The Pennsylvania State University

The Graduate School

Department of Earth and Mineral Engineering

CONDUCTING IN-SITU COMBUSTION TUBE EXPERIMENTS USING ARTIFICIAL NEURAL NETWORKS

A Thesis in

PETROLEUM AND MINERAL ENGINEERING

by

YOGESH BANSAL

Submitted in Partial Fulfillment
of the Requirements
for the Degree of

Master of Science

May 2009

The thesis of YOGESH BANSAL was reviewed and approved* by the following:

Turgay Ertekin
Professor of Petroleum and Natural Gas Engineering
George E. Trimble in Earth and Mineral Sciences
Graduate Program Officer in Petroleum and Mineral Engineering
Thesis Co-Advisor

Majid Ahmed Al- Wadhahi
Assistant Professor of Petroleum and Natural Gas Engineering
Sultan Qaboos University, Oman
Thesis Co-Advisor

Robert Watson
Associate Professor Emeritus
Petroleum and Natural Gas Engineering and Geo-Environmental Engineering

*Signatures are on file in the Graduate School

ABSTRACT

Artificial neural networks (ANNs), also known as expert systems, have become an increasingly important part of the petroleum industry for performance analysis of reservoirs. ANNs work similar to the biological brain which can make predictions based upon past experiences. ANNs used as a screening tool offer a low cost alternative to commercially available simulators that may require extensive data collection in order to build an effective model. The ANN serves to pare down the analysis so that a more focused data set and corresponding model can be developed. This screening tool consists of data sets usually referred as knowledge base and set of algorithms capable of predicting fact based results for an unexposed part of the input data set.

Artificial neural networks are widely used in the optimization of the reservoir parameters. These include operating conditions and reservoir performance, instantaneous and cumulative production, cyclic injection of fluids into the reservoir in order to maintain reservoir pressure for better recovery, field development and well stimulation, among others. The expert system developed during this research models in-situ combustion which is a technique utilized in heavy oil recovery. In in-situ combustion process oil is ignited in the porous matrix of the reservoir to improve the mobility of viscous oil using the heat generated. It is a complex process as the reaction parameters are unknown at the reservoir conditions, but the ANN is able to predict reliable results without a formal analysis of the mechanisms at work.

The ANN developed in this study is able to predict the cumulative production profile of oil, water and gas in a laboratory scale experiment utilizing the technique of in-

situ combustion under simulated reservoir conditions. Peak temperatures of the combustion zone, their positions and the velocity of the combustion front in the tube at 25%, 50%, 75% & 100% of the production time are predicted. One dimensional flow was analyzed and expert systems were prepared for both dry and wet combustion.

Understanding the ability of the network to predict the output parameters is a crucial task in this type of development. The complexity of the network is bound to increase with the number of the inputs and outputs. This problem becomes cumbersome because of the complexity of combustion reactions occurring in the porous media. The mechanisms of reactions have not been fully developed for different crudes with varying asphaltenes and maltenes compositions. By developing a data set for Athabasca crude, which already has a developed reaction mechanism in the literature, an expert system has successfully been developed each for dry and wet combustion processes in the combustion tube experiment.

TABLE OF CONTENTS

LIST OF FIGURES

LIST OF TABLES

ACKNOWLEDGEMENTS

I would like to express my deepest thankfulness and appreciation to my thesis advisors, Dr. Turgay Ertekin and Dr. Majid Al-Wadhai for their guidance and assistance throughout the development of this thesis without which this work would never have been completed. Acknowledgements are also extended to Dr. Robert Watson for his interest in serving as committee member and for his time and comments in evaluating this work.

I also would like to thank doctoral students Emre Ertun, Basar Basbug and Claudia Parada and Master's student Karthik Sriniwasan for their help at times of need and the Department of Energy and Mineral engineering for providing scholarship and fellowship during the course of my study at The Pennsylvania State University.

I am indebted to my mother, Kanta Bansal and to my father, Satpal Bansal, for being the endless source of support and encouragement. I would also like to thank my friends for their help and emotional support at different times.

Chapter 1

INTRODUCTION

Most of the light oil has already been exploited by natural or artificial lift of the hydrocarbons. Currently different methods are being employed for the recovery of heavy oil in the reservoir. These EOR methods include carbon di-oxide injection, water injection, steam injection, polymer flooding, *in-situ* combustion and the combination of these processes and are employed to mobilize the otherwise immobile oil. The proposed ANN model mimics the *in-situ* combustion tests carried in the laboratory. Each individual *in-situ* combustion experiment, in 2008 dollars, costs around $100,000-$150,000 and therefore, the total cost of experiments is huge as several runs are required to completely understand the recovery process. This work aims at reducing the experimental cost by means of mimicking the laboratory experiment so that the number of these cost intensive runs can be minimized for different conditions of operations.

During this study, history matching of published data was achieved during the initial stages so that the use of the commercially available software can be justified in generating the training data. The history matching of the process is referred to tune the numerical model* to a combustion tube experiment. Several different scenarios were generated where the properties of the system, the design parameter, and the controls of the experiment can be changed. During the initial stages system properties such as porosity, permeability and saturation of oil were changed to generate the training dataset

* Computer Modeling Group (CMG)

for the ANN. These properties are considerably different from the actual conditions found in the field. During the laboratory experiments reservoir rock is crushed and mixed with the desired saturations of water and oil. The porosity and the permeability values of the crushed sample cannot be lowered to the reservoir conditions. The ranges of the input variables are chosen from the published data by academic and research laboratories which are running the complex experiments successfully. A large number of data files for dry and wet combustion tube experiments are generated and the results of cumulative production, peak temperatures, their locations and combustion front velocities are extracted using the simulator. During the learning stage of ANN 90% of the sample inputs and their corresponding outputs are chosen randomly using a code and 5% of the total data set is used each for validation and testing of the network.

Chapter 2

LITERATURE SURVEY

Although *in-situ* combustion process is not as popular as other enhanced oil recovery methods, there are number of studies carried at laboratory and field scales since 1970. There have been many field tests and laboratory experiments carried by various academic laboratories and companies during the recent past. Although different companies like Oil and Natural Gas Commission of India Ltd. (ONGC) at Santhal field in India [Chattopadhyay et al., 2004], Shell oil at their pilot plant in Colorado, are carrying out this method successfully, the complete mechanism of the process is still not totally understood. *In-situ* process follows a complex reaction mechanism which requires an extensive study of reaction kinetics parameters in reservoir conditions. Combustion process encounters problems like propagation and sustainability of the combustion front. The complete understanding of the process will include knowledge of initial oil saturation required to start the process, amount of air (oxygen) required for complete combustion at the combustion zone and the amount of pre-heating of the system to achieve threshold temperature for self-sustaining combustion. In this chapter, a description of in-situ combustion, combustion reaction model, combustion tube and ANN are discussed.

2.1 *In-situ* combustion:

In-situ combustion is a process of igniting the oil in the porous matrix of the reservoir. In this process the generated heat is utilized for the following purposes:

- To reduce the viscosity of the oil
- To vaporize the water and crude oil to form steam and the gases
- To crack the heavy oil present in the subsequent zone to form the lighter and the heavier component

The produced vapors reduce the viscosity of the oil by dragging the liquid along with it and condensing in the colder region ahead of the combustion zone. The condensed vapor when mixes with the heavy oil reduces the viscosity considerably. As a result of the very high temperatures of the combustion zone (around 600˚F-1500˚F) cracking of the heavy oil takes place in the hydrocarbon zone ahead of the combustion zone. Cracking is helpful in the process as it provides lighter oil and coke. Lighter oil moves easily and is recovered. Whereas, the coke produced during the cracking process is the fuel to sustain propagation of the combustion zone. The processes that are taking place in *in-situ* combustion experiment can be explained with the help of the following Figure 1 [Chattopadhyay et. al. (2004)]

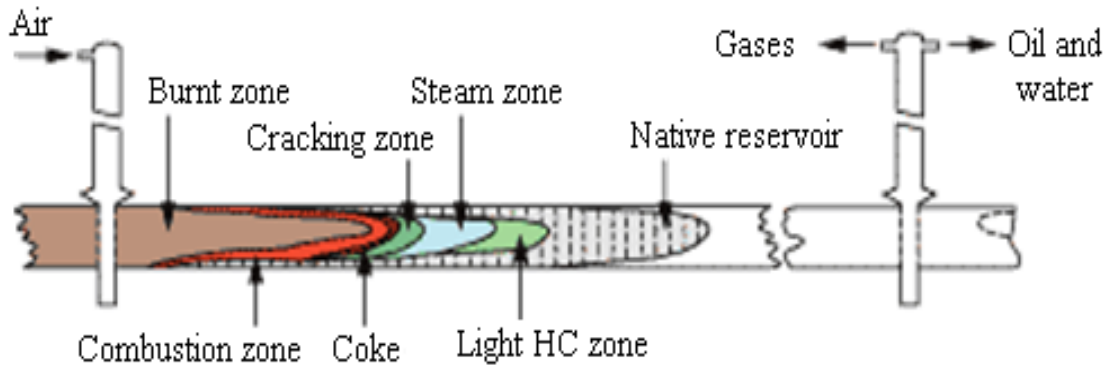

Figure 1: Various zones in *in-situ* combustion

In Figure 1, burned zone is the exhausted zone of the reservoir or the combustion tube, the combustion front has already past this zone utilizing the fraction of the heavy oil present in it and leaving behind the unburned fuel or residue in the incomplete combustion reactions. This zone is preceded by combustion zone where the oxidation reaction occurs. In this process coke and HCs* react with oxygen to form carbon dioxide (CO_2), carbon monoxide (CO), HC-acids, and steam. This zone is followed by a layer of coke which serves as fuel for the combustion front and helps in propagation of combustion. In the light HC zone, steam and HC-vapor condense and are mixed with the heavy crude of the reservoir. The process of mixing the heavy oil and the light HC yields an intermediate HC zone having low viscosity.

2.1.1 Types of *In-situ* Combustion

In-situ combustion process can be classified under forward and backward combustion methods. These two methods are based on the direction of the propagating combustion front with respect to the direction of producing fluid. In other words, if the fluid is moving in the same direction as the combustion front then it is called forward combustion and if the reservoir fluid move in the reverse direction as that of the combustion front then it is called reverse or backward combustion. The process can further be classified as dry *in-situ* combustion and wet *in-situ* combustion. Dry

* Hydro-Carbons

combustion employs the injection of only air whereas in wet combustion a combination of air and water is injected.

(A) Forward *In-situ* Combustion

In this process, preheating of the oil sand near the injection well is achieved. Once the oil sand reaches the desired temperature, injection of air or enriched air depending upon the design requirements at the injection well is started. When air reaches the heated zone (around the injection well) it starts reacting with the available fuel and leads to the development of the combustion zone. With continued injection of air (oxygen) this combustion front propagates in the direction of fuel as shown in Figure 2.

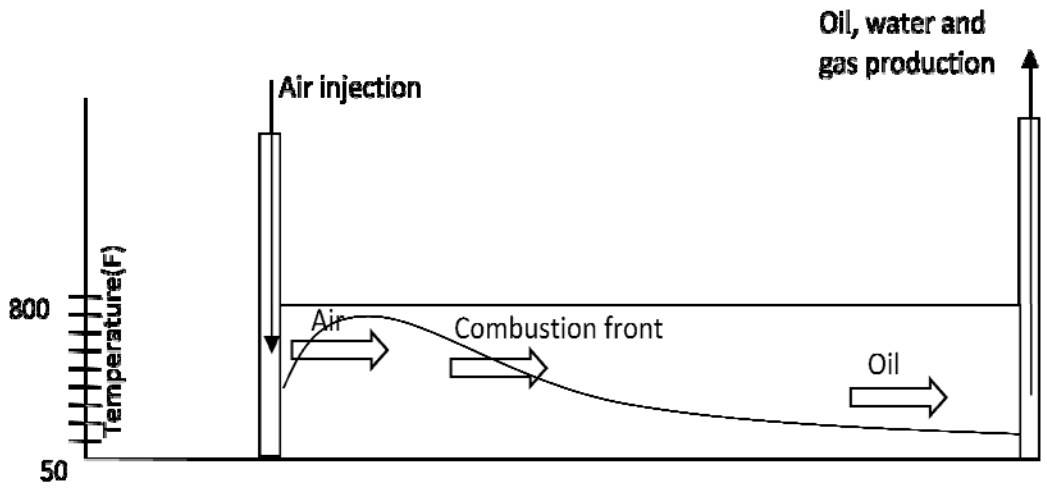

Figure 2: Forward Combustion

Chemical and physical properties of the fluid in the reservoir change as combustion front propagates in the reservoir [Burger et al., 1972]. As the combustion reaction takes place in the reservoir the temperature of the reservoir is increased. The level of temperature is largely determined by the amount of fuel available in the reservoir

[Mamora D.D., 1993]. The level of temperature in the reservoir is a highly important parameter in determining the production of the crude as it influences the viscosity of the heavy oil, quality of cracking and the extent of the combustion in the reservoir [Bousaid et al., 1968].

(B) Reverse Combustion

In reverse combustion, preheating of the oil sand near the production well is carried first. Once the oil sand reaches the desired temperature, air or enriched air injection is started depending upon the design requirements at the injection well. In this method, the combustion front moves in the backward direction and flows against the direction of the air flow. With continued injection of air (oxygen) this combustion front propagates in the direction of fuel and against the air flow as shown in Figure 3.

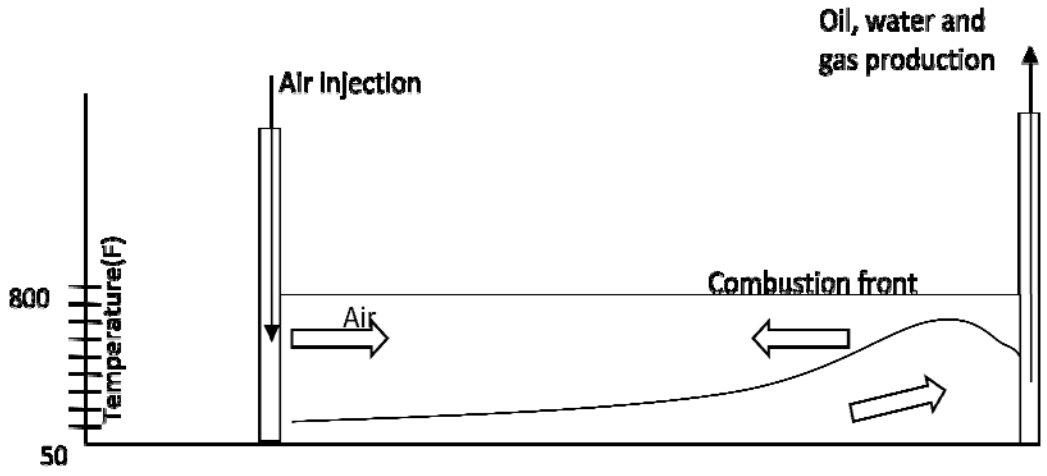

Figure 3: Reverse Combustion

As the combustion front moves towards the fuel, due to very high temperature of the zone, crude oil is cracked extensively and a relatively large amount of solid fuel is formed in the process. The solid fuel (coke) formed in the process serves as the fuel for the combustion front. The lighter fraction of HC formed during cracking reactions move in the direction of air flow. In this process, a relatively large amount of fuel is burnt; therefore, the amount of recoverable oil is smaller than that from the forward combustion or co-current process. The advantage of the process is that the cracking product flows through the combustion front and formation of oil bank is not observed; therefore, resistance to flow is pretty low as compared to forward combustion.

However, in reverse combustion, it is very difficult to sustain the combustion front because of the low availability of oxygen at the fire front [Dietz, 1968]. It has been experienced that the combustion front cannot be expected to last for more than few weeks [Dietz, 1968 and Chu, 1977]. It is also observed that the sustainability of the combustion front depends upon two factors, reactivity of the crude and the initial reservoir temperature [Burger et al., 1973].

2.1.2 Dry Combustion

The process of utilizing combustion inside the reservoir without injecting water after the combustion zone has been established is known as dry combustion. Experimentally, this process starts with the injection of an inert gas to set up the communication path between the injector and the producer via the rock matrix. During this stage, the initial zone of the reservoir is pre-heated to attain the threshold temperature. When the temperature of the zone is raised to the ignition temperature,

injection of the inert gas is stopped and is followed by the injection of air/oxygen. Continuous injection of air at the constant flux has to be maintained to sustain the combustion front. A calculated amount of air flux is required to maintain the continuous and effective sweep of the reservoir by the combustion front. If the air flux is insufficient then, the combustion front cannot be sustained. If the air flow is more than the required then, the front moves at an undesirably higher rate. As a result of higher air flux, combustion front will consume more oil in the reservoir and thus the cumulative oil production would be lesser than it could have produced. Figure 4 shows the idealized plot of temperature and oil saturation as a function of the length of the combustion tube.

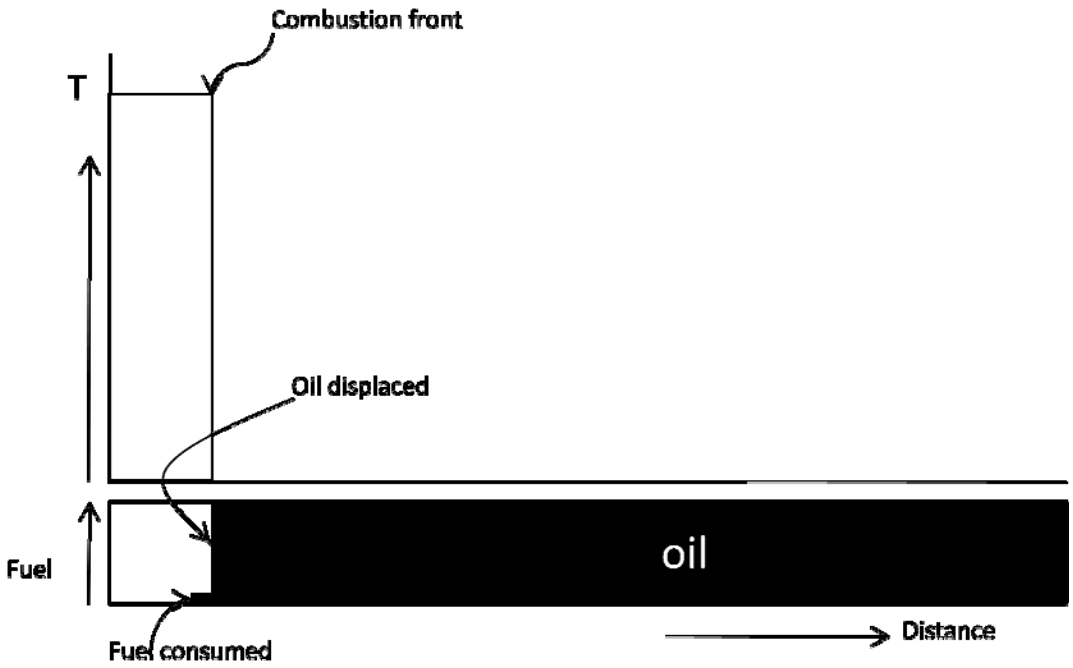

Figure 4: Dry Combustion (©1968 SPE-AIME)

Heat capacity of air is low; therefore, it cannot carry the heat of combustion from the combustion front along with it [Paarish et al., 1969 and Vekatesan et al., 1990].

Therefore, the heat efficiency of the dry combustion process is low as compared to other processes. Dry combustion when combined with water, chemical or polymer flooding yields better results as compared to dry combustion alone [Garon et al., 1974].

2.1.3 Wet Combustion

Wet *in-situ* combustion combines the benefit of both dry *in-situ* combustion and steam flooding [Burger et al., 1972]. The advantage of the wet combustion includes the improved utilization of the energy left behind and the development of larger steam zone ahead of the combustion front. In wet combustion a considerably reduced amount of air is required to burn a unit volume of reservoir [Garon et al., 1974]. This process faces complexities during recovery operations in tight sands where the co-injection of water and air is cumbersome therefore, simultaneous injection of air and water is carried in those situations. Wet combustion is a complex process and the addition of water corresponding to the "Water-to-Air-Ratio" (WAR) has been classified into three categories: normal wet combustion, incomplete wet combustion and super wet combustion.

2.1.3 (A) **Normal wet combustion**

In this case the injected water sweeps the heated zone and forms a steam front. This steam front moves well ahead of the combustion front. In the colder region of the reservoir, this steam front condenses and displaces the oil as the density of water is higher than oil in the pores. This process is accounted for most of the displacement occurring in the oil bank [Garon et al., 1974]. The thickness of the steam zone is a function of the amount of water injected. A contrast can be made with dry combustion, where, the steam zone is narrow because of the vaporization of the water contained in the rock matrix only.

But, by injecting water enlargement of steam zone is observed [Venkatesan et al., 1990]. In this case an optimum water to air ratio is injected once the combustion front is developed. The optimum range for WAR is suggested to be between 0.001(m^3/Sm^3) and 0.006(m^3/Sm^3) [Burger et al., 1972]. The evaporation curve of the water and the combustion front of the oil coincide with each other as a result most of the heat produced is used in vaporizing the water. In normal wet combustion, all the water injected gets vaporized and when this steam condenses in colder region, then, a larger quantity of oil is displaced as compared to incomplete and super wet combustions. In the combustion experiment with optimum WAR, exhausted zone is reported to be free from coke which entails complete utilization of fuel [Paarish et al., 1969]. All the coke formed due to cracking is consumed by the combustion reaction to produce flue gases, steam and raising the temperature of the combustion zone. Ignition phase lasts for a longer time when high water saturation is present in the combustion as more amount of heat is required to vaporize water to produce steam. Oxygen hindrance for the consumption in the reaction was not observed in the process of water injection [Paarish et al., 1969]. Figure 5 represents the optimal normal wet combustion.

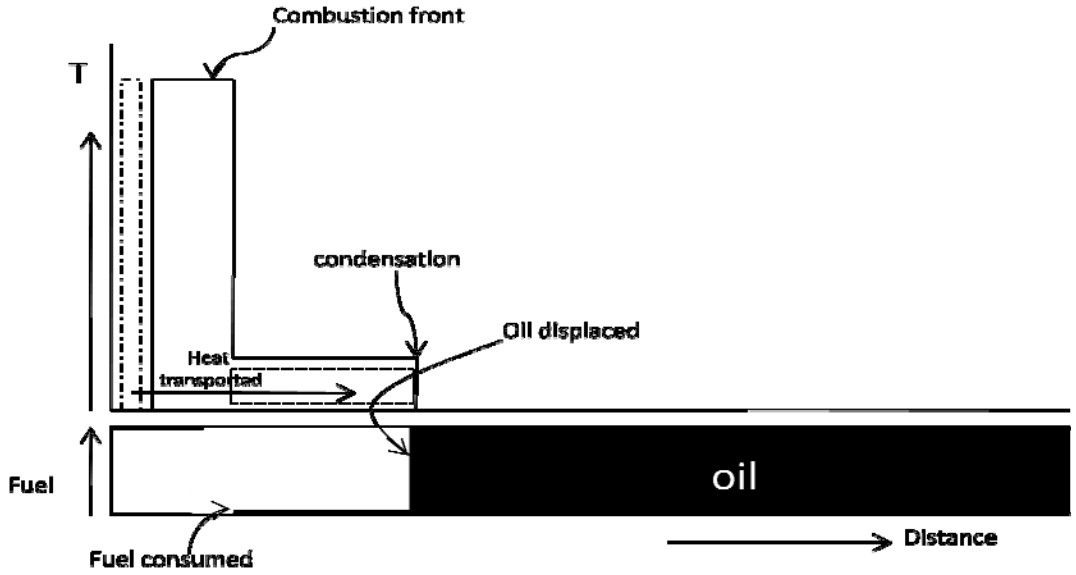

Figure 5: Normal wet combustion ©1968 SPE-AIME

2.1.3 (B) **Incomplete wet combustion**

In incomplete combustion, the cooling effect of the injected water is higher than combustion front, then, the combustion front does not reside long enough at the zone containing the coke. This results in incomplete combustion of the coke. A fraction of the unburned coke is left behind the combustion front and has been reported in the experiments [Dietz, 1970]. It has been reported that the oil recovery will be lesser than as compared to the normal wet combustion.

2.1.3.1 (C) **Super wet combustion**

This process indicates that more water is passed through the combustion front than it can be evaporated. When WAR is increased enough [a suggested range of $0.003(m^3/Sm^3)$ and $0.09(m^3/Sm^3)$] then evaporation front of water merges with combustion front [Dietz, 1970]. It has been reported that evaporation consumes most of

the heat produced by the combustion front and lowers the temperature of the front. Significant drop in temperature quenches the combustion. Once this condition is reached no more reaction occurs in the zone thus no more heat is produced and the temperature is dropped to a level where spontaneous ignition of crude cannot take place [Dietz, 1970]. Figure 6 represents the condition of super wet combustion.

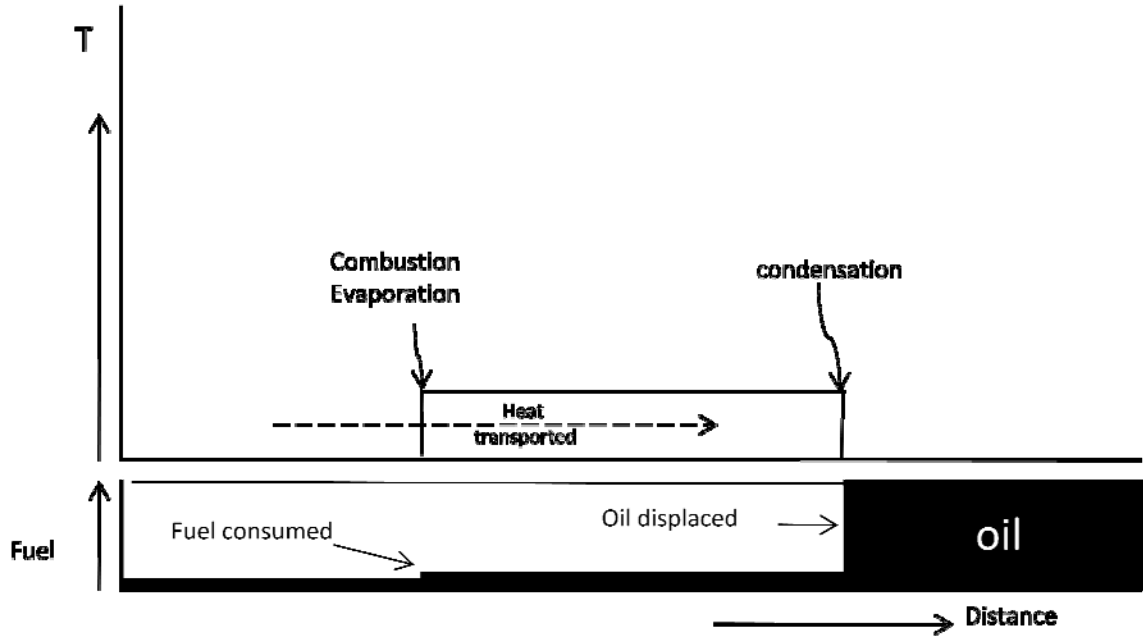

Figure 6: Super wet combustion © 1968 SPE-AIME

2.1.4 *In-situ* Combustion Reactions

During simulation runs, developed reaction model for water-free Athabasca crude oil is specified in the data files. The combustion reaction occurs in three stages: thermal cracking, low temperature oxidation (LTO), high temperature oxidation (HTO) [Belgrave et al., 1987]. In the development of the reaction model, bitumen was considered to be water free. This step is important as by this assumption bitumen can be considered as one

phase and water as another phase instead of water soaked bitumen which would otherwise be considered as one phase [Adegbesan, 1982]. Experiments for cracking were carried out in an inert environment so as to avoid combustion reaction. Cracking reaction occurs in three steps and each reaction follows first order rate reaction mechanism [Adegbesan, 1982]. In the first step, maltenes are converted into asphaltenes as shown in Equation 2.1. The rate constant† for this reaction is assumed to be 'K_1'. This reaction suggests that when one mole of maltenes reacts then 0.372 moles of asphaltenes are formed. In the second step, a parallel reaction is observed where asphaltenes, formed in the first step, is converted into coke by the action of heat as represented by Equation 2.2. The rate constant for this step is 'K_2'. In this reaction, one mole of asphaltenes reacts to form 82.223 moles of coke. Asphaltenes also react to produce some gas as shown in Equation 2.3. The rate constant is 'K_3' for this conversion. In this reaction, one mole of asphaltenes reacts to form 37.683 moles of gas.

$$\text{Maltenes} \xrightarrow{K_1} \text{0.372 Asphaltenes} \qquad (2.1)$$

$$\text{Asphaltenes} \xrightarrow{K_2} \text{83.223 Coke} \qquad (2.2)$$

$$\text{Asphaltenes} \xrightarrow{K_3} \text{37.683Gas} \qquad (2.3)$$

LTO reactions occur in two steps represented by Equations 2.4 and 2.5 [Adegbesan, 1982]. In the first step, one mole of maltenes react with 3.431 moles of

† Rate constant quantifies the speed of the chemical reaction.

oxygen to produce 0.4726 moles of asphaltenes as shown in Equation 2.4. The rate constant for this reaction is 'K_4'.In the second step, one mole of asphaltenes react with 7.513 moles of oxygen to form 101.539 moles of coke as shown in Equation 2.5. The rate constant for this reaction is 'K_5'.This reaction is very important in *in-situ* combustion as it provides fuel for the sustenance of combustion reaction. The amount of coke formation depends upon the amount of air available and the residence time of air at the combustion front.

$$\text{Maltenes} + 3.431O_2 \xrightarrow{K_4} 0.4726\ \text{Asphaltenes} \qquad (2.4)$$

$$\text{Asphaltenes} + 7.513O_2 \xrightarrow{K_5} 101.539\ \text{Coke} \qquad (2.5)$$

In high temperature oxidation (HTO), the coke obtained from the LTO reacts with oxygen to produce gas and water vapor (steam). This reaction occurs at the combustion front and during this reaction the temperature of the zone reaches around 600 ˚F–1500 ˚F [Adegbesan, 1982]. HTO reaction proposed is:

$$0.811\ \text{Coke} + O_2 \xrightarrow{K_6} 0.811\ \text{Gas} + 0.46\ H_2O \qquad (2.6)$$

Reaction rate constants are temperature dependent terms and are related by Arrhenius law. This relationship can be written as:

$$K_r = A_r . \exp\left(-E_r/RT\right) \qquad (2.7)$$

Where, K_r is the rate constant of the reaction *r*, A_r is the frequency factor of the reaction, E_r is the activation energy of the reaction, R is universal gas constant and T is the temperature of the reaction. Published values of reaction parameters are used in data file prepared for the numerical model and the values are represented in Table 1 [Coats et al., 1995].

Table 1: Rate constant parameters

r (reaction)	Reactant	A_r	E_r (J/gmole)
1	Maltenes	$7.86*10^{17}(d^{-1})$	$2.347*10^5$
2	Asphaltenes	$3.51*10^{14}(d^{-1})$	$1.772*10^5$
3	Asphaltenes	$1.18*10^9(d^{-1})$	$1.763*10^5$
4	Maltenes	$11.1*10^9(d^{-1}Kpa^{-1})$	$8.673*10^4$
5	Asphaltenes	$3.58*10^9(d^{-1}Kpa^{-1})$	$1.856*10^5$
6	Coke	$150.2(d^{-1}Kpa^{-1})$	$3.476*10^4$

2.2 Combustion Tube

Laboratory experiments are designed to study in-situ combustion method in one dimensional system. Studies are carried out where the tube is either horizontal, vertically up (injection well is at the bottom of the tube) or vertically down (injection well is at the top of the tube) [Moss et al., 1982]. The combustion tubes are designed to avoid heat losses; these designs are either insulated or adiabatic.

The reservoir rock is crushed and mixed with desired concentrations of heavy oil and water which then packed in the combustion tube and confined at the reservoir

pressure. Tube containing the reservoir rock is surrounded by an additional tube which has an electric heater installed in it. The purpose of having the heater is to heat the initial block of the tube and to bring the rock with crude to ignition temperature of the crude. Combustion tube is then insulated with fibrous insulator to ensure the adiabatic conditions [Belgrave, 1987]. Combustion tube has temperature probes to monitor the temperature at different locations along the tube length.

Some of the data utilized in this study came from a combustion tube which is 1.83 m long with a wall thickness of 1.067 mm and has the internal diameter of 9.94 cm. The tube is divided into 36 blocks of equal length and the temperature probs are placed in each of these blocks [Belgrave et al., 1993]. The combustion tube is produced at 9500 Kpa pressure at the production well and a constant flow rate of air is injected at the injection well for dry combustion experiment and a constant rate of air-water injection is used after dry air injection in wet combustion experiment. Figure 7 gives a schematic representation of the combustion tube.

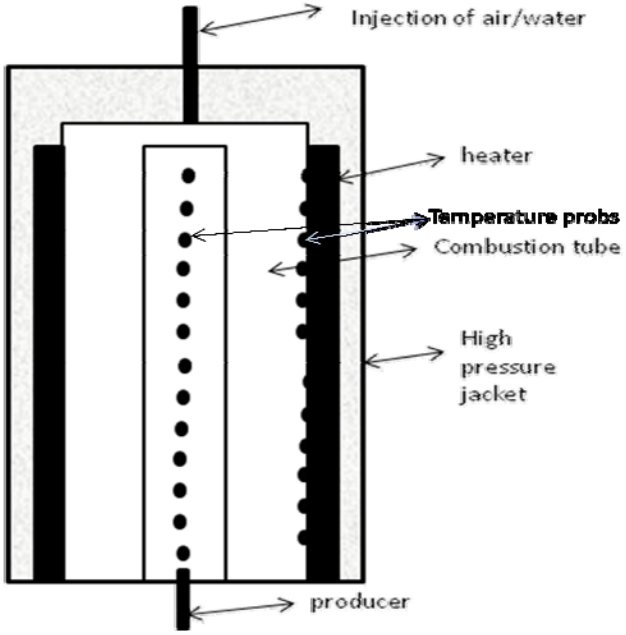

Figure 7: Combustion tube

2.3 Artificial Neural Networks (ANN)

Artificial Neural Networks are information processing models of human cognition of neural biological systems. ANNs are based on the following assumptions [Fausset, 1993]:

(a) The information is passed between neurons over connections links.

(b) Each link has some associated weight which is multiplied by signal transmitted.

(c) The capabilities and robustness of the neural network depends upon the learning abilities and can be applied to the pattern recognition problems and optimization techniques etc.

Each neural network contains one input layer, one output layer and one or more hidden layer and each layer contains different number of neurons which varies from problem to problem. The outermost layer that provides the output of the neural network is called as the output layer and the layer which provides the input to the network is known as the input layer and all layers in between are known as hidden layers. Each neuron is connected to other neurons by means of a communication link which has an associated weight with it [Fausett, 1994]. Each neuron sends one signal at a time although the signal is broadcasted to several other neurons in the next layer. A network has to be optimized for the number of the hidden layer and the number of neuron in each of the layers. It is a heuristic method which starts with one hidden layer and neurons equal to the number of output. Then we gradually increase the number of neurons in the first layer and also number of hidden layers in the architecture of the neural network. The structure that gives the least error on the testing sets is chosen as the final architecture of the neural network. A typical fully connected neural network looks like the one shown in the Figure 8.

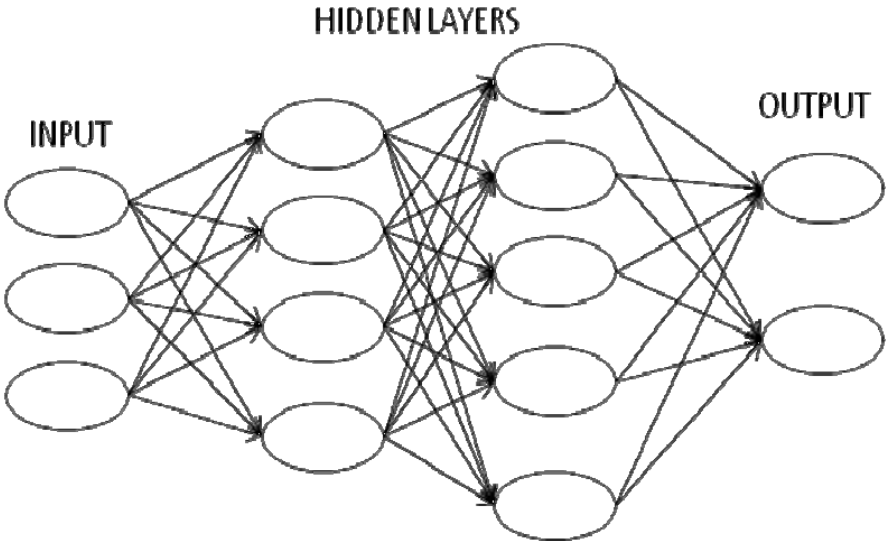

Figure 8: Typical Architecture of ANN

2.3.1 Feed Forward Backpropagation Algorithm

Backpropagation is a gradient decent algorithm in which weights and biases of the network are updated in the direction of the decreasing performance function or the negative of the gradient. Backpropagation network is also known as the generalized delta rule. This algorithm is based on other optimization techniques like conjugate gradient method and the Newton methods. One of the iteration of the algorithm can be written as:

$$X_{K+1} = X_K - \alpha_K g_K \qquad (2.8)$$

Where X_K is a vector of current weights and biases, g_K is the current gradient and α_K is the current learning rate. In a feed forward network, the flow of information is always carried in the forward direction starting from input layers to the hidden layers and finally to the output layer. In this process, each neuron receives a signal, calculates the weighted

input signal and then applies the activation function to calculate the output of the hidden unit and finally passes the signal to all the neurons in the next hidden layer. During the backpropagation stage, error and weights are calculated and updated for hidden and output layers [Fausett, 1994].

Chapter 3

DATA GENERATION

To train an ANN, it is necessary to know a number of reservoir and operating conditions in that reservoir. Available commercial reservoir simulation software[‡] is used to generate the data for ANN. This chapter describes the numerical model requirements, tuning of the numerical model, factoring out the crucial parameters and the data generation for the predictive model.

3.1 Numerical model for *In-situ* combustion

The model used was developed using CMG-STARS simulator module used for thermal recovery processes including steam injection, *in-situ* combustion processes etc. In order to use this model a data file is developed which includes properties of the porous medium, the operating conditions, rock and fluid properties and kinetics of the reactions. A sample file is attached in Appendix A.

In the initial part of the simulator's data file, the description of the reservoir is entered which starts with the type of the grid system used to solve the system, in the data files one dimensional Cartesian coordinate system with 36 blocks is used. During the description of the reservoir the permeability, porosity of the rock matrix, thermal properties of fluid and rock and the rock compressibility are also defined.

---

‡ Computer Modeling Group (CMG)

In the second part of the file, component present with their names are specified. In this part of the description, the type of model used for the reservoir is specified which depends upon the number of components in the reservoir. The model specified has 8 components in the reservoir viz. water, asphaltenes, maltenes, N_2, Gas, O_2, LTO coke and HTO coke. Then, the number of components in oil phase and number of components in the water phase are specified. During the definition of the system, the properties of the fluids in the reservoir that includes molecular weight, critical pressure and temperature for each of the components are also specified. This section also includes the definition of the values at the reference condition and specifying the thermodynamic properties of the fluid viz. vapor-liquid equilibrium constant values, enthalpies of the fluids and viscosity correlation of the fluids.

In an *in-situ* combustion reaction, the mechanism of the combustion in the rock matrix is specified by providing stoichiometry of the reactions with their frequency factors and the activation energy of each of the reaction. Rate constant of the reaction follows the Arrhenius equation given by:

$$K_r = f.exp(E_a \,/\, RT) \qquad (3.1)$$

In equation 3.1, where, K_r is the rate constant of reaction, f is frequency factor of the reaction, E_a is the activation energy of the reaction, R is universal gas constant and T is the temperature of the reaction. Since the temperature of the operation is not fixed therefore, the rate of the reaction will keep on changing. In order to overcome this situation, frequency factor and energy of activation are used for calculating the rate of the reaction in each simulation.

In the next section in the data file, rock and fluid properties of the system are defined. In this section, a table depicting the relationship between permeability and saturation is fed. After specifying the rock and fluid properties, the initial condition of pressure, saturation, temperature, mole fractions of asphaltenes and maltenes in the oil are specified. Then, parameters that control the simulator's numerical activities such as time step, iterative solution of non-linear flow equations, and the solution of resulting system of linear equations are defined. Finally, the well and recurrent data that has information like operating conditions of the wells at different times is defined. In this system, an injection well and a production well are used. Injection well operates at constant flow rate of nitrogen during the heating stage of the combustion tube and then it starts injection of enriched air (94.78% O_2) and in the final stage of injection of injection it injects either nitrogen or water depending upon dry or wet combustion process. A sample data file in Appendix A represents the complete structure of the input file.

3.2 Tuning of the numerical model

Data generation for learning and training of ANN heavily relies upon numerical model; therefore the numerical model must be calibrated for the published experimental data [Belgrave, et al., 1993 and Coats, et al., 1995]. During the initial stages of the work, validation of numerical model was carried by matching the aforementioned published experimental data. For validation, peak temperatures and the locations of the combustion front were matched with those published. A comparison of the experimental results and the results obtained from the numerical model was made to ensure a good calibration of

the numerical model. The experimental data is referred to the published data extracted from the figure [Belgrave, et al., 1993].

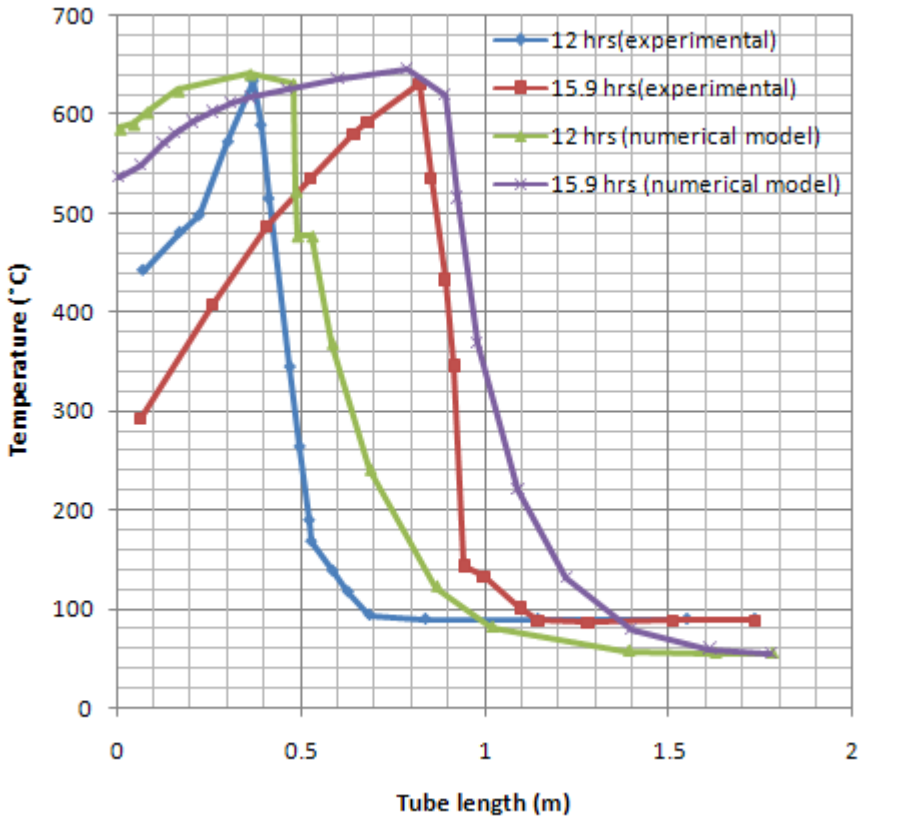

Figure 9: Comparison of numerical model and experimental results

The numerical model was tuned for the same properties used in the literature to generate the experimental data. The results obtained by the numerical model were extracted for 12 hrs and 15.9 hrs of production times. The comparison is made for the peak temperatures and the locations of the combustion front in the tube. These results match well with those published experimentally as shown in Figure 9. For this particular system, the combustion front traverses a distance of around 0.38 m after 12 hrs of combustion time and a distance of 0.82 m after 15.9 hrs of combustion time.

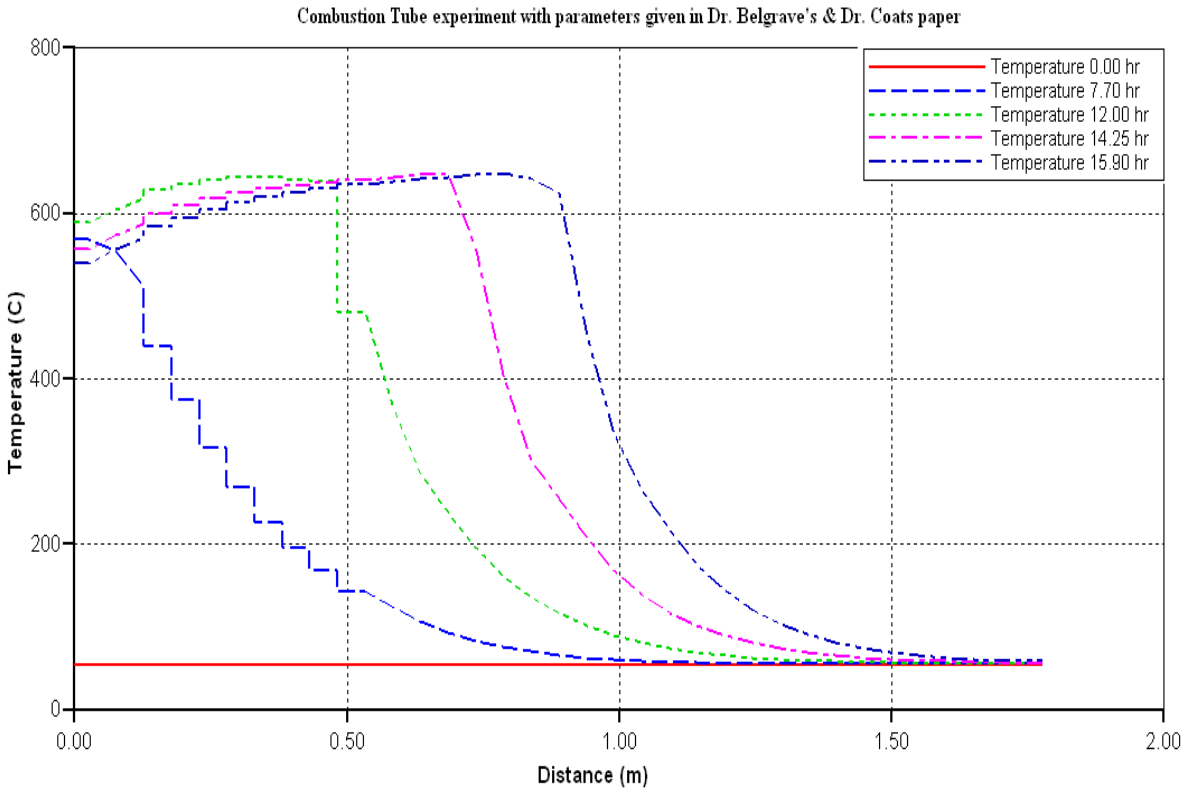

Figure 10: Numerical model results

Figure 10 shows the temperature profiles at different times obtained using the numerical model. These temperature profiles are obtained by using the combustion tube conditions mentioned in the literature [Belgrave et. al, 1993 and Coats et al., 1995]. Results for temperature profiles after 12 hours and 15.9 hours of combustion were extracted and plotted along with the experimental results. This figure also shows the movement of the combustion front with time.

3.3 Factors affecting the production

Preparing a list of all the parameters important to the *in-situ* combustion process is an initial task in the study carried out in this thesis. Only laboratory *in-situ* combustion experiments for heavy oil recovery are addressed in this study. It is a one dimensional vertical system where air is injected at the top and oil, gas, and water are produced at the bottom. In order to generate the data for this system a list of variables was prepared, important factors were chosen from the list of all the probable variables. Table 2 shows the list of crucial parameters to this experiment.

Table 2: List of parameters

Probable Parameters	(fixed/variable)
System Properties	
Size of the system	Fixed
Heat capacity of the rock	Fixed
Thermal conductivity of the rock	Fixed
Porosity	Variable
Permeability	Variable
Initial saturation of the oil	Variable
Initial pressure of the system	Fixed
Fluid properties	
Thermal conductivity of water	Fixed
Thermal conductivity of oil	Fixed
Thermal conductivity of gas	Fixed
Asphaltenes/maltenes ratio	Fixed
Solid density of the coke	Fixed
Critical conditions of Temperature & Pressure	Fixed
Viscosity of the fluid	Fixed
Chemical Reactions	
Rate of the reaction	Fixed
Frequency factor	Fixed
Activation energy	Fixed
Order of the reaction	Fixed

Operating conditions	
Time of heating	Variable
Heating rate	Variable
Injection flow rate of air	Variable
Concentration of air	Fixed
Time of air injection	Variable
Injection flow rate of water	Variable
Time of water injection	Variable
Water to air ratio	Variable
Sandface pressure of the production well	Fixed

This work focuses on studying in-situ combustion experiment on Athabasca crude oil. The data for crucial parameters for this oil and the ranges for the parameters were taken from published literature. The parameters representing the rate of reaction for Athabasca crude were taken from the published rate of reaction data [Coats et al., 1995]. Thermal conductivity of water, air and rock were fixed in generating the data files for the numerical model. Although the thermal conductivity of oil changes with composition, for one particular crude oil it can be taken as a constant by assuming that composition of the crude oil does not change during the combustion and heating process. In this analysis, the concentration of asphaltenes[§] and maltenes[**] in the crude oil is taken as constant. The complete data stating the rate of the reaction for different crudes have not been published and this restricts the work in analyzing the system over a variety of crude oils. Since this work mimics the laboratory experiment, the ranges for variables are observed to be different from the values found on the field scale. For example, porosity and permeability

[§] Asphaltenes are condensed aromatic HCs with side-chains up to 30 carbon atoms. Asphaltenes are insoluble in n-alkanes (pentane and heptanes)

[**] Maltenes are fraction of asphaltenes soluble in normal alkanes

in the sample sets are in a high range where we do not observe those high values on the field scale.

This thesis includes development of four models where the first two models serves as the basis for developing dry combustion and wet combustion model. The first model was developed to understand the variations in reservoir conditions of porosity, permeability and saturation of oil. In the second model tube dimensions, air injection and sandface pressure of the production well were also added in the list of variables of first model. The third model was developed for dry in-situ combustion. In this model, dimensions of only one tube are considered. Information on volume of air injected, amount of heat input in the beginning and amount of nitrogen injected in the combustion tube are also added in this model. Fourth model was developed on wet-combustion experiment. This model is an extension of the third model where the information on water injection flow rate and water to air ratio are added. All of the four models have been discussed in detail in Chapter 4.

3.4 Data File Generation

Data files represent information to the system which contains the values of permeability, porosity, initial oil saturation, initial water saturation and the operating conditions of *in-situ* combustion. All the variable parameters used in the data files are tabulated in Tables 3, 4, 5 and 6. For each of the abovementioned models a number of data files were generated by developing MATLAB codes. Once all the files of a particular model were generated then the batch files containing all the data files were run

in reservoir simulation model. The results of the simulation for each model were extracted by developing a code in MATLAB. This program extracts the cumulative production data at the end of the simulation, combustion front velocities, peak temperatures and its locations at 25%, 50%, 75% and 100% of the production time. A record of all the cases was stored in a matrix referred as ‘output matrix’ and the variable conditions of each simulation were stored in the different matrix referred as ‘input matrix’. These two matrices represent the database for the intelligent system to be built.

Chapter 4

Stages of Development

In this chapter, different stages of the model development are discussed. First, variable reservoir condition model is explained in which reservoir conditions of saturation, porosity and permeability were varied. Second, variable tube dimensions model is described where tube dimensions were added to the list of variable from the first model. Finally, dry combustion tube model and wet combustion model are explained in this chapter.

4.1 Variable Reservoir Conditions Model

Development of the first model started with three parameters in the input layer. Based on the literature study and sensitivity analysis of the parameters using the numerical model, a list of the parameters critical to the study was developed. Based on the availability of data and sensitivity to the process, some of the parameters were fixed and the other parameters were chosen as variables, as shown in Table 2.

At this stage, porosity, permeability and the initial saturations of oil, water and gas were taken into consideration. In the study, it is assumed that gas is not present in the beginning of the experiment, as when the combustion tube is prepared for the experiment then the reservoir rock is crushed and mixed with the desired volumes of oil and water. Since there is no initial gas present in the rock matrix, when the saturation of oil is changed in the rock matrix then the water saturation is automatically fixed in a particular

experiment as the summation of the saturation values of oil and water is unity. In this way, the initial variables in terms of porosity, permeability and saturation of oil/water were selected for the input layer. Ranges of parameters are selected through literature and are shown in Table 3.

Table 3: Input layer for Variable Reservoir condition model

Parameter	Lower Limit	Upper Limit	Number of cases
Porosity (ϕ)	20%	40%	5
Permeability (K)	3D	12D	12
Saturation(S_o)	30%	90%	13

Considering the number of cases shown in Table 3, a total of 780 cases were generated out of these combinations 39 cases were used for testing, 39 of the cases were used for validation of the data the rest of the 702 cases were used for training. This network predicts oil, water and gas production rates at the end of the numerical experiment and peak temperatures of the combustion front at 615, 735, 954 and 1200 min after the combustion was started. In this model the experiments were carried at the same conditions of injection rate, heating rate, total volume of the air injected, heating time, combustion time and the final production time.

The extracted data was used for training the ANN. Initially, an ANN structure with only one hidden layer was used with the same number of neurons as outputs and gradually the numbers of the neurons were added with subsequent run. Different combinations of number of neurons and number of hidden layers were tested. All the

architectures were tested on different transfer functions between the layers to optimize the performance of the network. The architecture with three hidden layers having 67, 45, and 52 neurons in each layer with 'tansig' transfer function for each layer was accepted as the final architecture as the errors in the prediction were less than 5% for each of the outputs. A number of functional links in the input and the output layers were used for better learning of the network. In this network, saturation of water is used as one of the functional link in the input layer. The final optimized ANN architecture is shown in Figure 11.

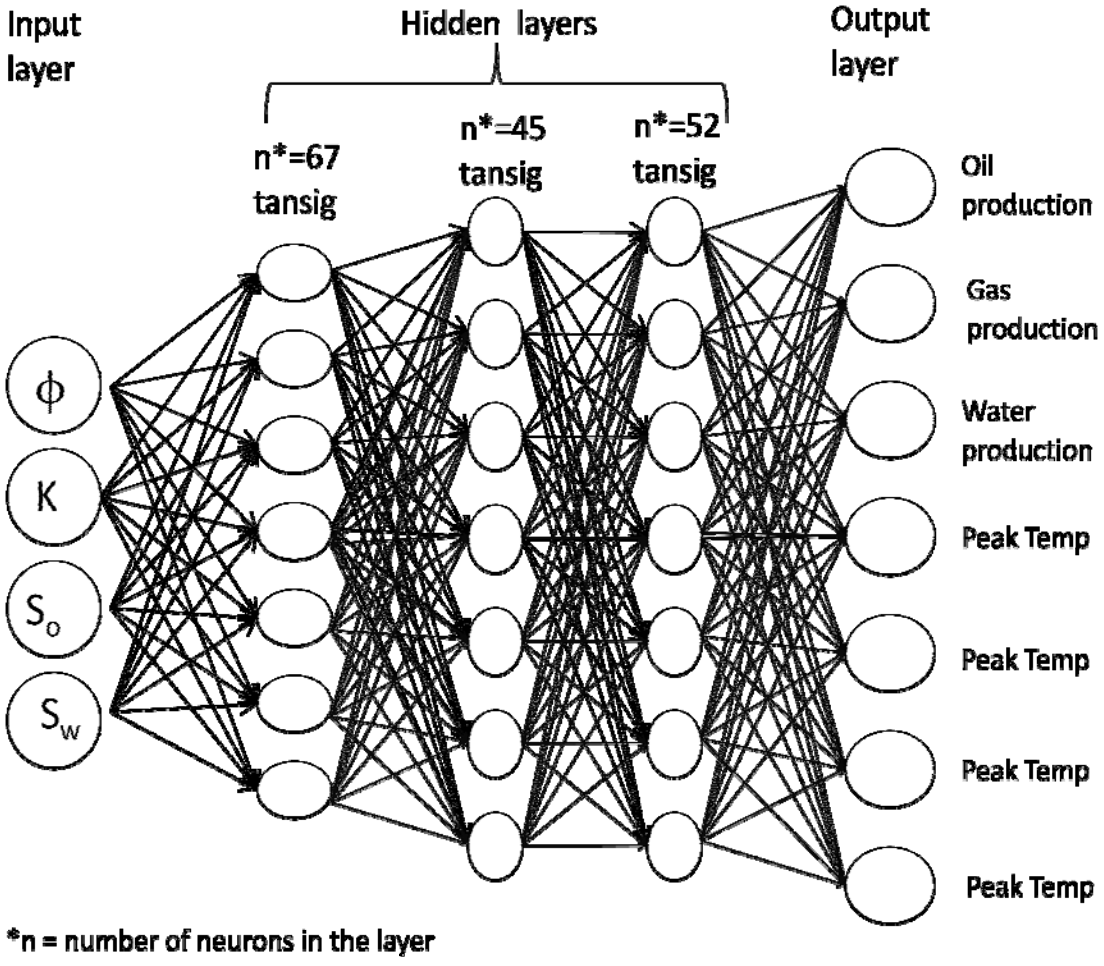

Figure 11: ANN architecture variable reservoir condition model

4.2 Variable Tube Dimensions Model

The desirable accuracy levels achieved with the neural network motivated to develop a more generalized model that can predict the combustion experiment in different tubes having different dimensions. In this model, additional variables providing information about the size of the system were added. All of the values of the variables were selected from the previous data set and literature survey; and are listed in Table 4.

Table 4: Range of variables for variable tube dimensions model

Parameter	Lower Limit	Upper Limit
Porosity (ϕ)	20%	40%
Permeability (K)	3D	12D
Saturation(S_o)	30%	90%
Air injection(Q_{in})	0.5 m^3/hr	3 m^3/hr
Diameter of tube(D)	5.08 cm	9.94 cm
Length of tube(L)	25 cm	183 cm
P_{sf}(production well)	4100 Psia	9500 Psia

From the ranges shown in Table 4, a total of 2358 cases were generated; out of these cases 118 cases were used for testing, 118 cases were used for validation of the data and the rest of the 2122 cases were used for training the network. This network predicts oil, water and gas production rates at the end of the simulation, peak temperatures and the location of the combustion front at 25%, 50%, 75% and 100% of the total production time. In this model, two different tube lengths were used and the final production times

were different for each of the combustion tube. In this process data is extracted at time interval of 0.24 hrs (0.01 days). In order to keep the output data file consistent, it was assumed that the simulation continues for 1 hr and 36 minutes after the combustion was started.

The extracted data generated using the numerical model was used for training ANN. Optimizing the architecture of the ANN follows the same design heuristics as was followed for the first model. Finally, the architecture with three hidden layers having 67, 45, and 52 neurons in each layer with 'tansig' transfer function for each layer was accepted as the final architecture as the errors in the prediction were less than 5% for each of the outputs. In this network, ration of porosity over initial oil saturation, and Leveret-J function (square root of permeability over porosity) were used as functional links in the input layer. In addition, temperature divided by the square root of normalized[††] distance was used as a functional link in the output layer for better learning of the network. This model is developed for different tube lengths, therefore, in order that the ANN learns better; all the distances were normalized against the respective tube lengths. The final optimized architecture is shown in Figure 12.

[††] A ratio of the distance covered by the combustion front over the tube length

Figure 12: ANN architecture for variable tube dimensions model

4.3 Dry Combustion Tube Model

After successfully training the network for "variable tube dimension model," different crude oils were planned to be added in order to extend the model. Numerical reservoir simulation model needs data like kinetic parameters for the crude oil that include activation energy, frequency factor of the reaction and the stoichiometry of the reaction. In addition to this data, it also needs values of constants used to calculate the viscosity of fluids as shown in the Equation 4.1. These constants are function of temperature and pressure. This equation requires these constants typically for asphaltenes and maltenes. Due to unavailability of complete data, this model could not be extended further. Therefore, after the previous activity, the developed model was used as benchmark and a dry combustion model for Athabasca crude oil was developed.

$$\mu = a.e^{\left(\frac{b}{T}\right)} \qquad (4.1)$$

In this development, instead of developing the model for different tube dimensions, a single tube length was used as most of the research laboratories now use the same standard combustion tube. In this model, the flow of fluid and the combustion front is studied only in one direction i.e. z-direction. Porosity and the permeability of the system are assumed to be constant throughout the tube. This model is developed for Athabasca crude oil which has a fixed concentration of Asphaltenes (8.49 %) and Maltenes (91.51%).

Viscosity coefficient values for this model are taken from the published literature [Coats, et al., (1995)]. The values of 'a' are 4.89E-25 and 1.94E-05 for asphaltenes and maltenes, respectively. Also, values of 'b' are 33147 and 5270.4 for asphaltenes and maltenes,

respectively. The total amount of heat supplied to the system assumes complete adiabatic conditions and the amount of heat is sufficient to initiate the reactions. For this system the list of parameters and its ranges are listed in Table 5.

Table 5: Parameter ranges for dry combustion

Parameter	Lower Limit	Upper Limit
Porosity (ϕ)	20%	40%
Permeability (K)	3D	12D
Saturation(S_o)	30%	90%
Air injection($Q_{a,in}$)	1 m^3/hr	3 m^3/hr
Heat rate (Q_{heat})	$1.1*10^5$ J/Day	$2.2*10^5$ J/Day
Time for heating (t_{heat})	0.15 Day	0.2 Day
Time for air injection (t_{air})	0.15 Day	0.3 Day

A total of 1440 cases were generated each with different combination of parameters listed in Table 5. All the cases were simulated using the numerical model and the results were extracted at a regular simulation time of 0.24 hrs or at .01 days starting from the onset of combustion in the tube. In order to keep the output data file consistent it was assumed that the simulation at least runs for 1 hr and 36 minutes after the combustion was started. By this selection criterion, a total of 1140 cases were used in the study. Out of these cases, 57 were used each for testing and validation of the data, and the rest of 1026 cases were used for training the network. This network predicts the

cumulative oil, cumulative water and cumulative gas production at the end of the simulation, peak temperatures, location of the combustion front and the velocity of the combustion front at 25%, 50%, 75% and 100% of the total production time.

The data generated in this model was optimized using different architectures of the neural network. The optimization of the network follows the same procedure as was followed for the previous models. An architecture with three hidden layers having 67, 62, and 65 neurons in each layer with 'logsig' transfer function for first two hidden layers and 'tansig' transfer function for the third hidden layer was designed. A number of functional links in the input and the output layers were used to optimize the performance of the network. In this network following functional links were used in the input layer:

- Ratio of porosity over saturation of oil
- Leveret-J function[‡‡]
- Total amount of air injected
- Total amount of heat supplied
- Logarithm of heat supplied
- And, logarithm of the ratio of permeability over porosity

Also, product of temperature and distance was used as a functional link in the output layer. The final optimized ANN architecture is shown in Figure 13.

[‡‡] Square root of the ratio of permeability over porosity

Figure 13: ANN architecture for dry combustion tube model

4.4 Wet combustion tube model

The combination of dry combustion followed by water flooding is termed as wet-combustion process. Air has a low heat capacity and as a result it leaves behind most of the heat generated by combustion process and later lost in the process. Where, if water is injected once 25% or more of the reservoir has been covered with the dry-combustion then water carries forward the heat as it has a higher heat capacity [Dietz et al.,1968]. It has been observed that this process recovers more of the original oil in place than dry-combustion process alone. As reported earlier, this project heavily relies on water-air ratio (WAR) and the position of combustion front when water injection is started. Therefore, in this process it becomes really important to find the right combination of water to air ratio and the time to start water injection.

This model assumes that injected water does not hinder the kinetics of the combustion reactions occurring in the combustion tube. This model will also experience some cases where the water is injected at a higher rate or WAR is too high such that it extinguishes the combustion reaction and the later part of the experiment will simply become water flooding. Also, if water injection rate or WAR is low then the injected water will be converted into steam even before it reaches the combustion front. In both the cases it is very difficult to quantify our result in this aspect but the comparison of performance will be made on oil recovered during the process. This network predicts the cumulative oil, cumulative water and cumulative gas production at the end of the simulation, peak temperatures, location of the combustion front and the velocity of the combustion front at 25%, 50%, 75% and 100% of the total production time.

In this model, a minimum value of 0.001 (m^3/sm^3) and a maximum of 0.006 (m^3/sm^3) are used for WAR. A water injection range of 0.5-1 m^3/day is used. All the other parameters are taken from the dry combustion experiments and the complete list of variable parameters is shown in Table 6.

Table 6: Parameters ranges for wet combustion

Parameter	Lower Limit	Upper Limit
Porosity (ϕ)	20%	40%
Permeability (K)	3D	12D
Saturation(S_o)	30%	90%
Air injection($Q_{a,in}$)	1 m^3/hr	3 m^3/hr
Water injection($Q_{w,in}$)	0.5 m^3/hr	1 m^3/hr
Heat rate (Q_{heat})	$1.1*10^5$ J/Day	$2.2*10^5$ J/Day
Time for heating (t_{heat})	0.15 Day	0.2 Day
Time for air injection (t_{air})	0.15 Day	0.3 Day
Water to air ratio (WAR)	0.001 (m^3/sm^3)	0.006 (m^3/sm^3)

With variables listed in Table 6, a total of 4320 cases were generated by writing a MATLAB code and later a different code was prepared to extract the results for optimizing the ANN. Data extraction follows the same assumptions as were assumed in the dry-combustion model. After selecting the cases based on the assumptions a total of 3144 cases were left. The method for optimization of the network follows the same procedure as is followed for the previous models. All the architectures prepared in this

model were tested on different transfer functions between the layers to optimize the performance of the network and overtraining of ANN was avoided. The architecture with three hidden layers having 69, 62, and 65 neurons in each layer with 'logsig' transfer function for all the hidden layers was decided as the final. A number of functional links in the input and the output layers were used to test the performance of the network. In this network following functional links were used in the input layer:

- Ratio of porosity over saturation
- Leveret-j function
- Amount of air injected
- Amount of water injected
- Amount of heat supplied
- Logarithm of heat supplied
- And, logarithm of WAR

Also, product of temperature and distance was used as a functional link in the output layer. The final optimized ANN architecture is shown in Figure 14.

Figure 14: ANN architecture for wet combustion tube model

Chapter 5

RESULTS AND DISCUSSION

In this chapter, results obtained for the four models developed in this study are discussed. The study is divided into four parts and this chapter briefly discusses the results obtained from each of the model.

5.1 Introduction to discussion of results

In order to train the network, number of neurons and hidden layers in the architecture has to be optimized following a heuristic procedure. There is rule of thumb to start with total number of neurons in the structure, and it is always recommended that we start with one hidden layer and keep on adding neurons and layers to the network for improved predictions. The procedure is tedious and time consuming but once the network is optimized, the parameters of the network can be saved for future reference and predictions.

During the optimization process it has to be made sure that model is not over-trained, an undesirable situation, which can arise because of numerous reasons. The situation may arise because of more number of neurons in the hidden layers, more number of layers, or over-specified training dataset used in the network. The situation may also arise from combinations of the aforementioned problems. It is recommended that a record of number of hidden layers, number of neurons in each layer, transfer

function between each layer, and the performance of the network is kept as it helps in reducing the time to analyze the results on a later date and avoids repetition of the runs.

In the process of optimizing, a database is required which comprises of input files (tells about the reservoir and operating conditions) and output files (tells about the production and combustion zone). The database prepared has a large range of numerical values that ranges from 10^{-3} to 10^{5} with such a range it becomes difficult for the network to understand the relationship between the inputs and the outputs. Therefore it is important to reduce this range by mathematical operations and these changes have to be reverted back once the training, validation and testing is completed. In the beginning of the optimization process logarithmic function was used to reduce the range but when an inbuilt function for reducing the range from -1 to +1 was used then a better learning was observed. The inbuilt function 'minmax' allows to store the parameters used to reduce the range and can be used to map the changes made.

The prepared database is randomly divided into three sets viz. training set, validation set and testing set using MATLAB's internal function. For each run the division is random and due to this reason little deviation from the previous result is bound to happen. But, in an optimized network the deviation is not expected to be significant. Division of the sets in different fractions can also be used to avoid over-training in the network. In this problem different fraction of the sets were tested and later on the fractions were fixed as 90% for training, 5% each for validation and testing, as this combination gave better performance than the rest of the cases.

In this problem, default values for initial weights and biases for the hidden layers are assigned using an inbuilt function of MATLAB. There are different algorithms for

training and learning but for this problem cascade feed forward back propagation network works better for learning and gradient descent with momentum weight and bias learning function works better. In the cascade feed forward back propagation network, the inputs to each layer come from all the layers before it. When other back propagation network was used then error were not reducing at a rapid rate as has been suggested.

There are different algorithms to train the network viz. Fletcher-Powell conjugate gradient algorithm, the BFGS quasi-Newton algorithm (trainbgf), scaled conjugate training algorithm (trainscg), the Levenberg-Marquardt algorithm (trainlm) and the Powelle-Beale conjugate gradient algorithm. The Levenberg-Marquardt algorithm (trainlm) is the strongest algorithm but requires an extensive memory space. Due to this disadvantage the method could not be tested on the available machines. Different other methods were tested and scaled conjugate training algorithm proves to be the best for the type of systems in this study.

For performance of the network, mean square error regularization (MSEREG) method was used in the networks developed in the study. This function not only calculates the mean squared errors but also weight and biases values which are updated at the end of each epoch. Different functions for example, mean-square error (MSE) and mean-squared error performance derivatives function (DMSE) were also tested but the former function proves better than the other functions.

In the activity of training the network, a more or equal expertise in the technical details of *in-situ* combustion process is required. It is really important to prepare a database which includes the crucial parameters of the system. In order to start preparing the network one needs to really understand the basics of the problem which tells about

the importance of parameters and their relative impacts on the results. Once the database is prepared it is important to check the possibility of the results in the actual application.

5.2 Results from variable reservoir conditions model

This model discusses about varying system conditions, when reservoir has varying saturation of oil, porosity of the reservoir and the saturation of the oil. The architecture of the model is represented in Figure 11 and the ranges of variable are given in Table 3. Sample runs were carried out for this model before coming up with this structure of the ANN. Figures 15 and 16 make a comparison between the values obtained from the numerical reservoir model and the values obtained from ANN developed for this model. Figure 15 shows the comparison between the oil production rates, water production rates, gas production rates, peak temperatures at 615 minutes, 954 minutes, 735 minutes and 1200 minutes after the combustion was started. The comparison is made for 39 cases selected for testing the performance of the network. The results show a good match between the values predicted by the network as prediction curve closely follows the curve representing the numerical model.

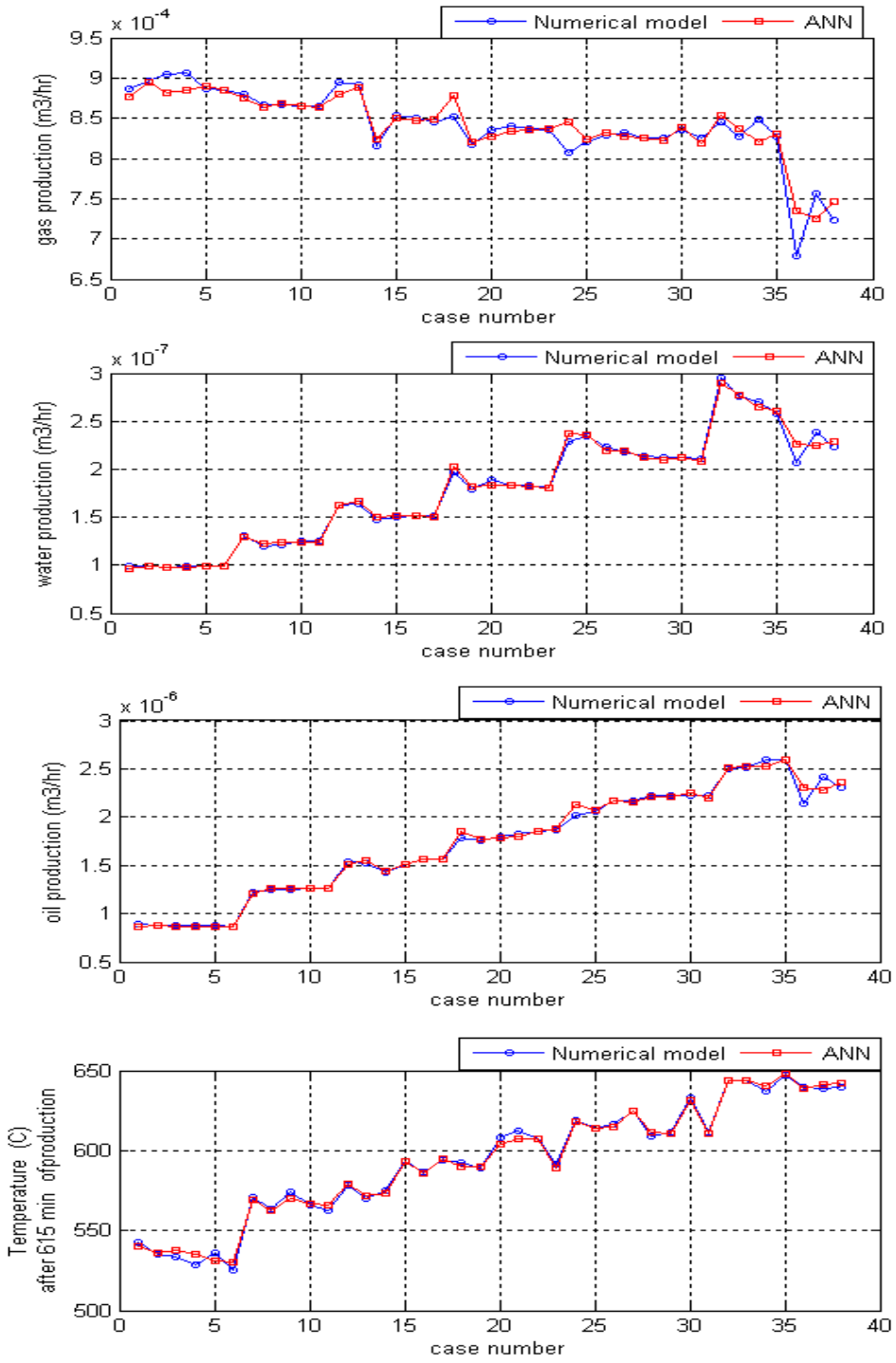

Figure 15: Comparison of results from numerical model and ANN for variable initial conditions-I

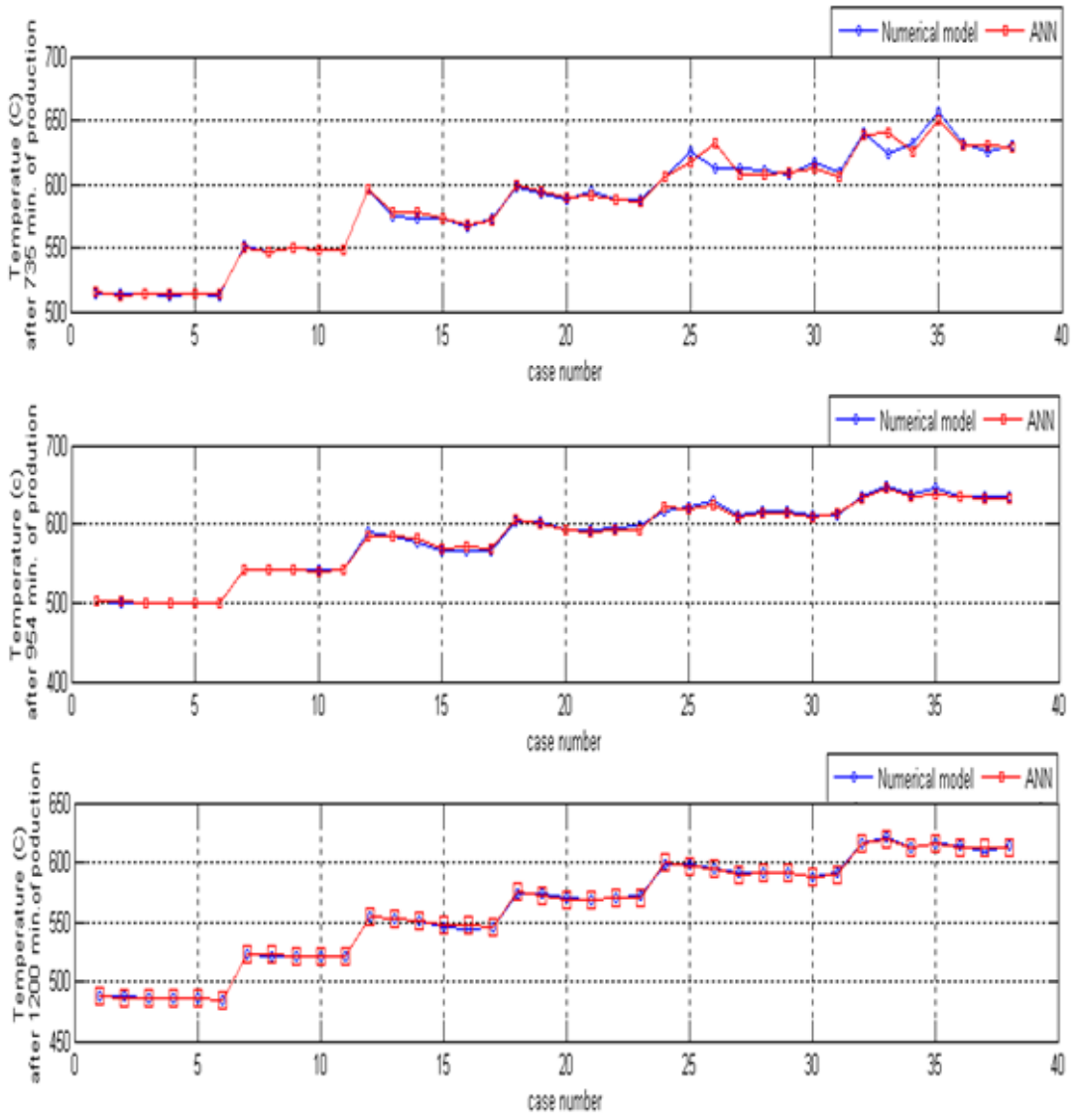

Figure 16: Comparison of results from numerical model and ANN for variable initial conditions-II

5.3 Discussion of results for variable reservoir conditions model

As it can be seen from the results shown in Figures 15 and 16, a good match of results from numerical model is predicted by ANN; except for the gas production rate. A very good match of gas production is observed for the initial cases as ANN does not see a significant change in the gas prediction. For the last three cases, ANN was not able to comprehend a sudden change in the gas production by the numerical model. A similar pattern is observed in water and oil production rates but the errors in the later cases are less than the error observed with the predictions in gas production. These predictions could not be improved further by either increasing number of neurons, number of layers or both.

5.4 Results from variable tube dimension model

This model is developed for variable combustion tube dimension ranging from 0.25m-1.83m in length. The architecture of the model is represented by Figure 12 and the variable range is given by Table 7. Sample runs were carried out for this model before coming up with the structure of the ANN. Figure 17 makes a comparison between the values obtained from the numerical reservoir model and the values obtained from ANN developed for this model for oil production rates and gas production rates. Figure 18 makes the same comparison between water production rates and peak temperature of the combustion front at 25% of the production time. In this model, production time has been normalized for different tube lengths as the total production time is different for different combustion tubes. Figure 19 shows the comparison made between actual peak temperatures and the one obtained from ANN for 50% and 100% of the production times.

Whereas, Figure 20 and Figure 21 shows the comparison between the peak temperatures at 75% of the production time and distance covered by the combustion front at 25%, 50%, 75% and 100% of the production times. The comparison is made for 154 cases selected for testing the performance of the network. These cases were isolated from the training set for ANN. Once the network was trained then the testing set was used to check the performance of the network. The results show a good match between the values predicted by the network as prediction curve closely follows the curve representing the numerical model.

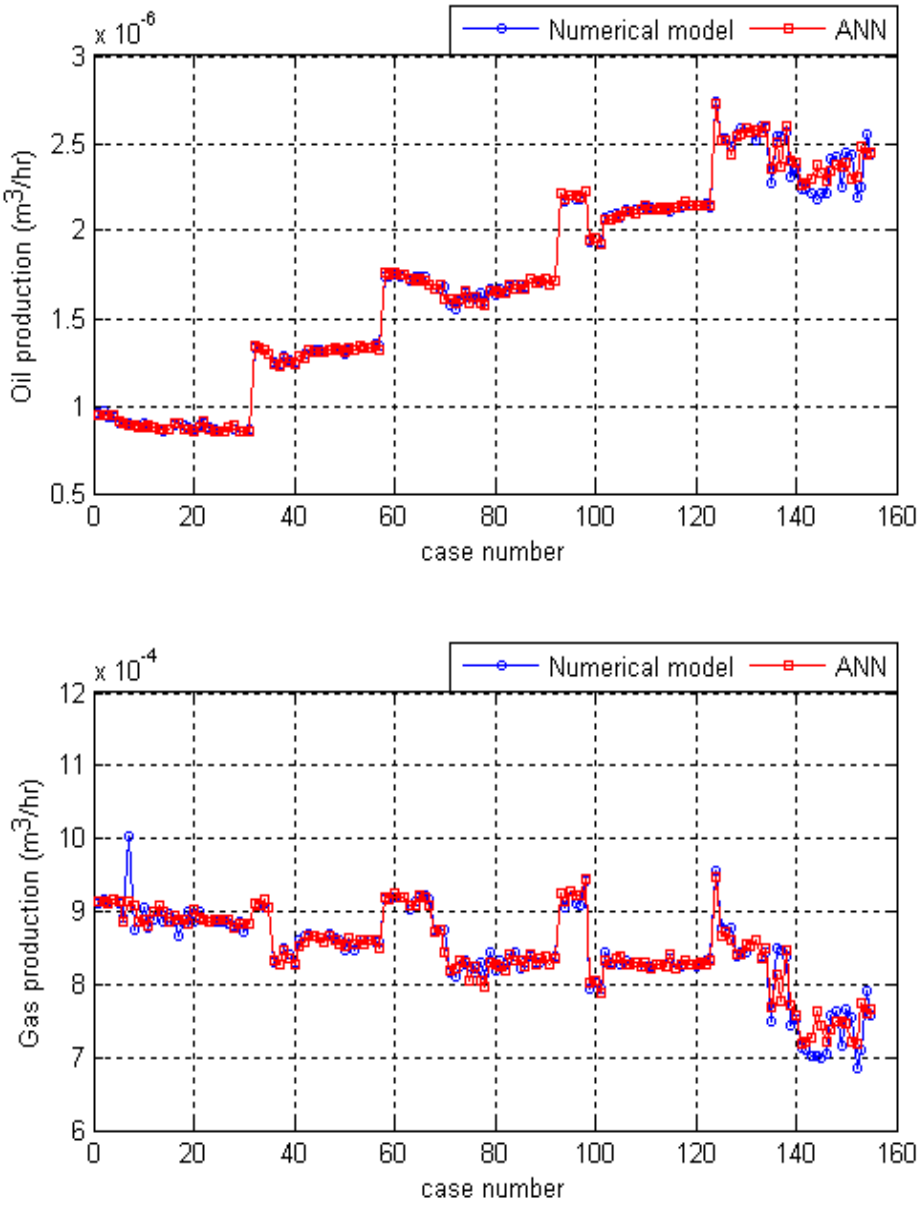

Figure 17: Comparison of results from numerical model and ANN for variable tube dimension model-I

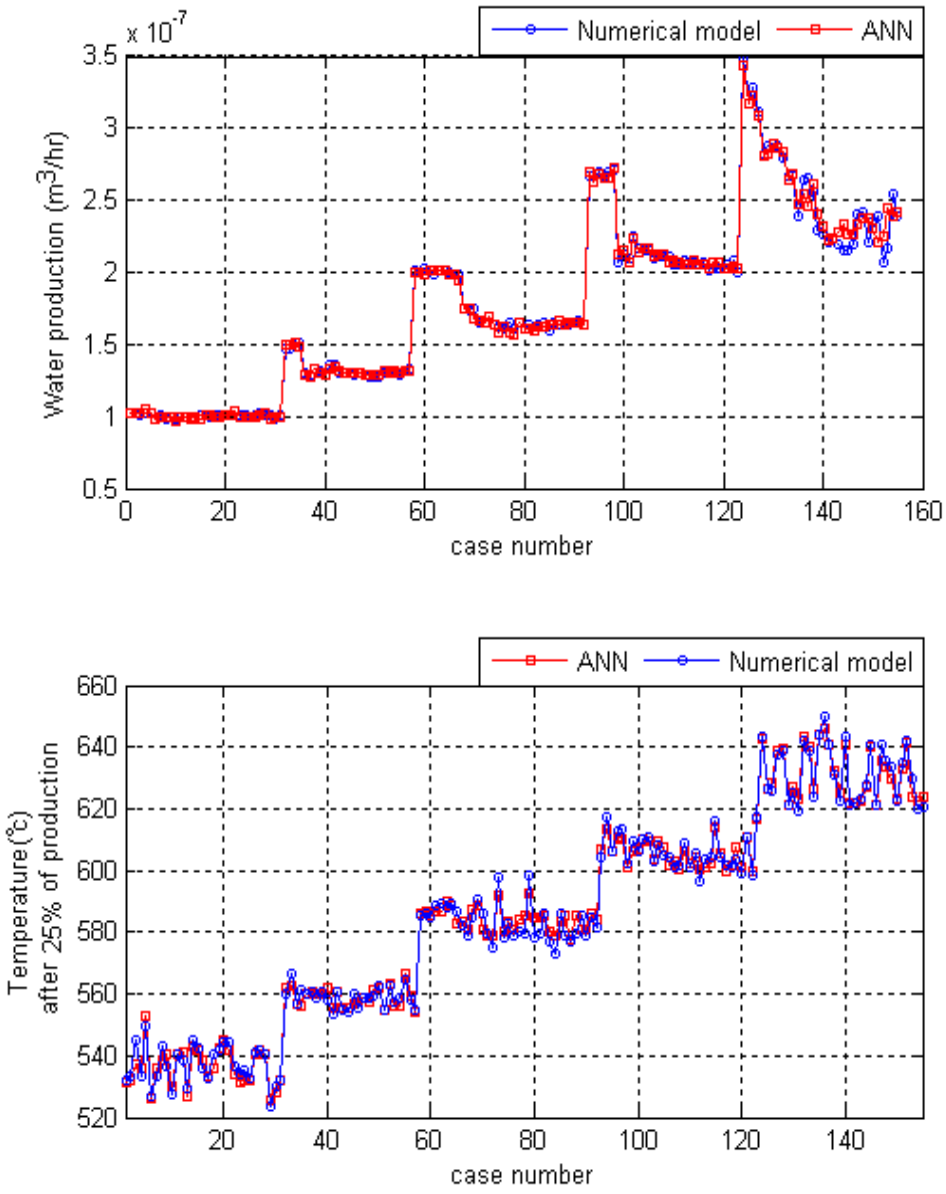

Figure 18: Comparison of results from numerical model and ANN for variable tube dimension model-II

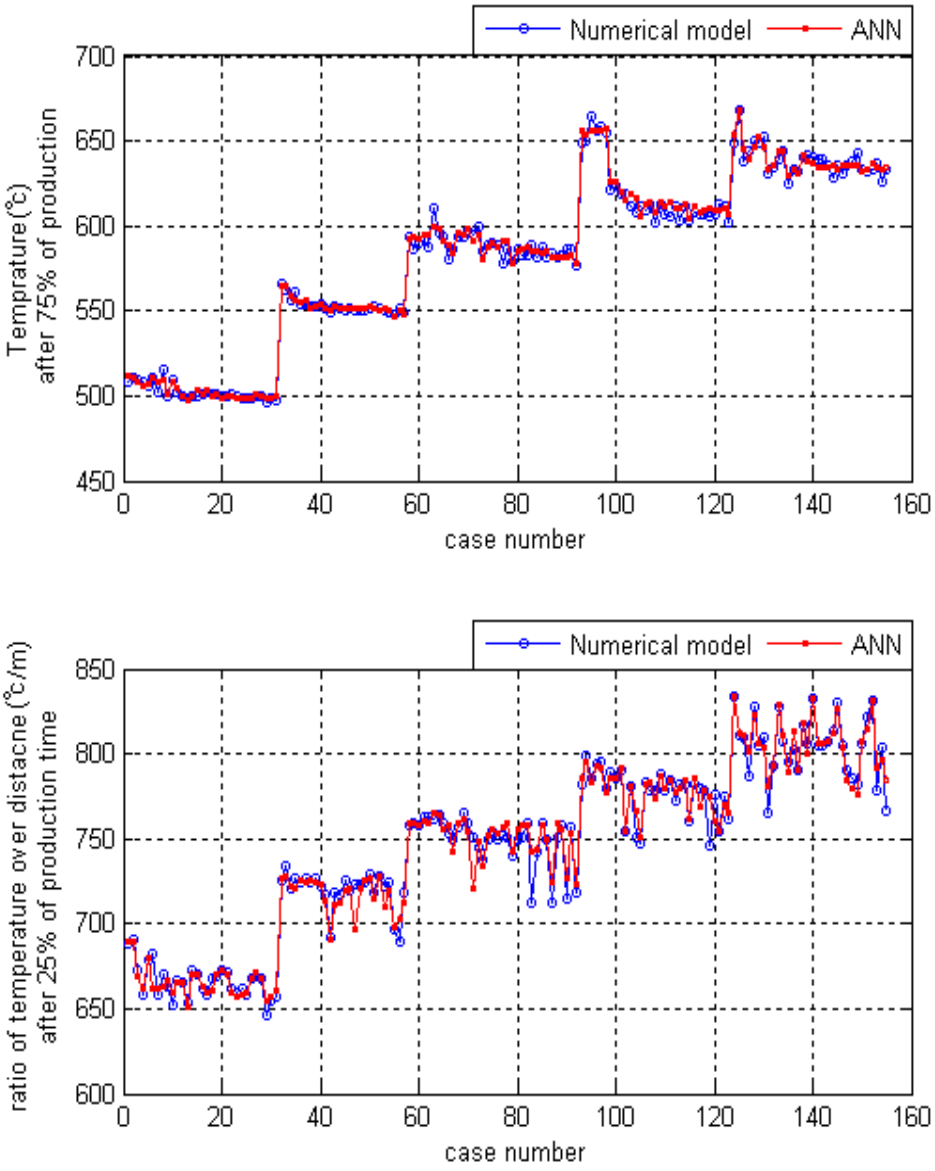

Figure 19: Comparison of results from numerical model and ANN for variable tube dimension model-III

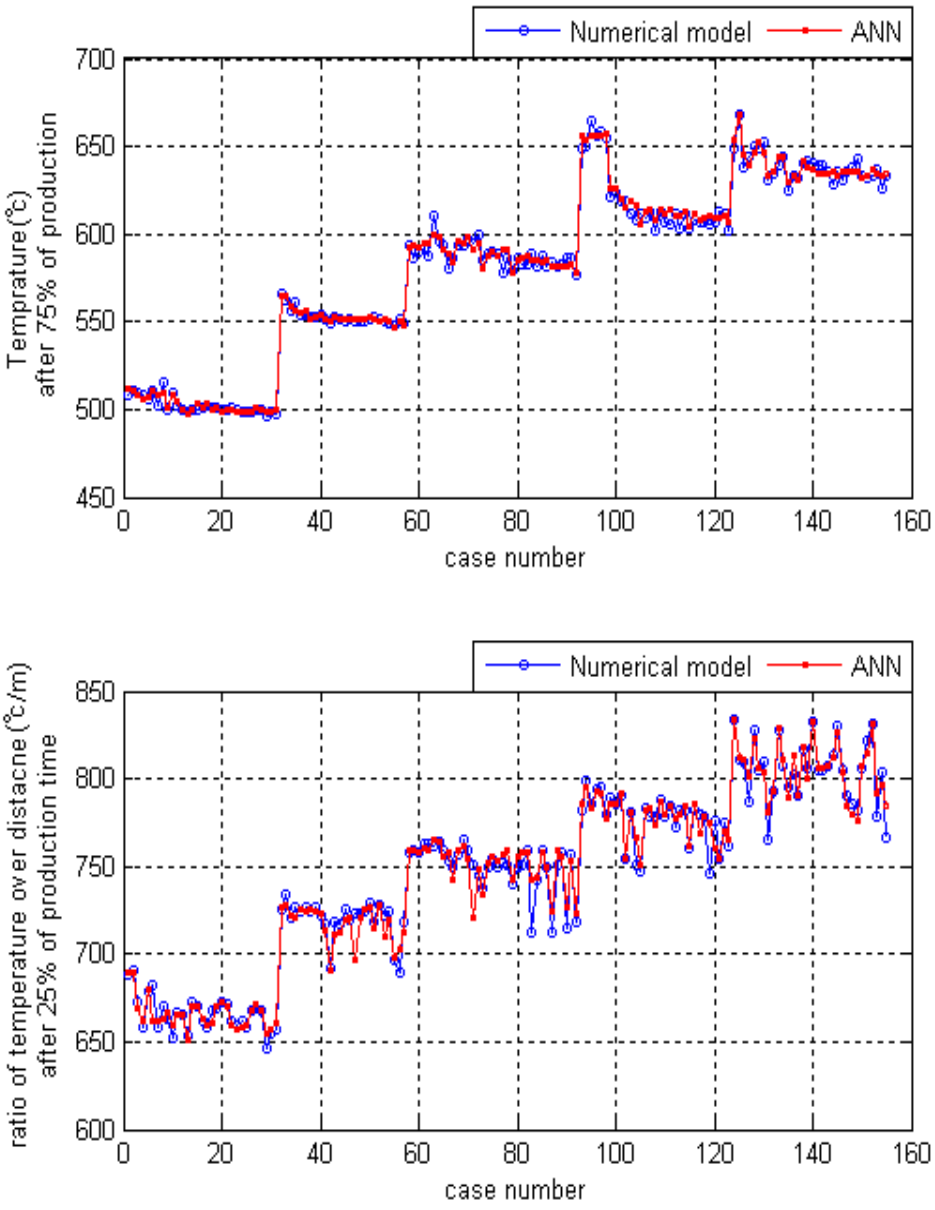

Figure 20: Comparison of results from numerical model and ANN for variable tube dimension model-IV

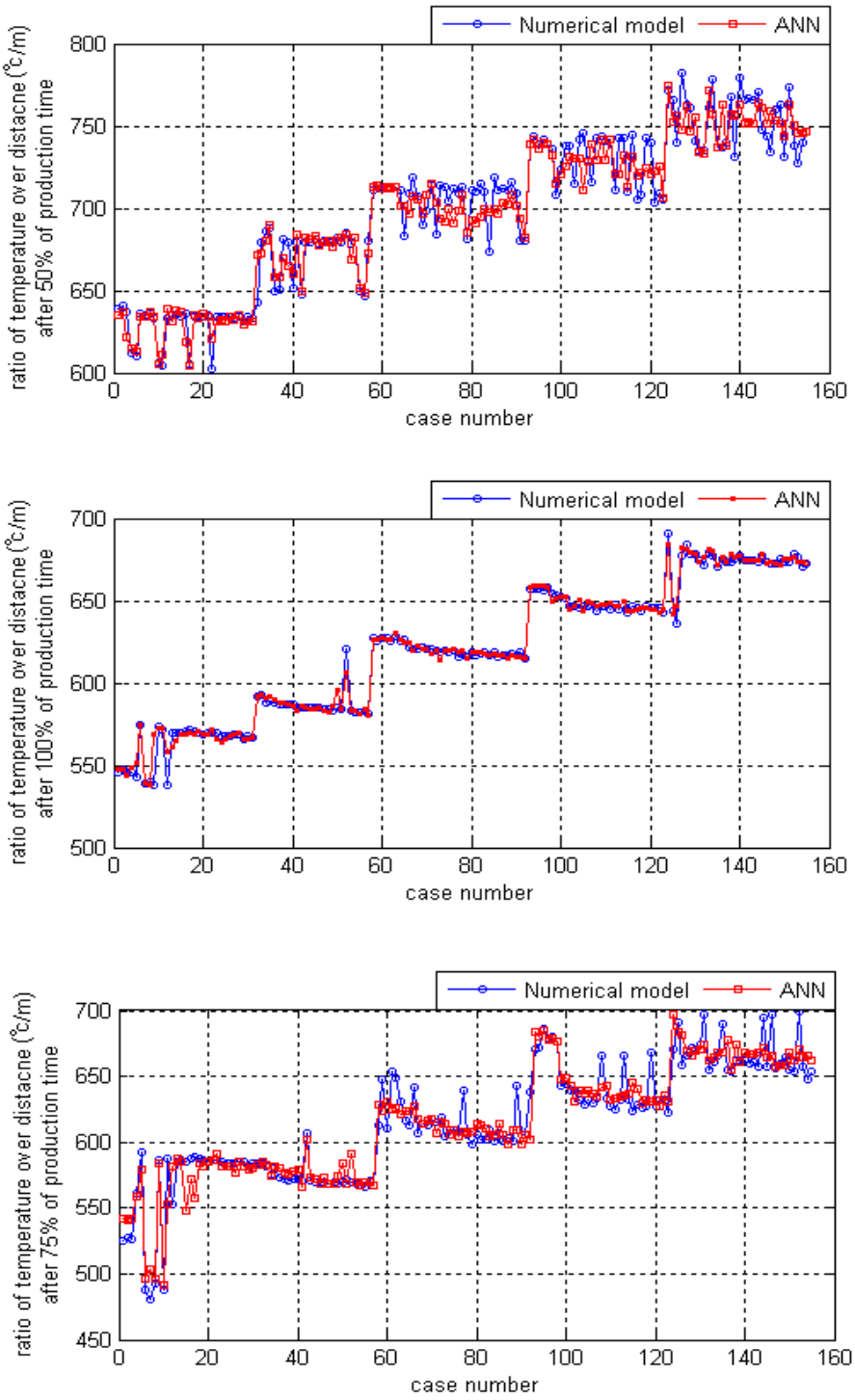

Figure 21: Comparison of results from numerical model and ANN for variable tube dimension model-IV

5.5 Discussion of results for variable tube dimension model

The results presented in the section are promising as a good match is observed between the results predicted by ANN and the results from the numerical model. In these results there is a slight off-set from the results by the numerical model for gas prediction. Initially, in the development of this model, distance covered by the combustion front could not be predicted accurately by the network. Therefore, a functional link (ratio of temperature over distance) was setup to predict the values. As, it can be seen that the results for the functional link for 50% and 75% of the production times could not be predicted as effectively for case numbers[§§] 60-180 as they are predicted for case numbers 1-59. The reason for these off-sets includes the oscillatory nature of the results obtained by the numerical model. The results predicted by numerical model are changing significantly for each of the case number presented in the figures for 50% and 75% of the production times. These errors could not be lowered further by changing the numbers of neuron or by number of hidden layers in the ANN architecture.

5.6 Results from dry combustion tube model

This model predicts the process for dry combustion In-situ process in a single tube dimension and for Athabasca crude oil. The architecture of the model is represented by Figure 13 and the variable range is given by Table 8. Sample runs were carried out for this model before coming up with the final structure of the ANN. Figures 22-23 make a

[§§] Case numbers represents a set of conditions for the combustion tube which includes system properties and operating conditions. One case number represents a unique combination of these properties in the data set.

comparison between the values obtained from the numerical reservoir model and the values obtained from ANN developed for this model for cumulative oil production, cumulative water production and cumulative gas production at the end of the simulation. Figures 23-25 make a comparison between peak temperatures of the combustion front obtained from the numerical model with the peak temperatures of the combustion front obtained from ANN at 25%, 50%, 75% and 100% of the production time. Figures 25-27 make a comparison between distance traveled by the combustion front obtained from the numerical model with the distance traveled by the combustion front obtained from ANN at 25%, 50%, 75% and 100% of the production time. Figures 27-28 make a comparison between velocity of the combustion front obtained from the numerical model with the velocity of the combustion front obtained from ANN at 25%, 50%, 75% and 100% of the total production time. Figure 29 shows the variation of peak temperature with saturation of oil. In this figure, values obtained from ANN at various production times are also compared with the values obtained from the numerical model at the respective times. Figures 30-32 show the cross plots of cumulative oil production, cumulative water production, cumulative gas production, peak temperatures, distance covered by the combustion fronts and velocity of the combustion fronts at 25%, 50%, 75% and 100% of the total production time. In this model, production time has been normalized for each case as the total production time differs for each combination of combustion tube properties and the operating conditions imposed on the combustion tube. The comparison is made for 55 cases selected for testing the performance of the network. These cases were isolated from the training set for ANN. Once the network was trained then the testing set was used to check the performance of the network. The results show a good

match between the values predicted by the network as prediction curve closely follows the curve representing the numerical model.

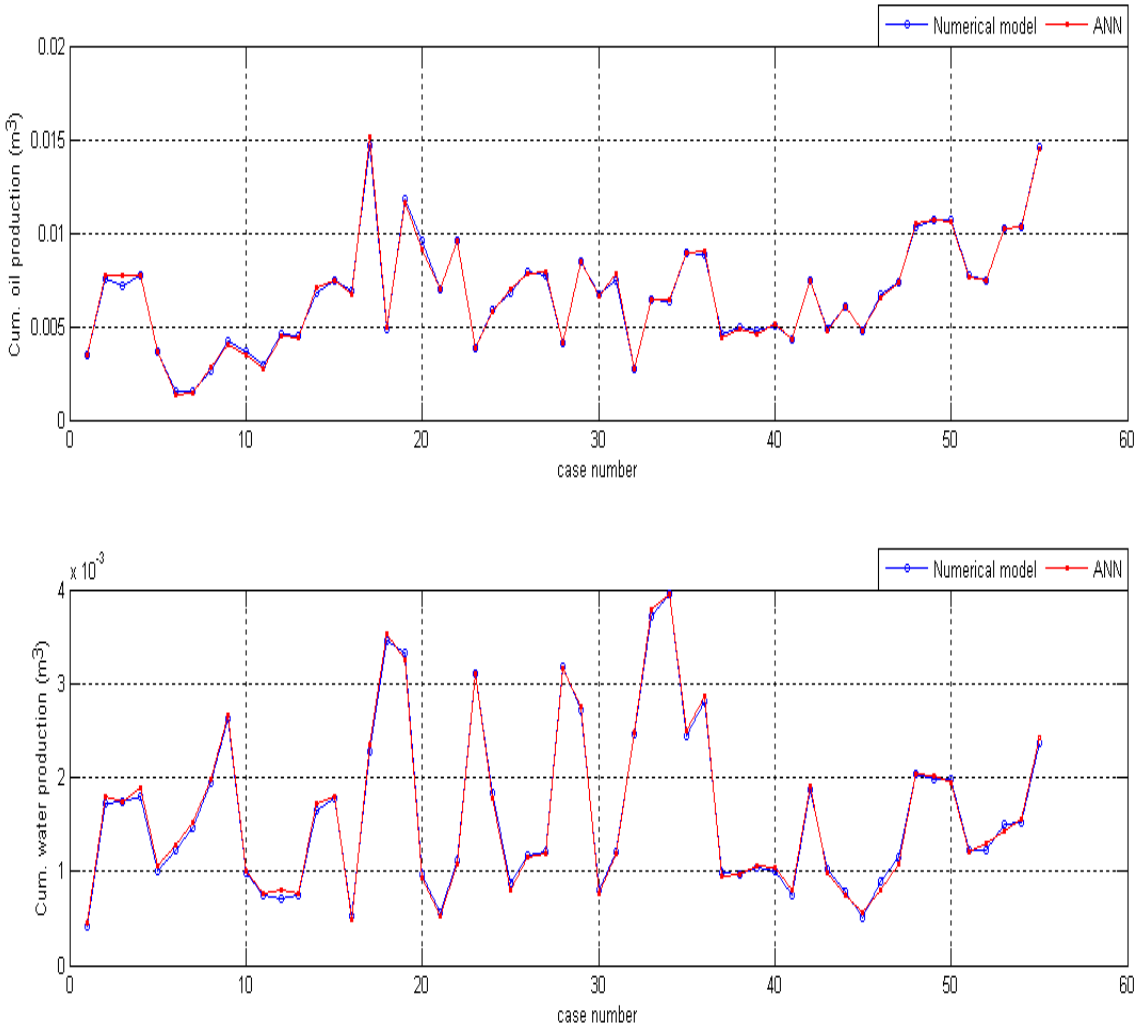

Figure 22: Comparison of results from numerical model and ANN for dry combustion tube model-I

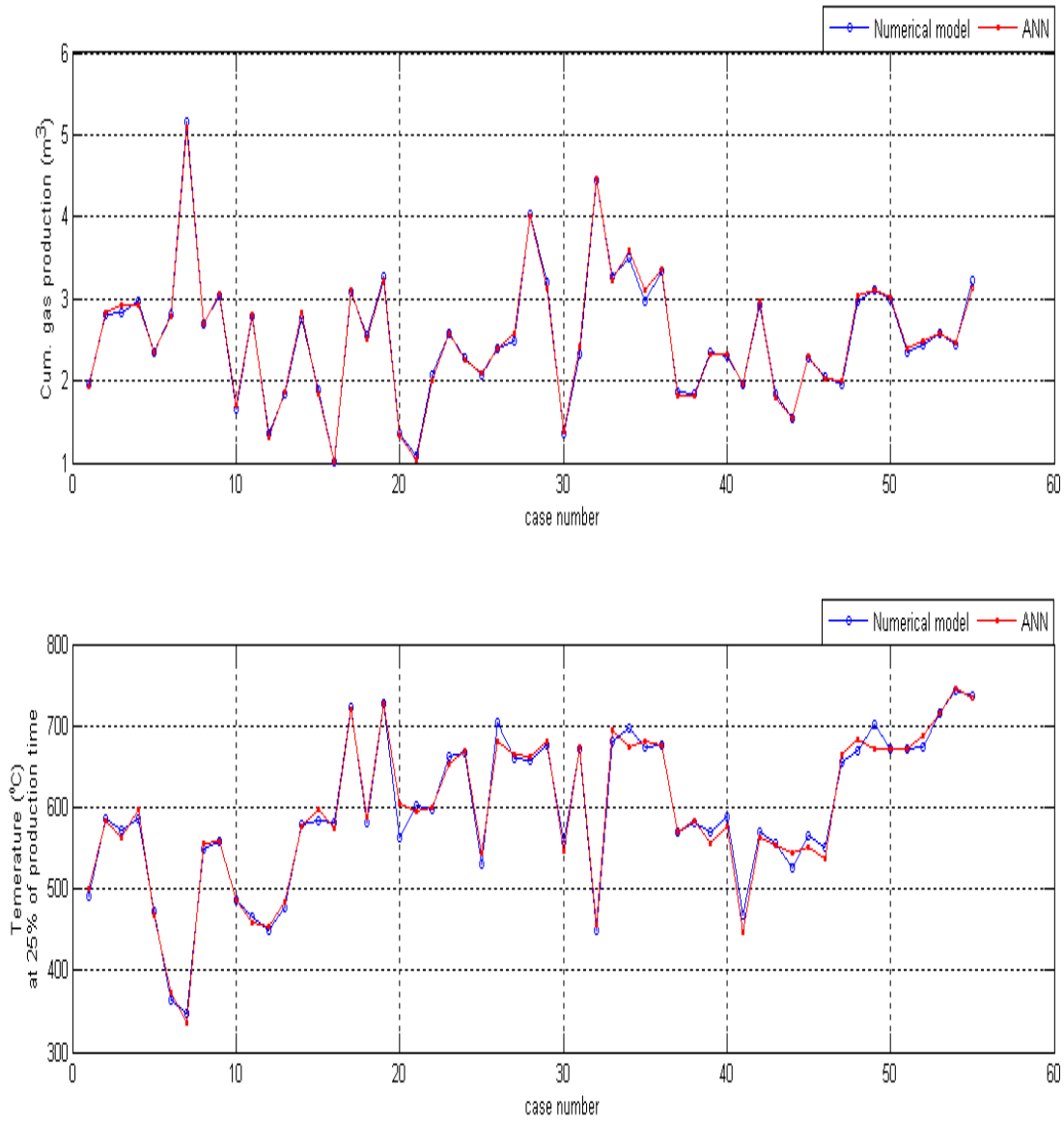

Figure 23: Comparison of results from numerical model and ANN for dry combustion tube model-II

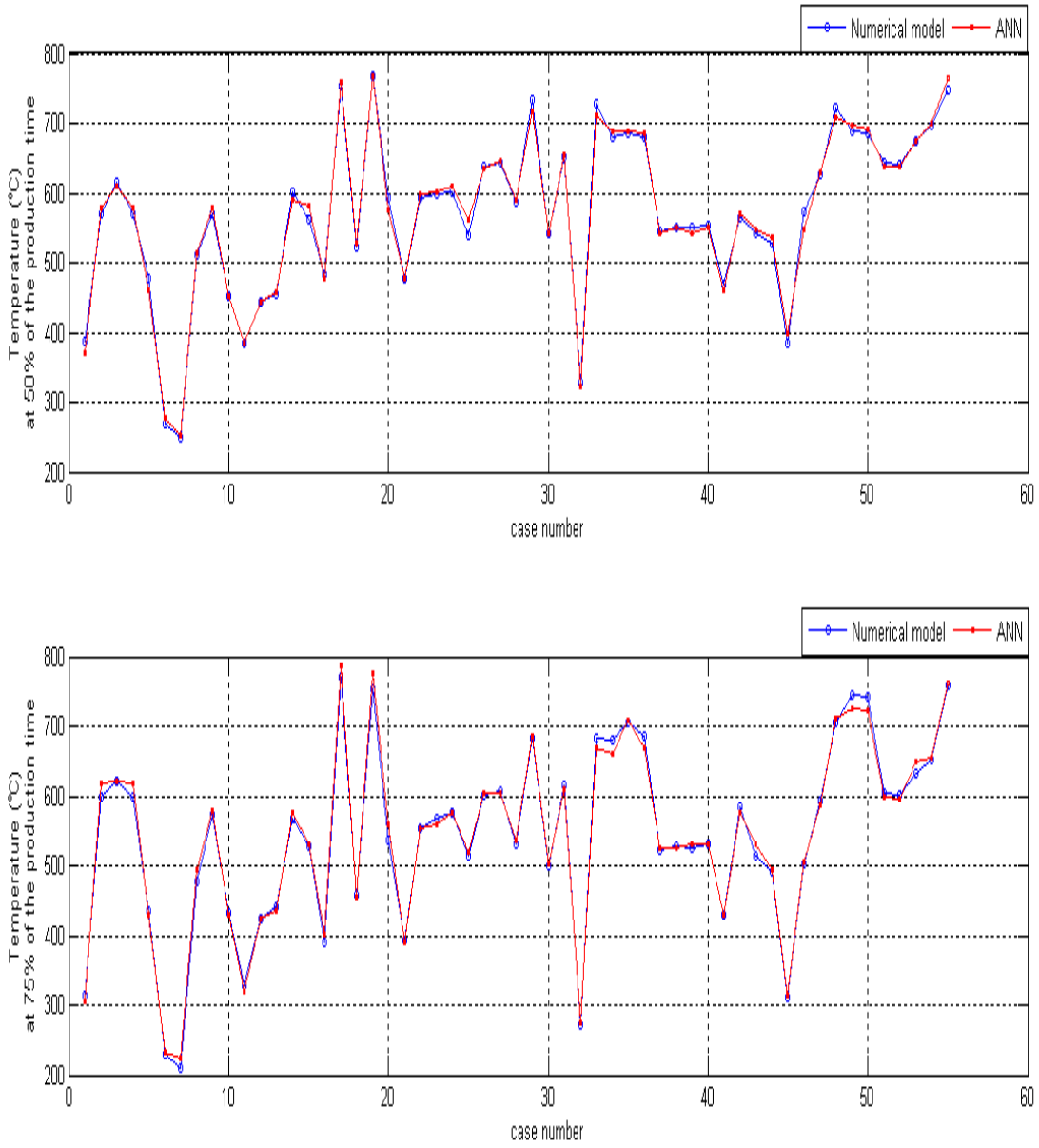

Figure 24: Comparison of results from numerical model and ANN for dry combustion tube model-III

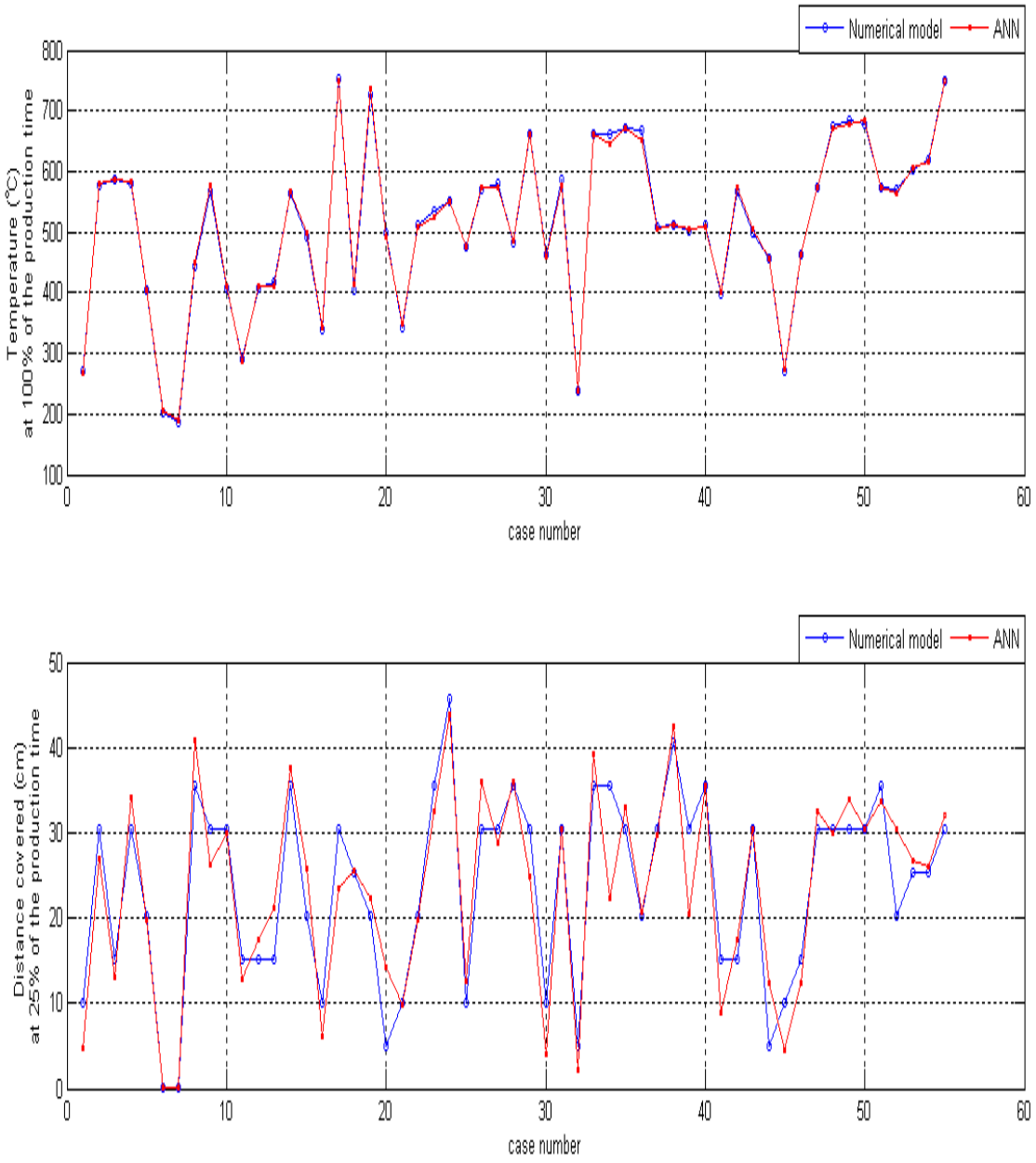

Figure 25: Comparison of results from numerical model and ANN for dry combustion tube model-IV

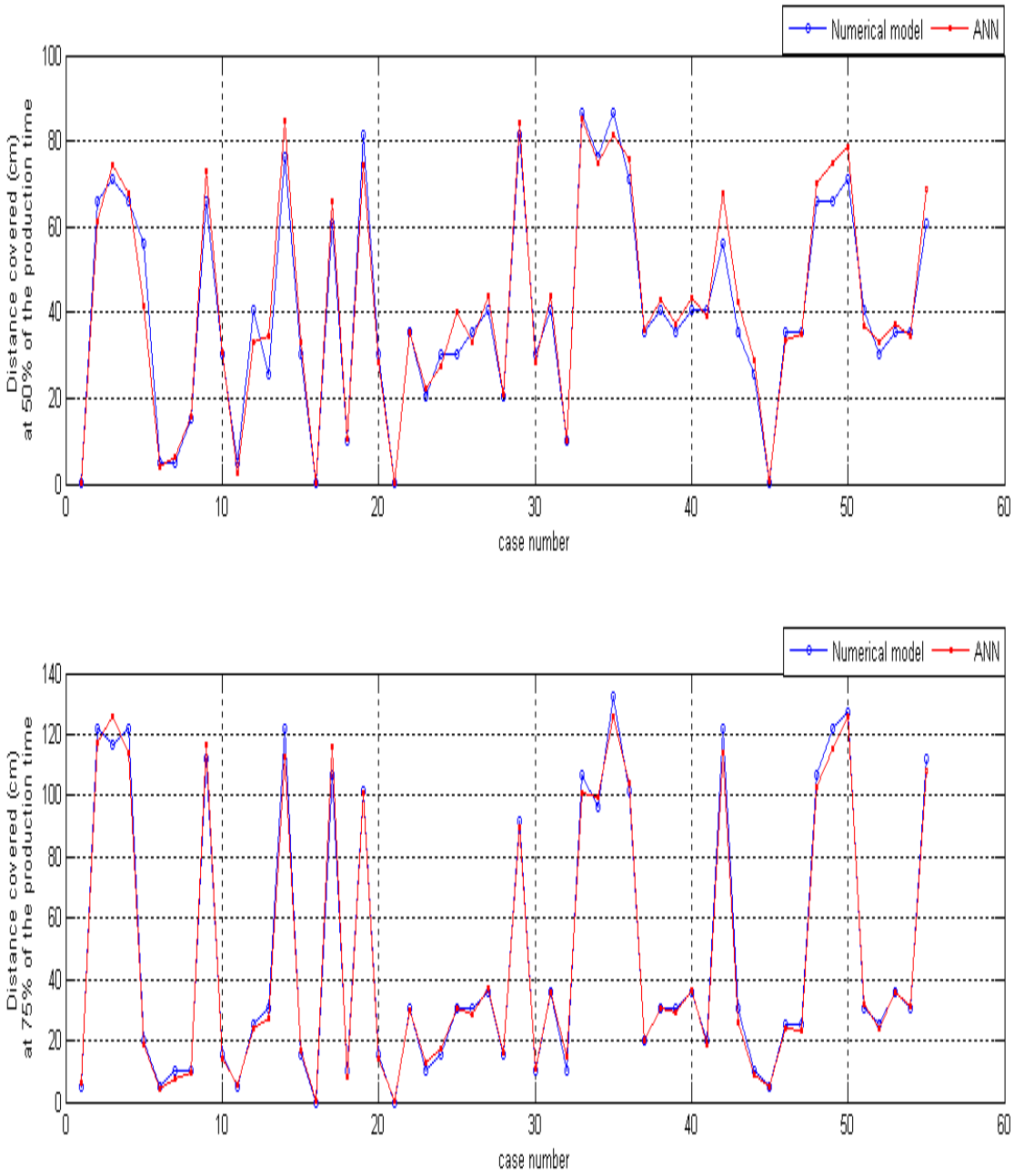

Figure 26: Comparison of results from numerical model and ANN for dry combustion tube model-V

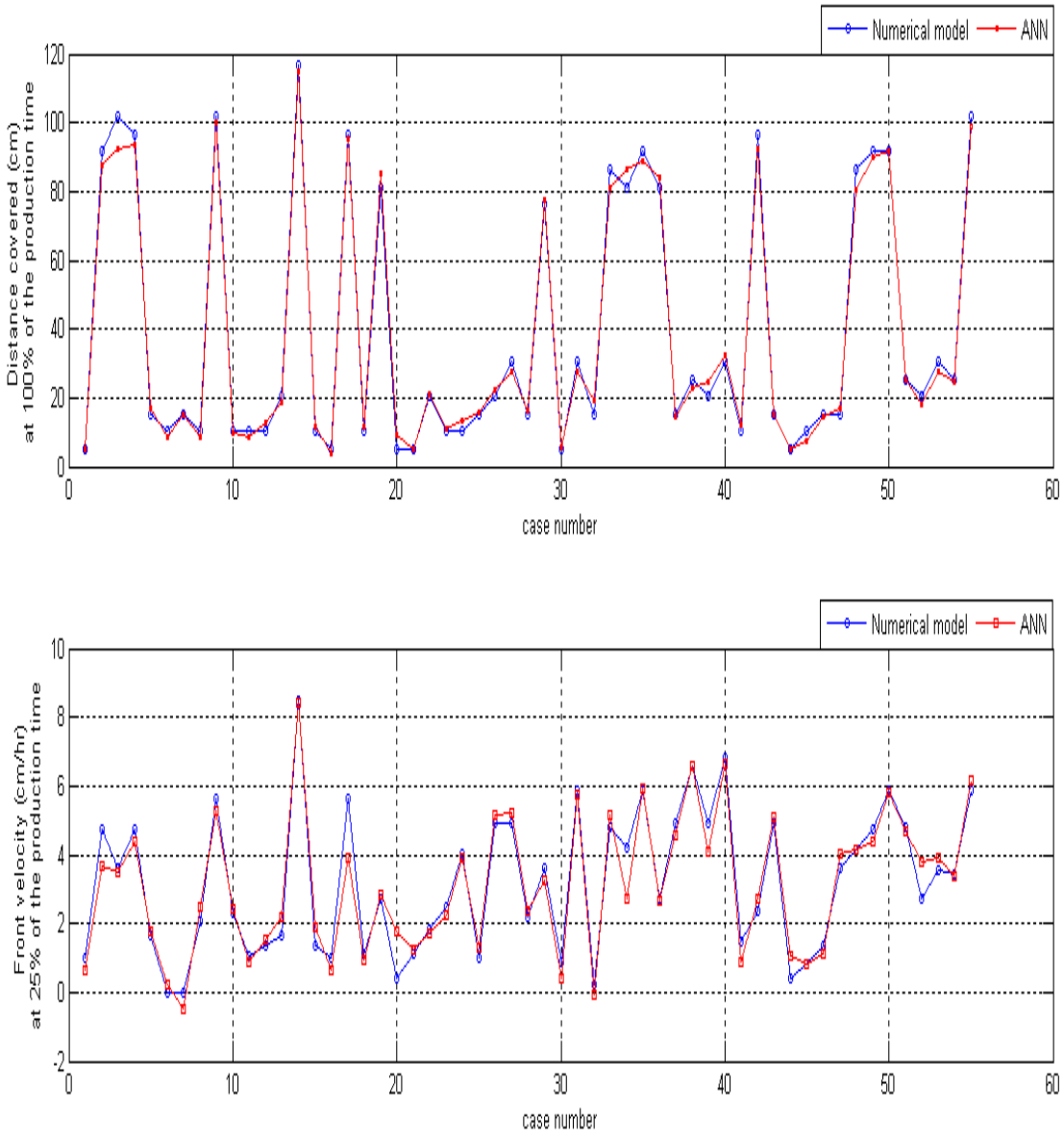

Figure 27: Comparison of results from numerical model and ANN for dry combustion tube model-VI

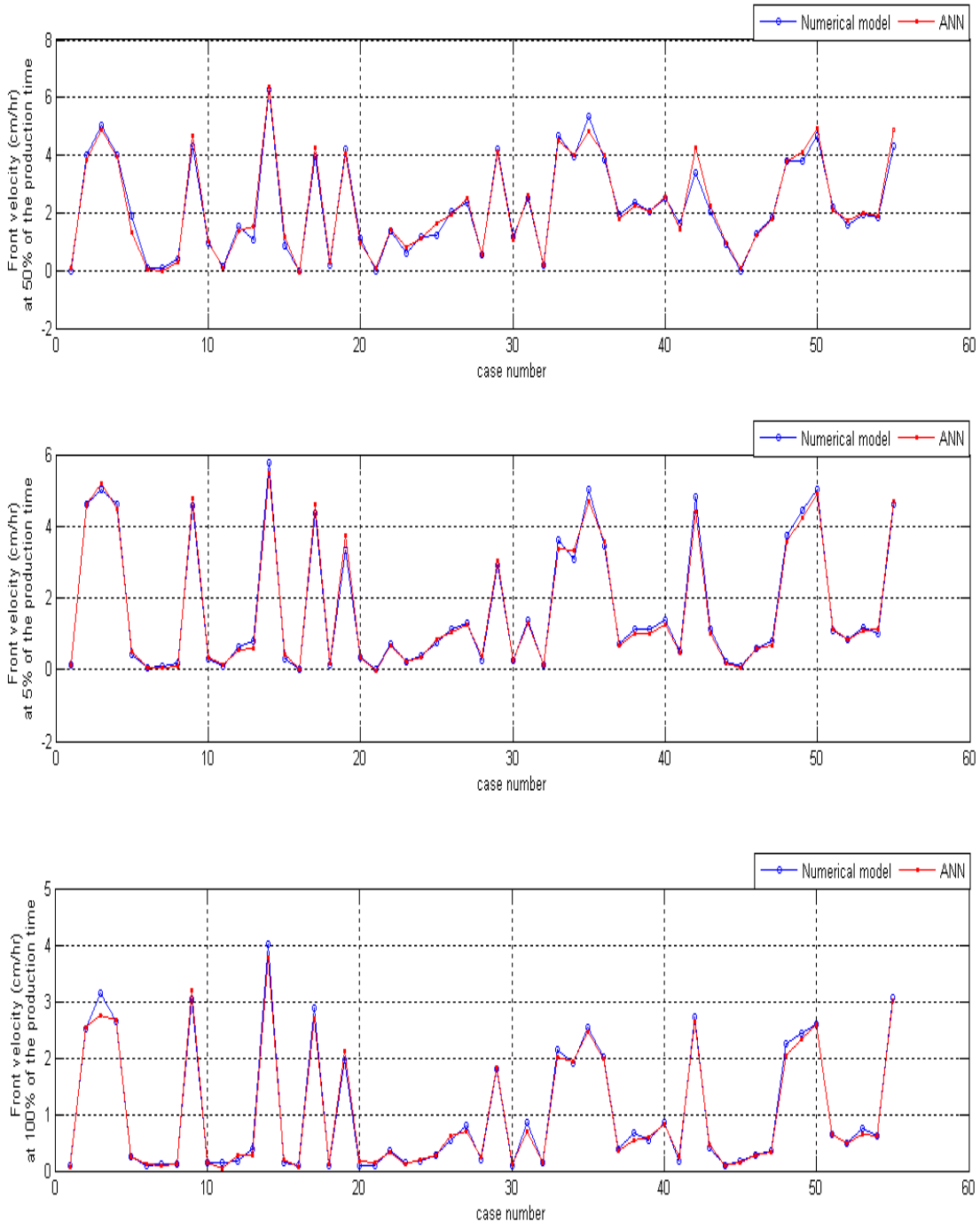

Figure 28: Comparison of results from numerical model and ANN for dry combustion tube model-VII

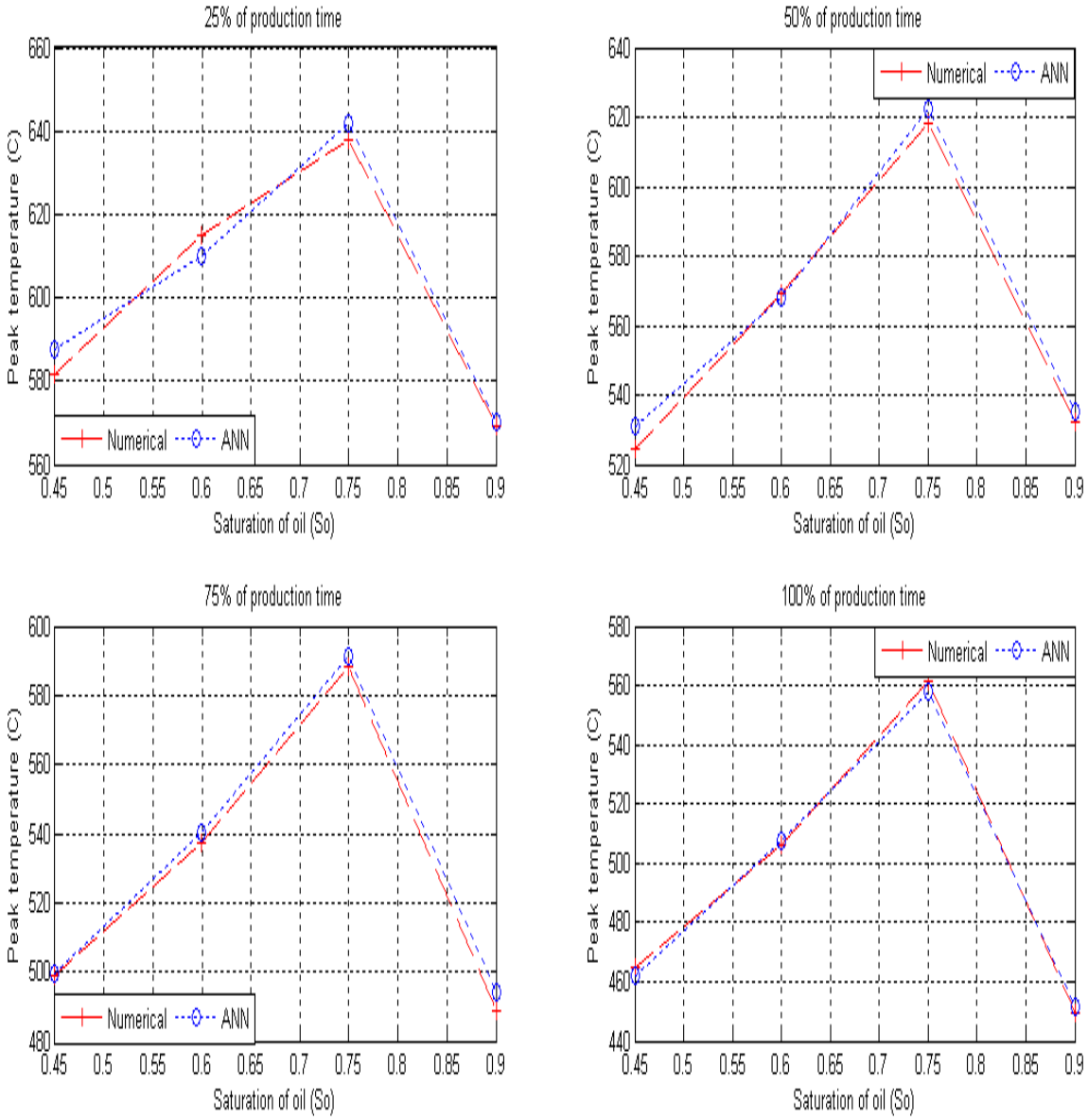

Figure 29: Peak temperature variation with oil saturation at different times in dry combustion

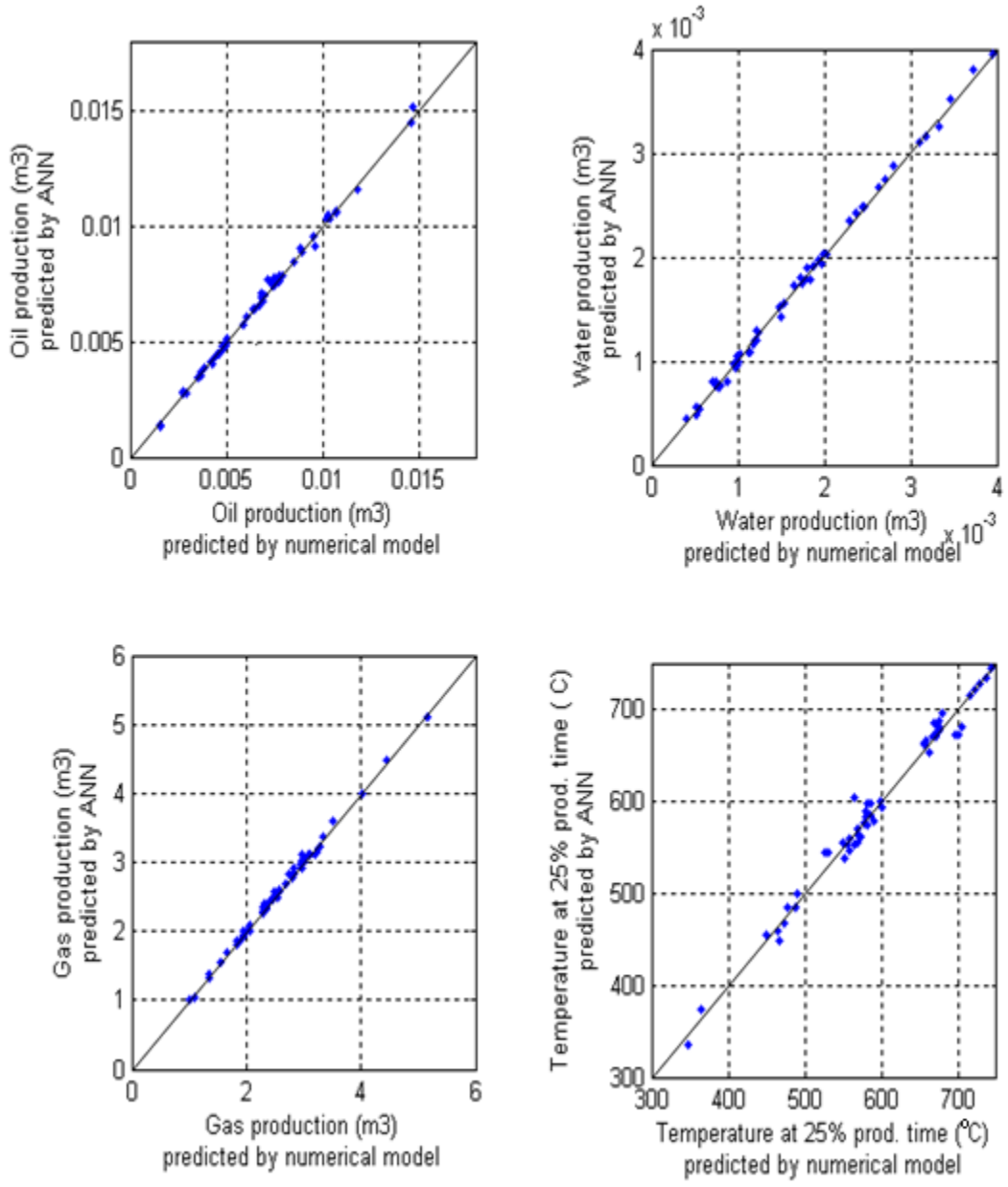

Figure 30: Cross plots of ANN vs numerical model for dry combustion tube model-I

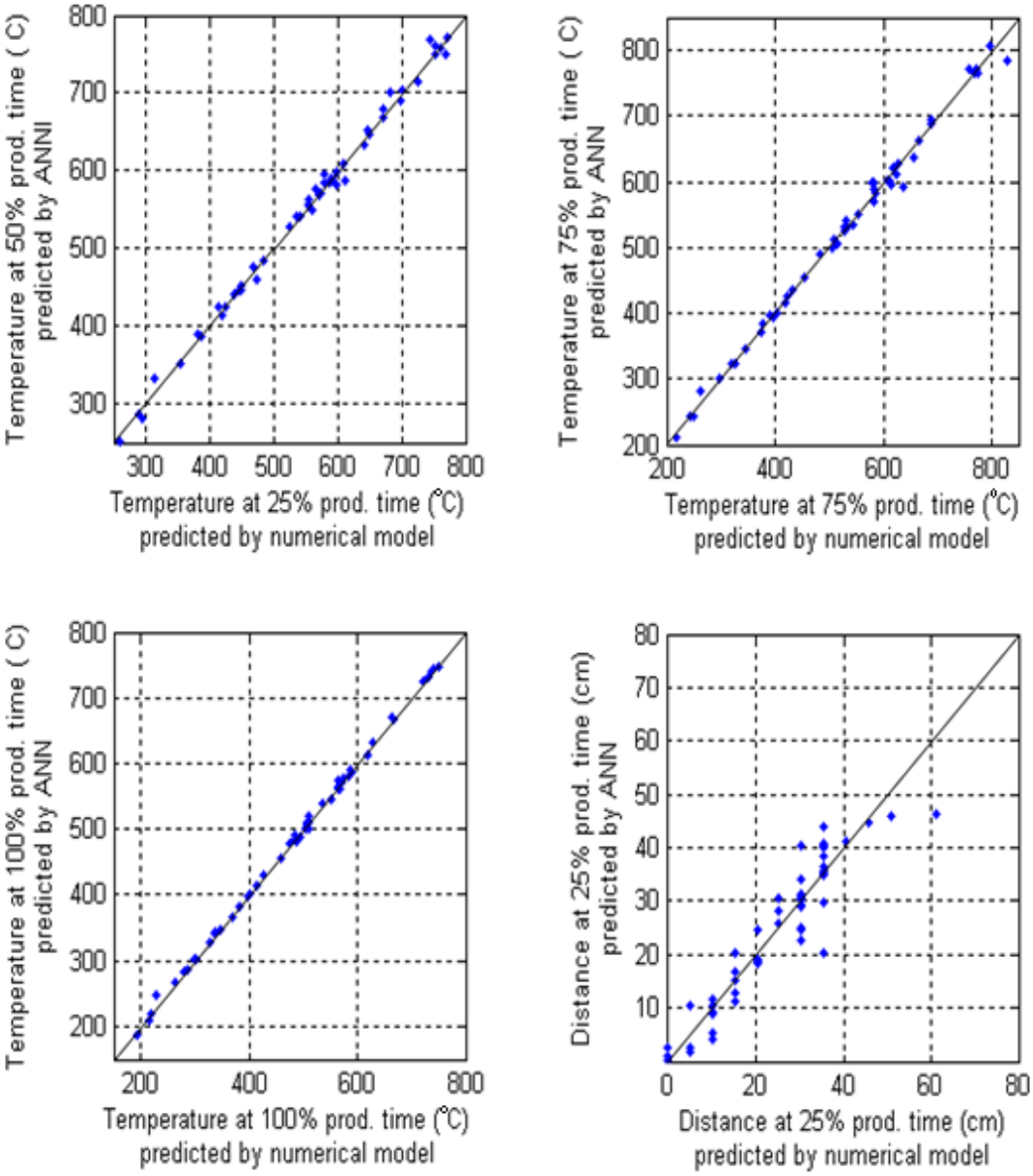

Figure 31: Cross plots of ANN vs numerical model for dry combustion tube model-II

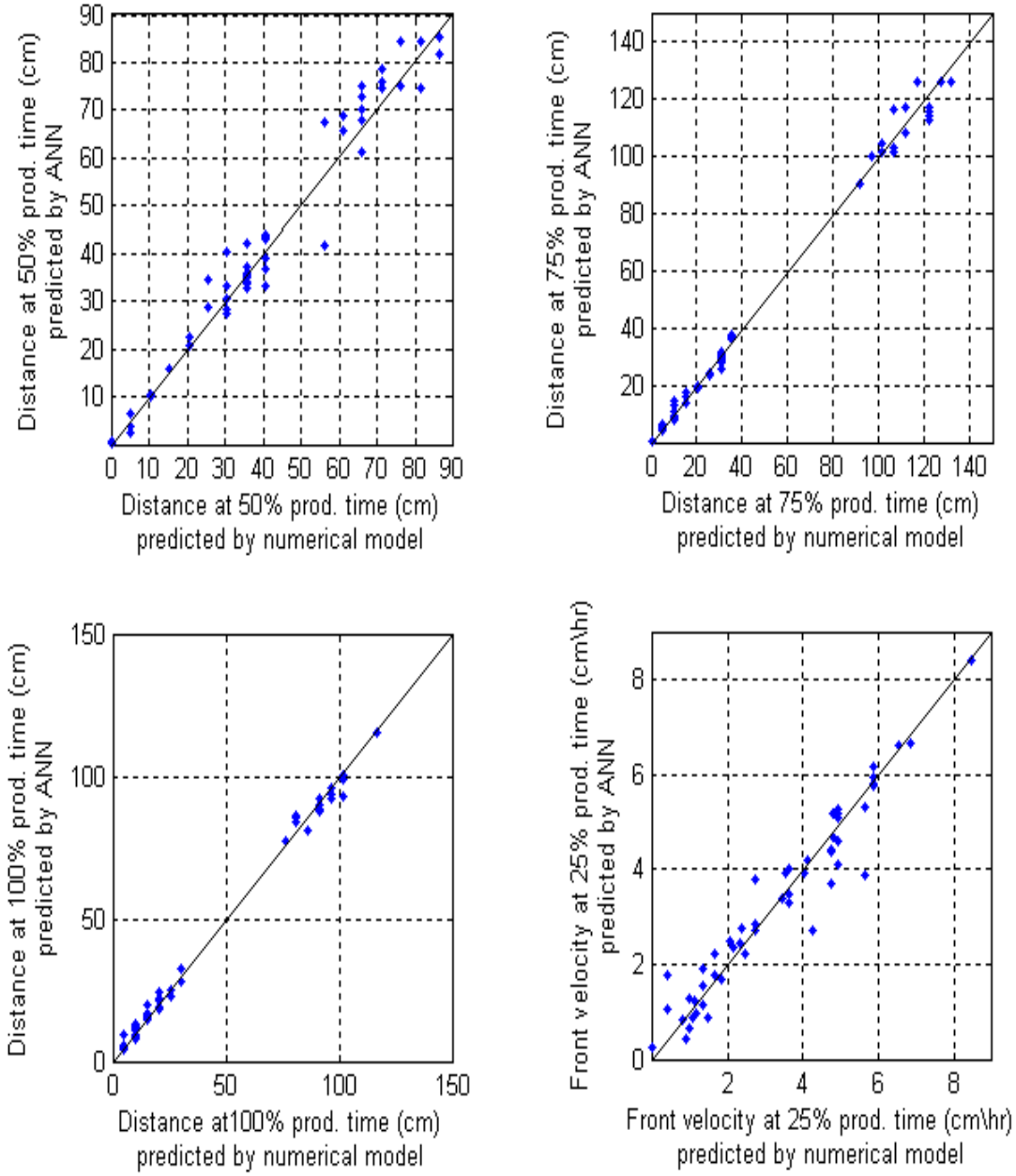

Figure 32: Cross plots of ANN vs numerical model for dry combustion tube model-III

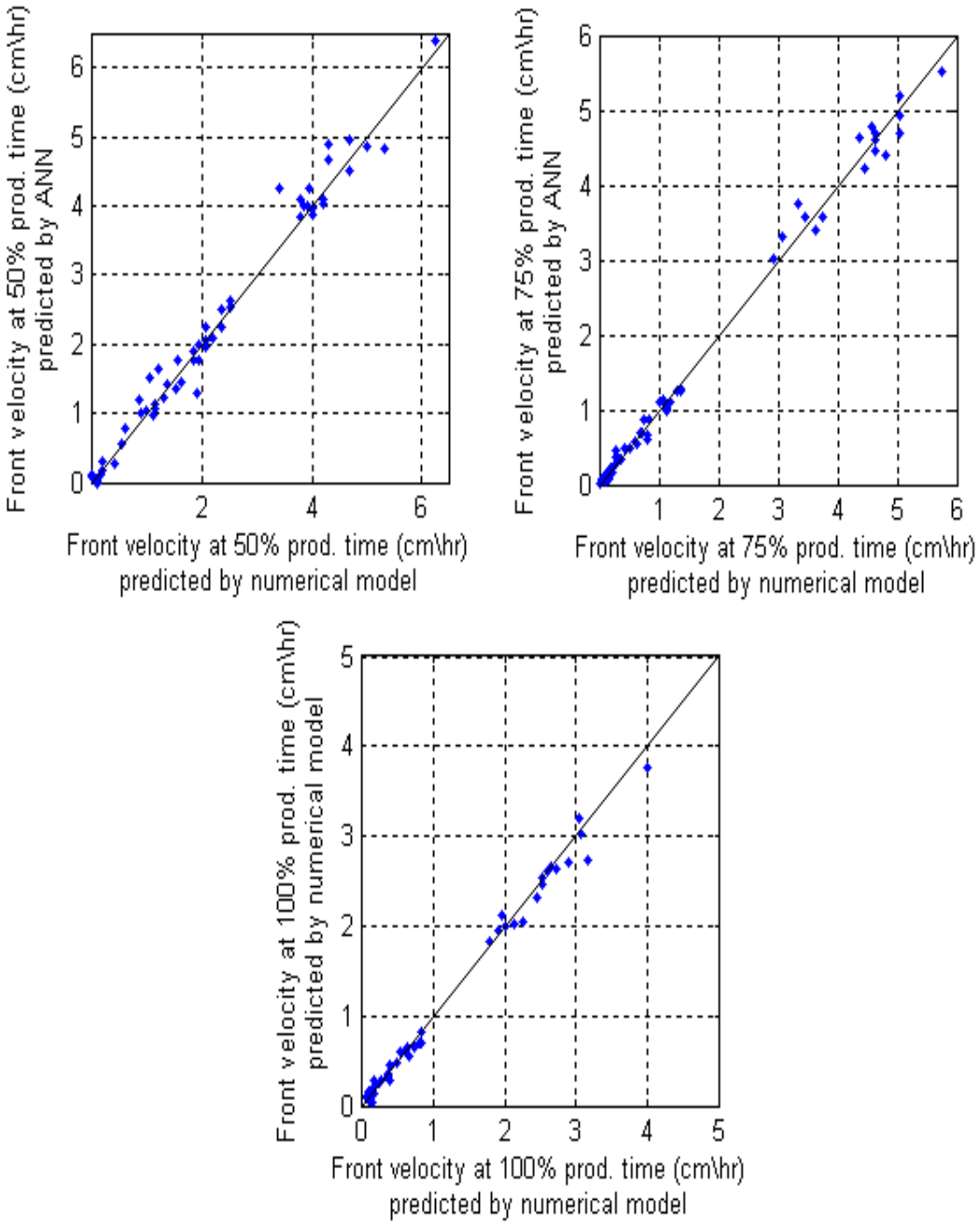

Figure 33: Cross plots of ANN vs numerical model for dry combustion tube model-IV

5.7 Discussion of results for dry combustion tube model

The comparison of results, obtained by neural network and the numerical model, shows promising predictions typically for cumulative oil, water, and gas production. These results also show a good match between the peak temperatures at 25%, 50%, 75%, and 100% of the production times. But the network shows variations in the predictions of distance covered by the combustion front and the velocity of the combustion front typically for 25%, 50%, and 75% of the production times. In the beginning of the in-situ combustion process, the initial part of the combustion tube is heated by external heaters and the combustion zone in the combustion tube is fully developed. For some scenarios developed in the training data set the combustion front moves faster and for some cases it moves a bit slower than the rest of the cases. The combustion front movement typically depends upon saturation of oil, porosity of the rock matrix and, air injection rate. For a slight change in any of the property a significant different result was observed. ANN is not able to comprehend these changes as predicted by numerical model for distance and velocity of the combustion front as effectively as other results like cumulative oil, water, and gas productions, and peak temperatures of the combustion front at 25%, 50%, 75% and 100% of the production times. Different architectures were tested by using different number of layers and neurons but the results could not be improved further.

5.8 Results from wet combustion tube model

This model predicts wet combustion *in-situ* process studied in combustion tube for Athabasca crude oil. The architecture of the model is represented by Figure 14 and the variable range is given by Table 8. Sample runs were carried out for this model before coming up with the final structure of the ANN. Figures 34 and 35 make a comparison between the values obtained from the numerical reservoir model and the values obtained from ANN developed for this model for cumulative oil production, cumulative water production and cumulative gas production at the end of the simulation. Figures 35 through 37 make a comparison between peak temperatures of the combustion front obtained from the numerical model with the peak temperatures of the combustion front obtained from ANN at 25%, 50%, 75% and 100% of the production time. Figures 37 through 39 make a comparison between distance traveled by the combustion front obtained from the numerical model with the distance traveled by the combustion front obtained from ANN at 25%, 50%, 75% and 100% of the production time. Figures 39 through 40 make a comparison between velocity of the combustion front obtained from the numerical model with the velocity of the combustion front obtained from ANN at 25%, 50%, 75% and 100% of the total production time. Figure 41 shows the variation of peak temperature with saturation of oil. In this figure, values obtained from ANN at various production times are also compared with the values obtained from the numerical model at the respective times. Figures 42 through 45 show the cross plots of cumulative oil production, cumulative water production, cumulative gas production, peak temperatures, distance covered by the combustion fronts and velocity of the combustion fronts at 25%, 50%, 75% and 100% of the total production. In this model, production

time has been normalized for each case as the total production time differs for each combination of combustion tube properties and the operating conditions imposed on the combustion tube. The comparison is made for 157 cases selected for testing the performance of the network. These cases were isolated from the training set for ANN. Once the network was trained then the testing set was used to check the performance of the network. The results show a good match between the values predicted by the network as prediction curve closely follows the curve representing the numerical model. Following figures show the results obtained with this model.

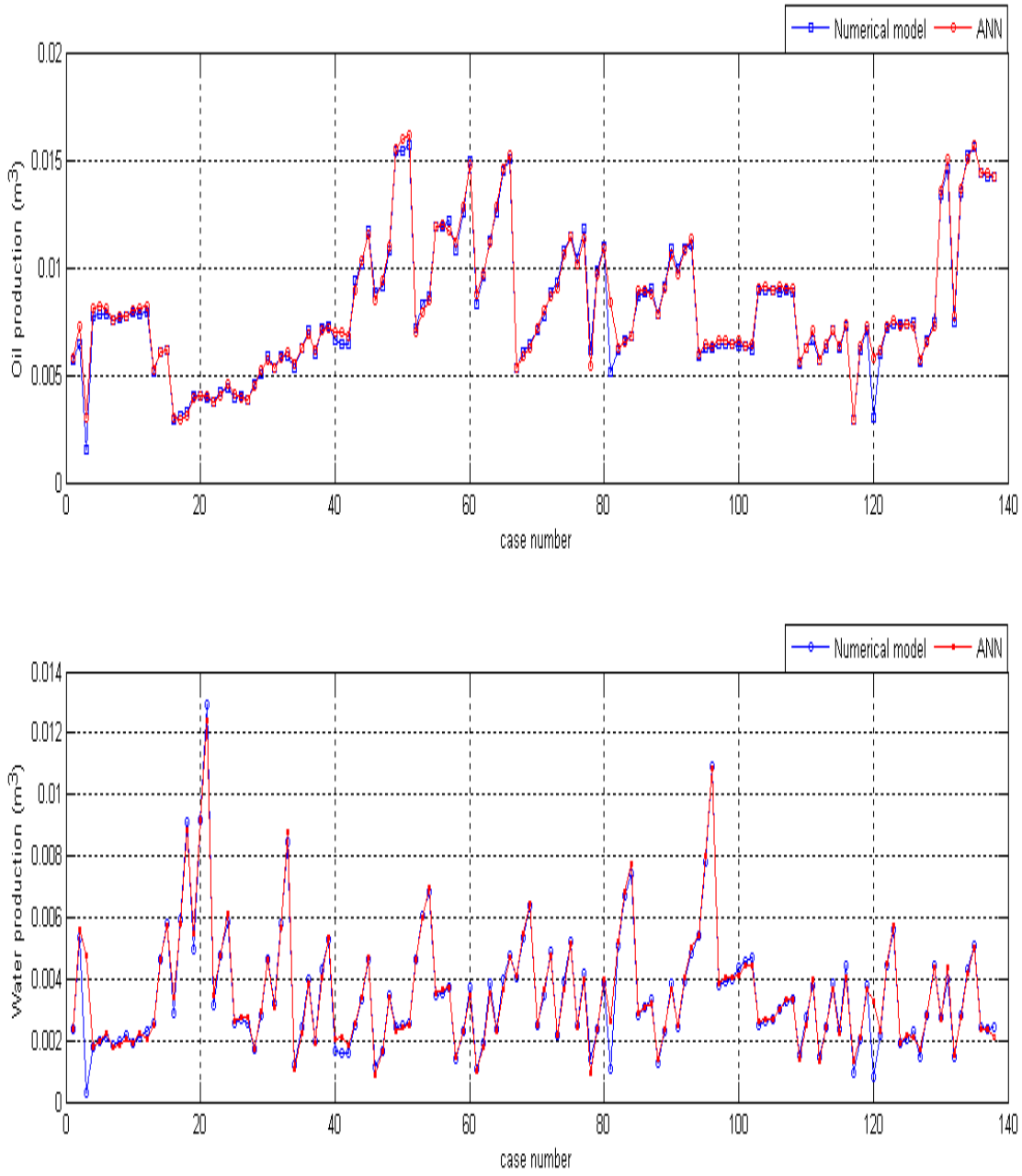

Figure 34: Comparison of results from numerical model and ANN for wet combustion tube model-I

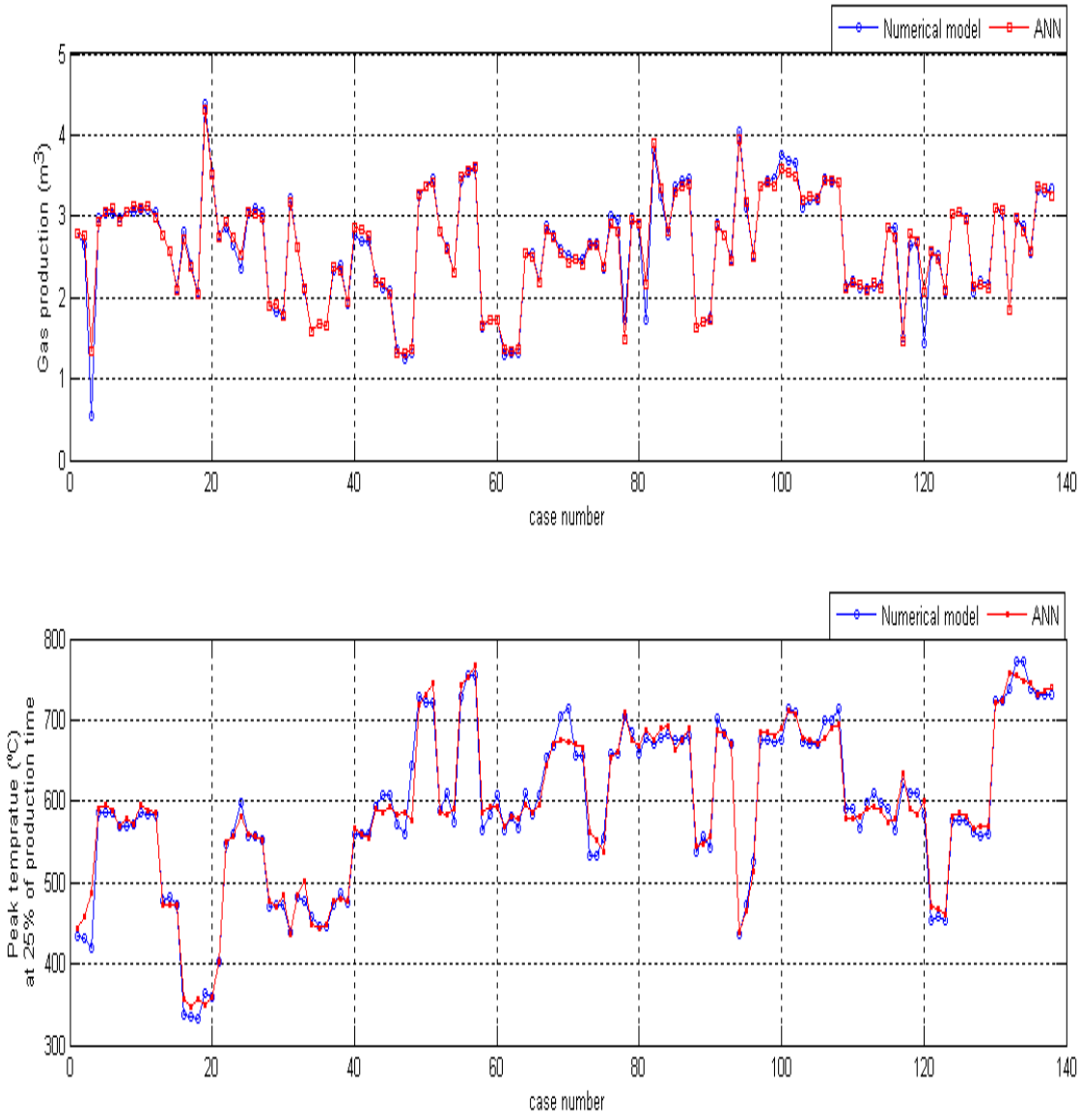

Figure 35: Comparison of results from numerical model and ANN for wet combustion tube model-II

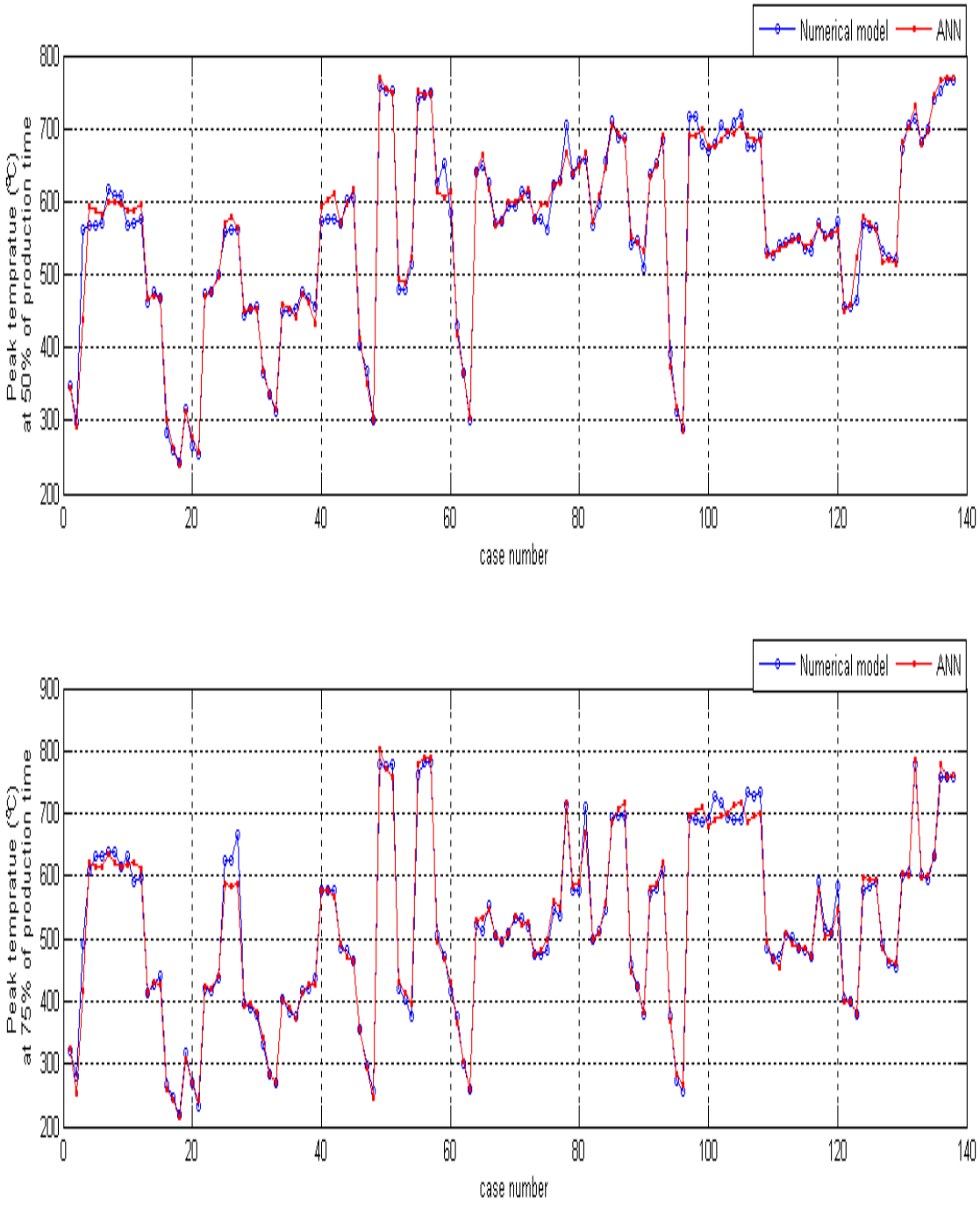

Figure 36: Comparison of results from numerical model and ANN for wet combustion tube model-III

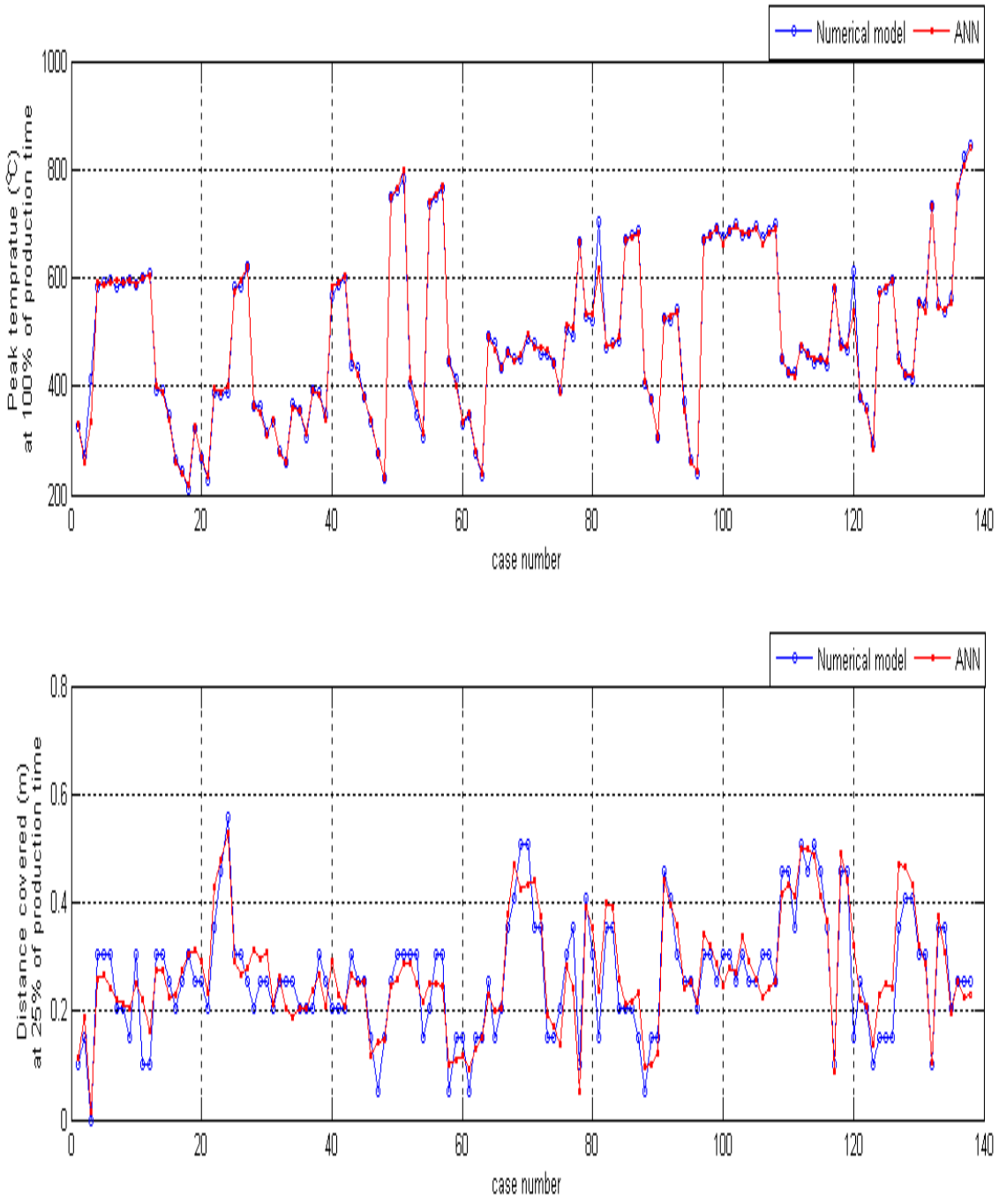

Figure 37: Comparison of results from numerical model and ANN for wet combustion tube model-IV

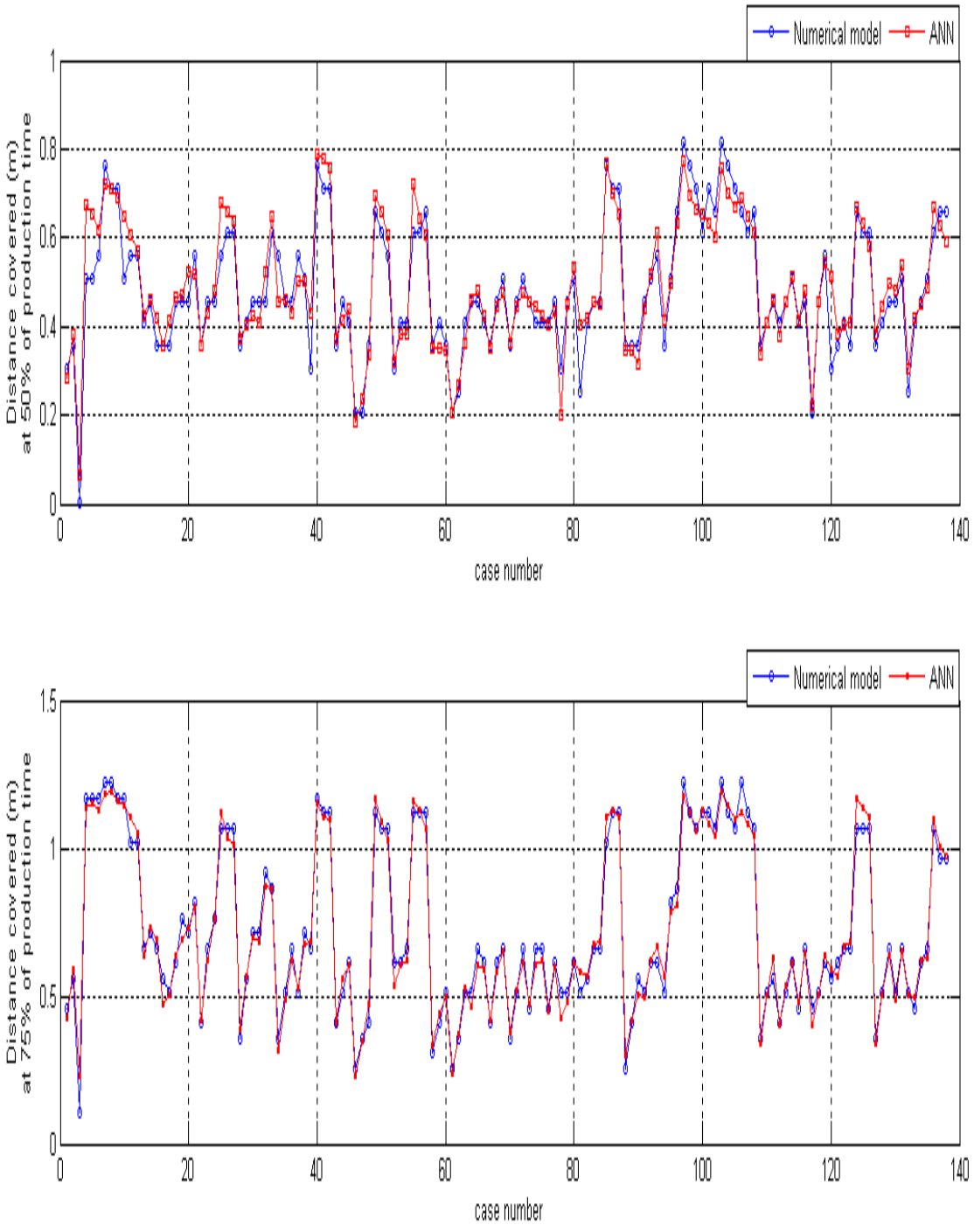

Figure 38: Comparison of results from numerical model and ANN for wet combustion tube model-V

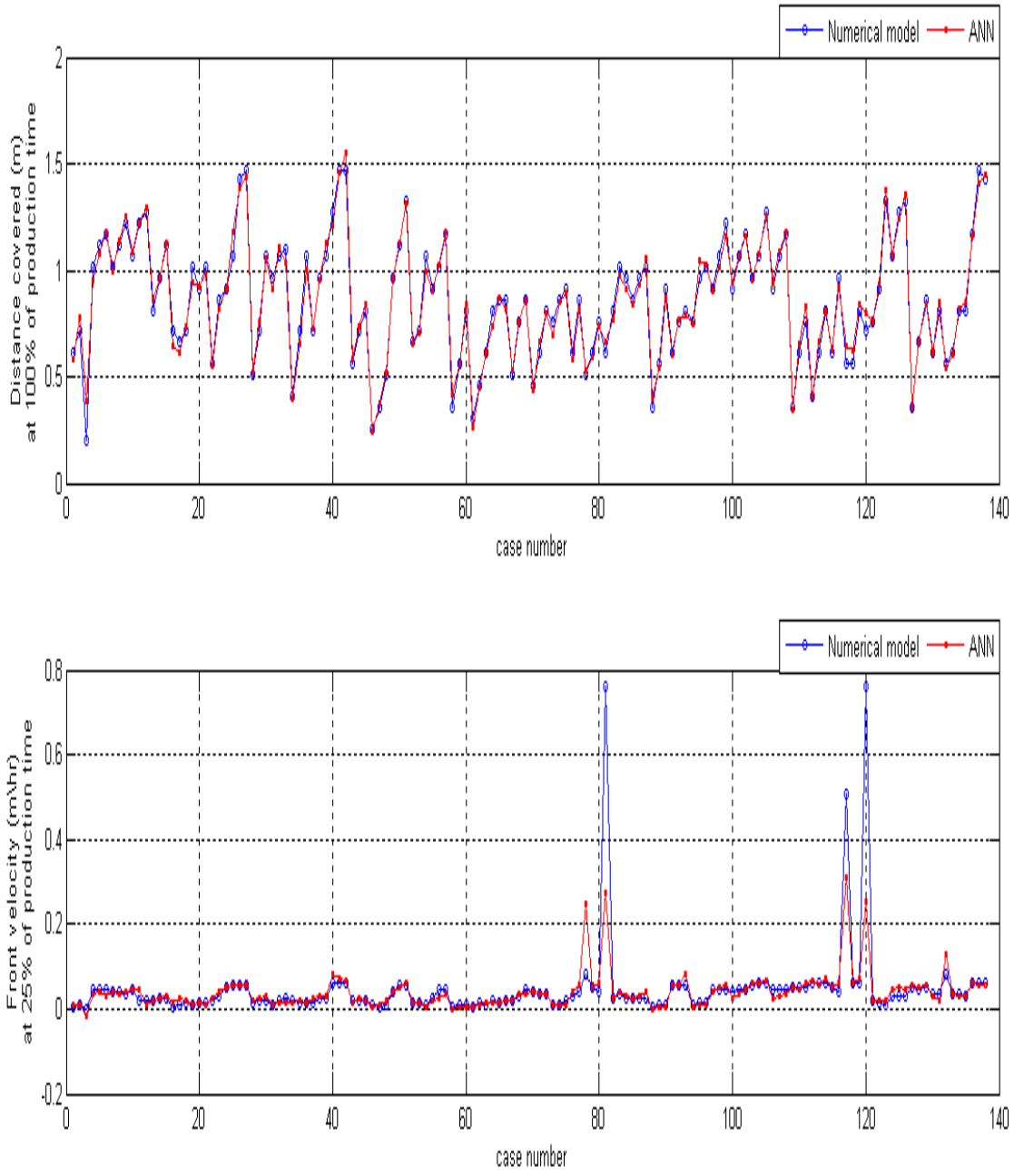

Figure 39: Comparison of results from numerical model and ANN for wet combustion tube model-VI

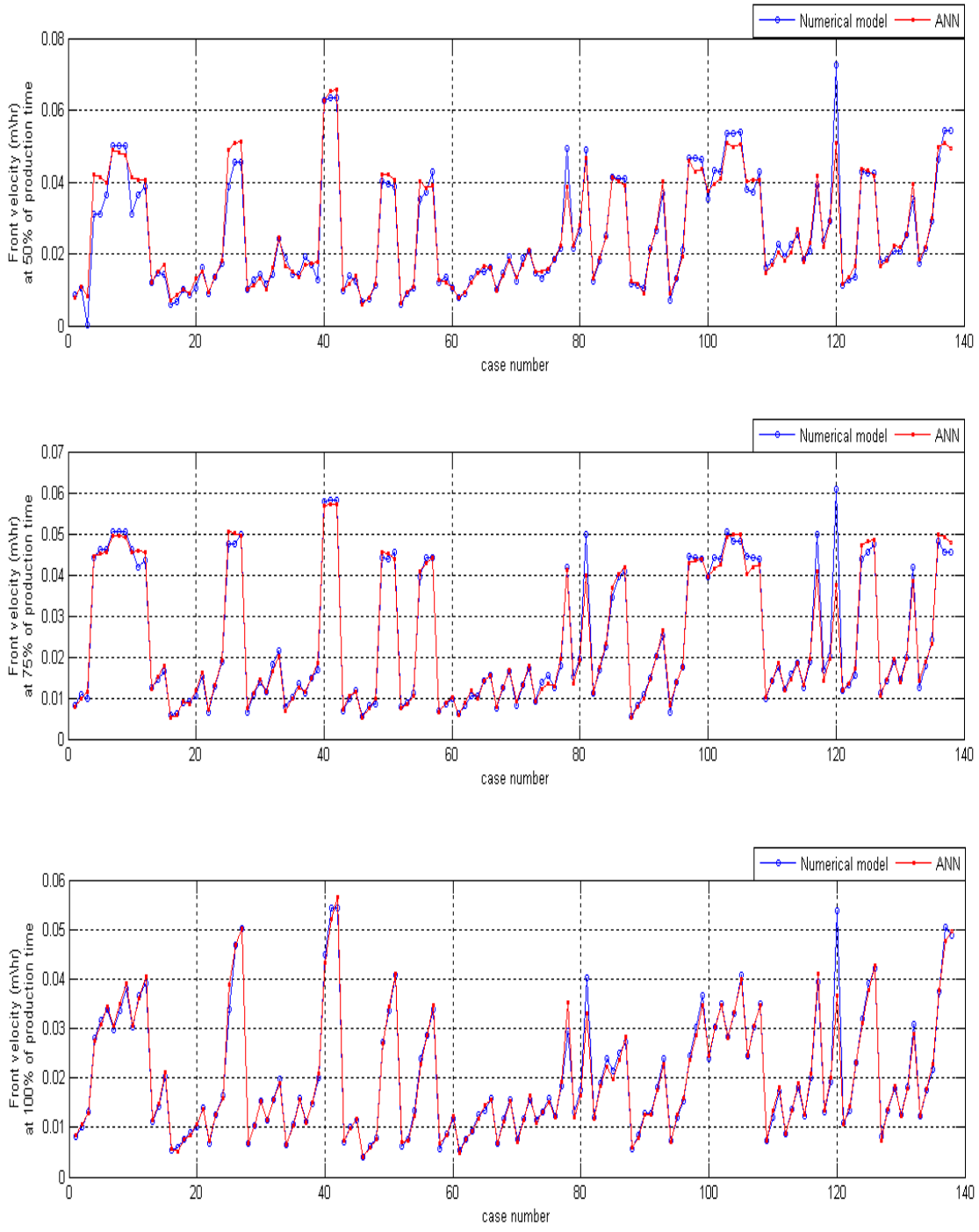

Figure 40: Comparison of results from numerical model and ANN for wet combustion tube model-VII

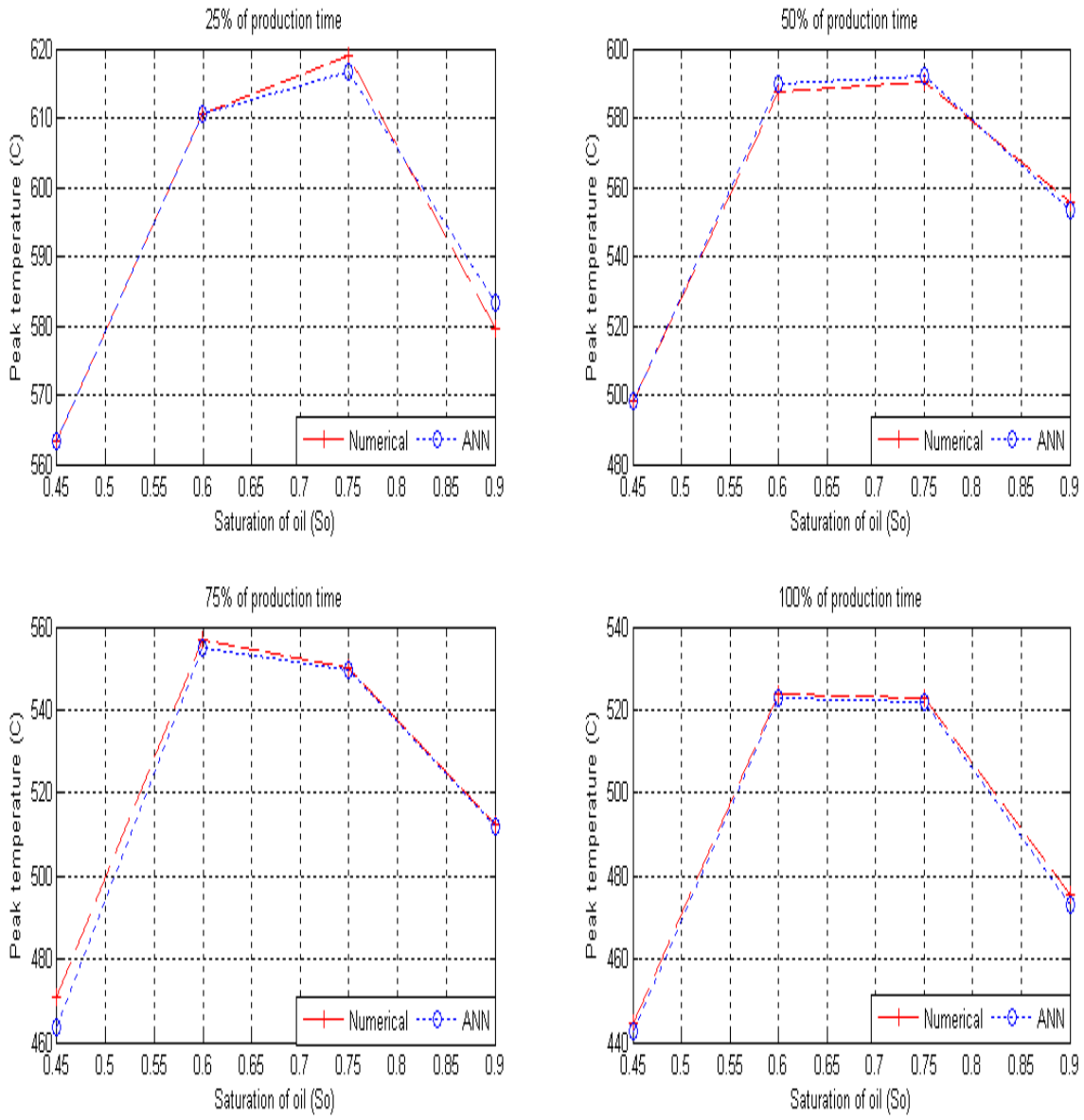

Figure 41: Peak temperature variation with oil saturation at different times in wet combustion

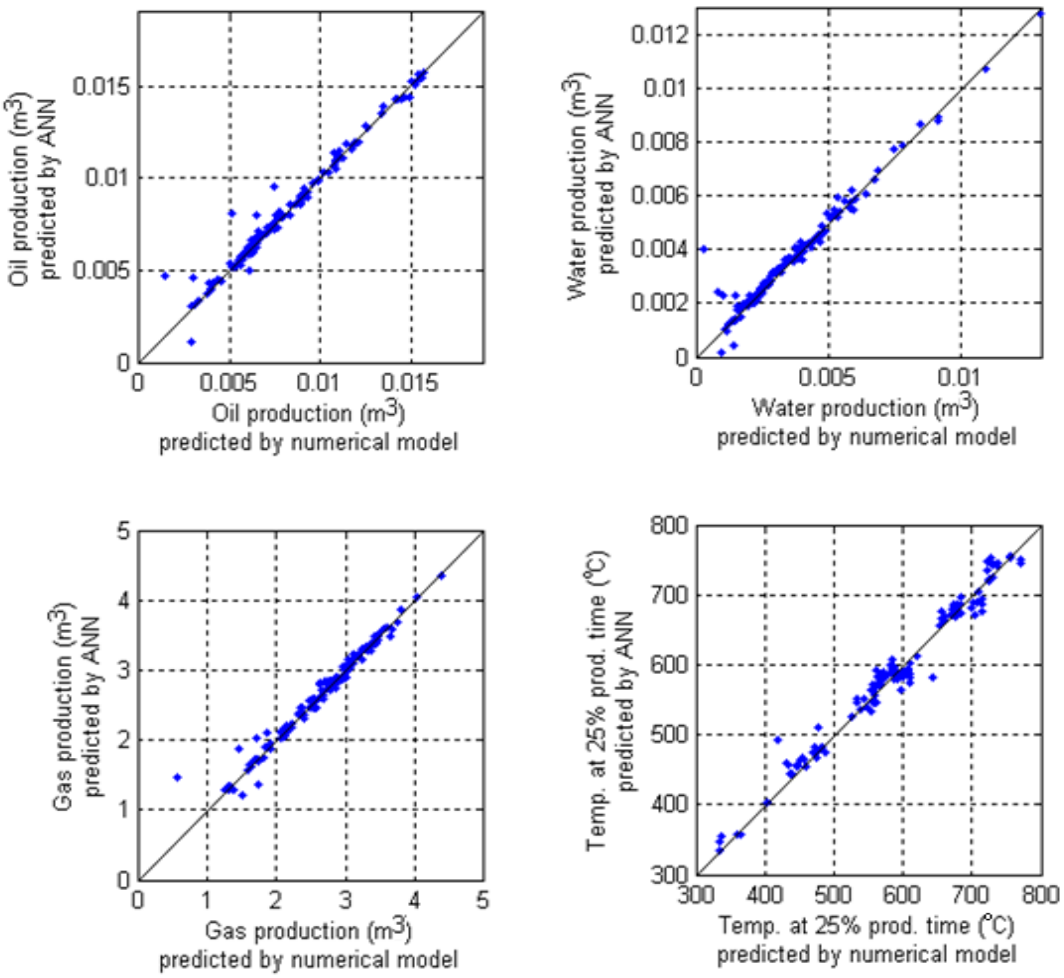

Figure 42: Cross plots of ANN vs. numerical model for wet combustion tube model-I

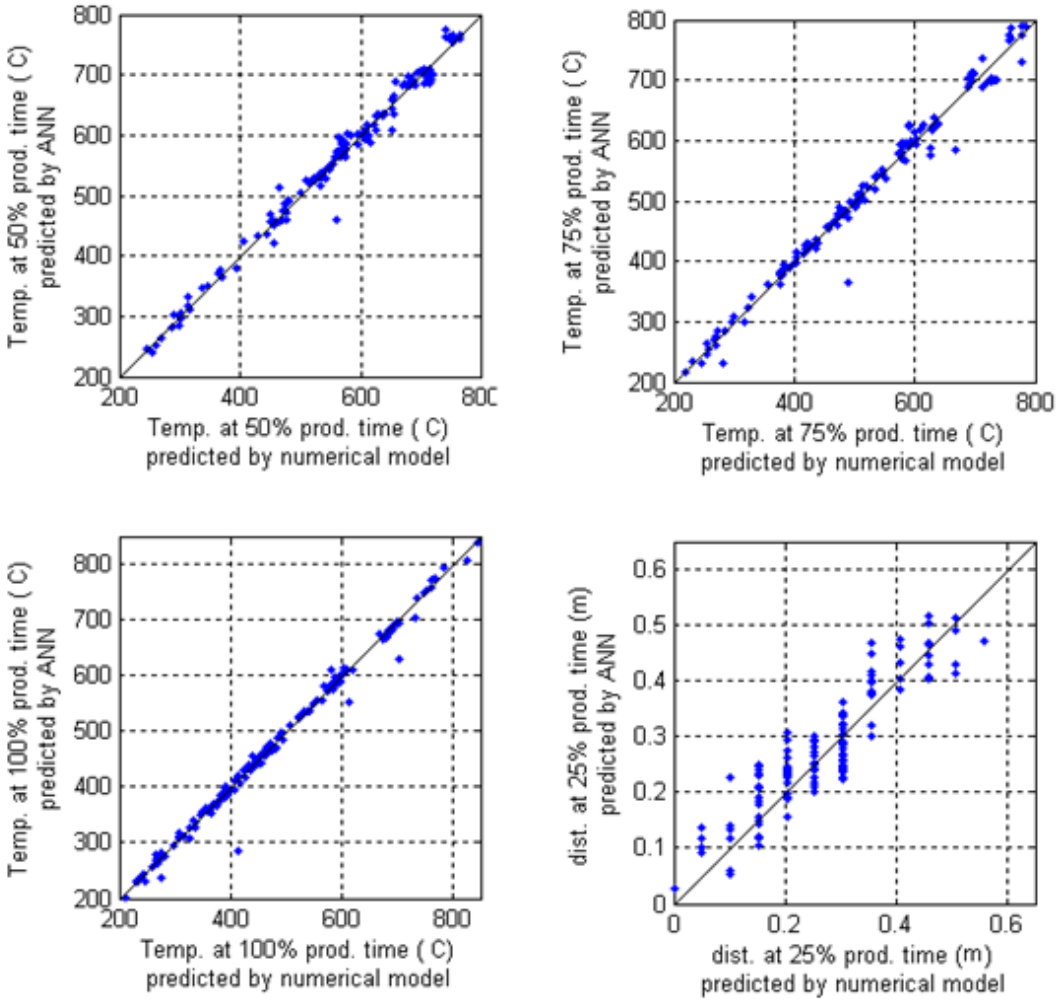

Figure 43: Cross plots of ANN vs. numerical model for wet combustion tube model-II

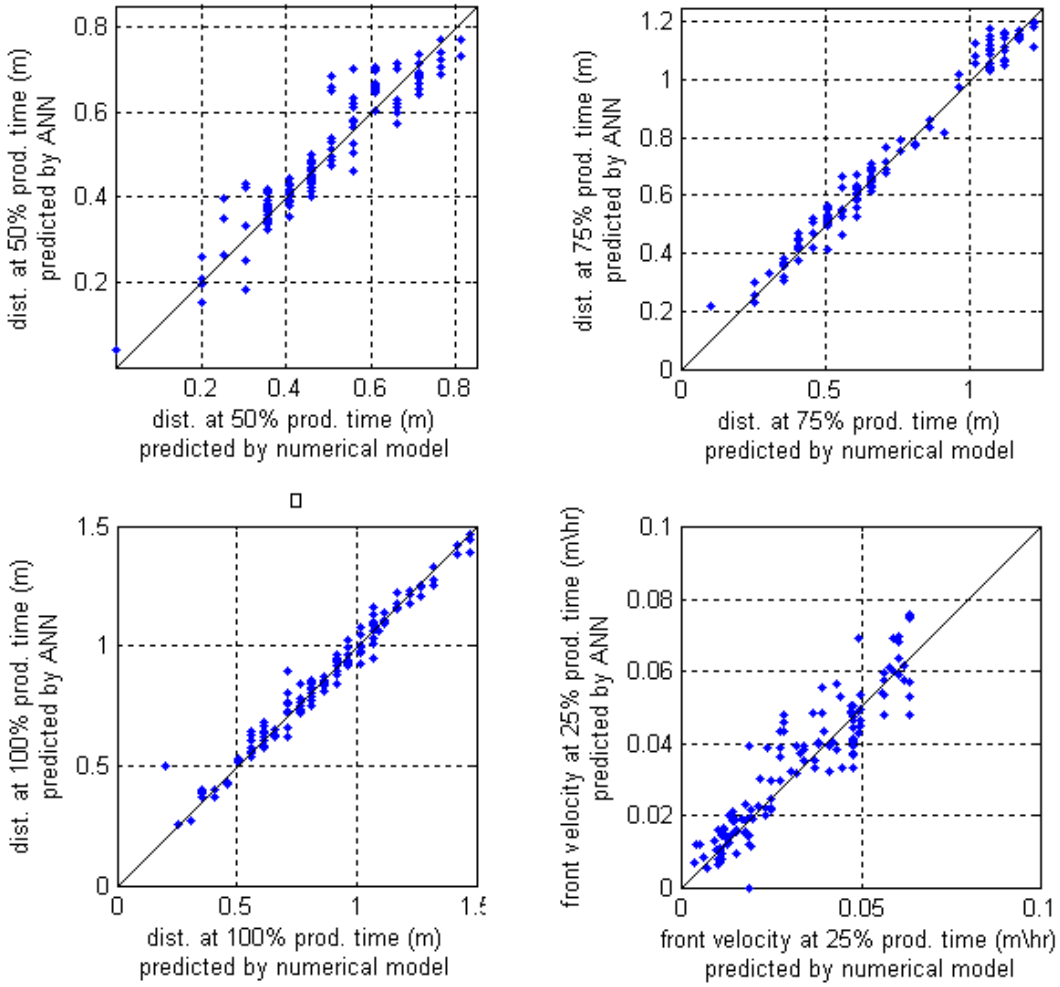

Figure 44: Cross plots of ANN vs. numerical model for wet combustion tube model–III

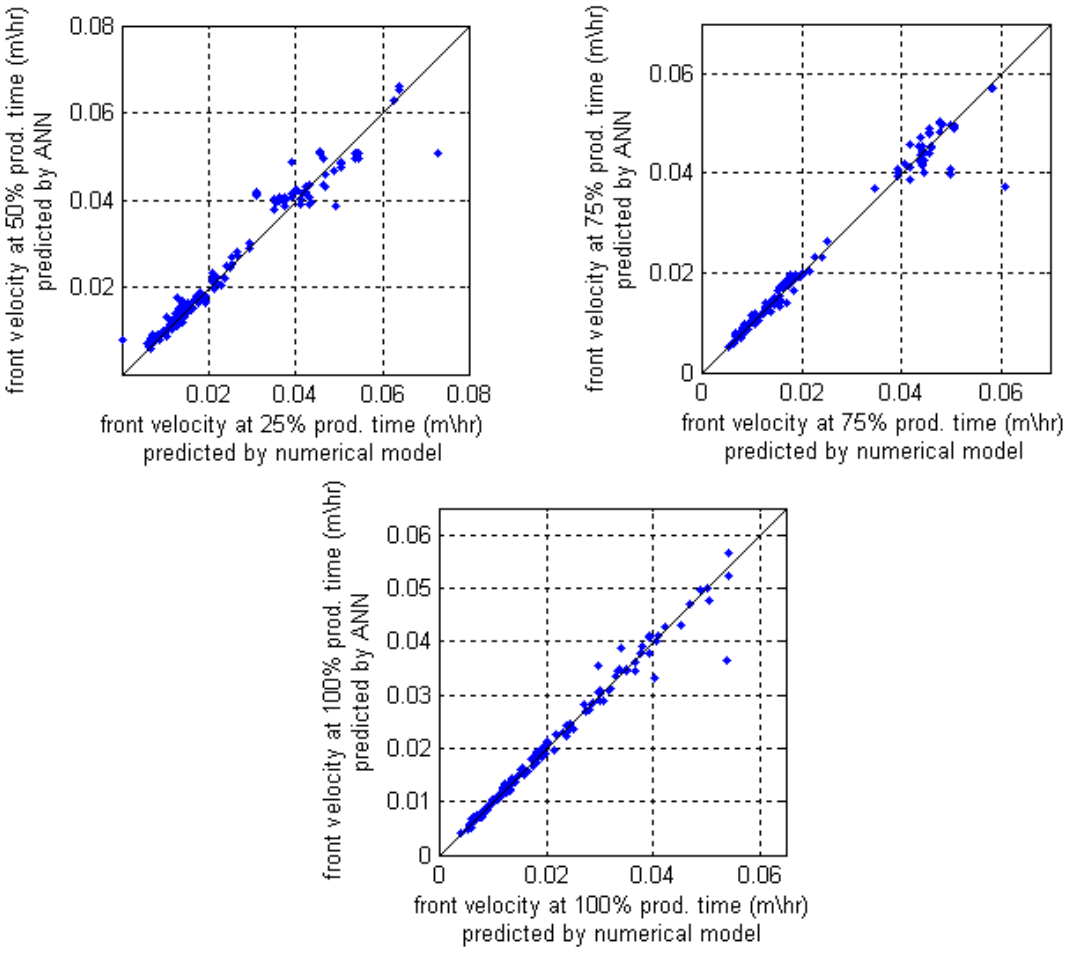

Figure 45: Cross plots of ANN vs. numerical model for wet combustion tube model–IV

5.7 Discussion of results for wet combustion tube model

The results, represented by Figures 33 through 43, shows promising predictions typically for cumulative oil, water, and gas production. These results also show a good match between the peak temperatures at 25%, 50%, 75%, and 100% of the production times. But the network shows variations in the predictions of distance covered by the combustion front and the velocity of the combustion front typically for 25% and 50% of the total production times. Velocity of the combustion front is a function of the distance traveled by the combustion front therefore, a similar behavior in the results for velocity of combustion front is observed. The combustion front movement in a wet combustion typically depends upon saturation of oil, porosity of the rock matrix, air injection rate, and water to air ratio. For a slight change in any of the above mentioned properties a significantly different result was observed. ANN is not able to comprehend these changes expected by numerical model for distance and velocity of the combustion front as effectively as other results like cumulative oil, water, and gas productions, and peak temperatures of the combustion front at 25%, 50%, 75% and 100% of the production times. These predictions could not be improved further by changing the number of neurons and the number of layers in the ANN architecture shown in Figure 14.

Chapter 6

CONCLUSTION AND RECOMMENDATIONS

This chapter concludes the important observations made in carrying out the study and states the broad horizon of the process which is still needed to be covered in order to fully explore *in-situ* modeling. The study carried out proved to be helpful in developing the in-situ combustion model at the laboratory scale and with the experience generated during the study it is recommended to expand the model to reservoir scale and for different crudes.

6.1 Conclusions

Dry and wet *in-situ* combustion recovery processes were studied for the system and predictive ANN based models for both of the systems were prepared. A total of 1105 cases were generated for dry combustion whereas for wet combustion model a total of 3144 cases were generated. ANN was prepared for each of the models by optimizing the number of neurons and number of layers in the neural architecture.

Reliability of the network was tested by exposing the network to the part of the dataset it has never seen before. The developed model can be used to predict the recovery processes for Athabasca crude in the combustion tube. The following inferences could be made from the study:

- Cumulative production of oil, water and gas, peak temperatures of combustion front, distance traveled by the combustion front, and velocity of the combustion front at 25%, 50%, 75%, and 100% of the production times in a wet-combustion

tube experiment can be predicted by using a feed-forward backpropagation network with three hidden layers and 69, 62 and 65 neurons in each layer.

- Cumulative production of oil, water and gas, peak temperatures of combustion front, distance traveled by the combustion front, and velocity of the combustion front at 25%, 50%, 75%, and 100% of the production times in a dry-combustion tube experiment can be predicted by using a feed-forward backpropagation network with three hidden layers and 67, 62 and 65 neurons in each layer.
- Distance traveled by the combustion front and the velocity of the combustion front was found to be sensitive of initial saturation of oil, porosity of the rock matrix, air injection rate, and water-to-air ratio.

6.2 Recommendations

This work can further be improved by carrying out the following studies in addition to this work.

- Kinetics for different crude oil and systems can be included in the study.
- This work deals with one-dimensional analysis and the work can be extended to 2-D and 3-D representations.
- This work deals with homogeneous properties of the reservoir and this model can be improved by incorporating heterogeneity of the system.
- This work can be extended to field scale.
- An inverse system should be developed to optimize the design of the in-situ experiments.

Chapter 7

REFERENCE

- Adegbesan K.O.:"Kinetic study of Low Temperature Oxidation of Athabasca Btumen", Ph.D. Thesis, The University of Calgary, Alberta (1982)
- Belgrave J.D.M.:" An experimental and Numerical Investigation of *In-situ* Combustion Tube Tests," Ph.D. Thesis, July 1987, The University of Calgary.
- Belgrave J.D.M., Moore R.G., Ursenbach M.G., Bennion D.W.:" A comprehensive approach to *In-situ* Combustion Modeling," April 1993, SPE Advanced Tech series, 98-107
- Burger J.G.: " Spontaneous Ignition in oil reservoirs," Soc. Pet. Eng. J., April 1976, 73-81
- Burger, J.G., Sahuquet, B.C., "Chemical Aspects of *In-situ* Combustion – Heat of Combustion and Kinetics," Soc. Pet. Eng. J. (October 1972), p. 410-422
- Burger J.G., Sahuquet B.C.:" Laboratory Research on wet combustion", J. PetTech., Oct 1973, 1137-1146
- Chattopadhyay, S.K., Ram Biany, Bhattacharya, R.N. and Das, T.K., "Enhanced oil recovery by *In-situ* combustion process in Santhal field of Cabay Basin, Mehsana, Gujarat, India- A case study," SPE/DOE Symposium on Improved Oil Recovery, (April 2004)
- Chu, C., "A study of fire-flood field projects," J. PetTech. (February 1977), pp. 111-120

- Coats, R., Lorimer, S., Ivory, J.:" Experimental and numerical simulation of a novel Top down *In-situ* combustion process", SPE international heavy oil symposium, June 1995, 487-498
- Dietz D.N.: " Wet Underground combustion, state of the art", JPT, May 1970, 605-617
- Dietz, D. N., and Weijdema, J.: "Wet and partially quenched Combustion," J. Pet. Tech., April 1968, p. 411
- Farooq Ali, S. M."A current appraisal of in situ Combustion Fiels Test," J. PetTech. (April 1972), p.477
- Fausett L.,"Fundamentals of Neural Networks Architectures Algorithms and Applications," Prentice Hall, 1994
- Garon A.M., Wygal R.J., Gulf research & development Co.: "A laboratory investigation of fire-water flooding",SPE J. , December 1974
- Mamora D.D.:"Kinetics of *In-situ* combustion", Ph.D. Thesis, Stanford University (1993)
- Moss. J. T., White, P. D., McNeil, J. S., Jr.: " In-situ combustion process – Results of a five-well field experiment in southern Oklahoma," Trans AIME, 1951
- Parrish, D. R., and Craig, F. F., "Laboratory study of a combustion of Forward combustion and water flooding – The COFCAW Process," J. Pet. Tech (June 1969), p. 753

- Onyekonwu, M.O., Pande, K., Ramey Jr. H.J., and Brigham, W.E., "Experimental and simulation studies of laboratory *In-situ* combustion Recovery," S.P.E. California Regional Meeting, (April 1986), p. 483-488
- Panait-Patica, A., Serban, D., Ilie, N., "Suplacu de Barcau Field – A case history of a successful *In-situ* Combusiton," S.P.E. Europec/EAGE Annual Conference and Exhibition (June 2006)
- Petit, H.J.M., Thiez, P. Le, and Lemonnier, P., "History Matching of a heavy-oil combustion pilot in Romania", S.P.E./D.O.E. Enhanced Oil Recovery Symposium, (April 1989), p. 737-749
- Tingas, J., Greaves, M., and Young, T.J., "Field scale simulation study of *In-situ* combustion in high pressure light oil reservoirs," S.P.E. Improved Oil Recovery Symposium (April 1996), p. 599-621
- Venkatesan N.N., Sampath K., Otto J.B. :" Oxygen Fireflooding: Determination of Maximum water/oxygen ratio for normal wet combustion", CIM/SPE International Technical Meeting, June 1990.

Appendix A

Sample data file used in CMG

```
*RESULTS SIMULATOR STARS
*interrupt *stop
*title 'combustion tube test'

*inunit  *SI  *except 6 1    ** darcy instead of md
*outunit *SI  *except 6 1    ** darcy instead of md
                *except 1 1   ** Hrs. instead of days
*outprn *grid pres sw so sg temp y x solconc obhloss viso cchloss
*outprn *well *all
*wrst
*rewind 1
*wprn *grid 300
*wprn *iter 300
outsrf well component all mass mole downhole
outsrf grid pres sw so sg temp y x w solconc obhloss
                masdenw masdeno  masdeng pcow pcog visw viso visg
        krw kro krg kvalyw kvalyx cmpdenw cmpdeno cmpvisw
        cmpviso cmpvisg cchloss dyngrddevg dyngrddevo
        dyngrddevw dyngrddeve dyngrddevt dyngrddevs dyngrddevz
outsrf special avgvar temp
                                avgvar pres
          blockvar              temp   1        1       36
          blockvar              temp   1        1       35
          blockvar              temp   1        1       34
          blockvar              temp   1        1       33
          blockvar              temp   1        1       32
          blockvar              temp   1        1       31
          blockvar              temp   1        1       30
          blockvar              temp   1        1       30
          blockvar              temp   1        1       28
          blockvar              temp   1        1       27
          blockvar              temp   1        1       26
          blockvar              temp   1        1       25
          blockvar              temp   1        1       24
          blockvar              temp   1        1       23
          blockvar              temp   1        1       22
          blockvar              temp   1        1       21
          blockvar              temp   1        1       20
          blockvar              temp   1        1       19
```

```
blockvar              temp   1        1        18
blockvar              temp   1        1        17
blockvar              temp   1        1        16
blockvar              temp   1        1        15
blockvar              temp   1        1        14
blockvar              temp   1        1        13
blockvar              temp   1        1        12
blockvar              temp   1        1        11
blockvar              temp   1        1        10
blockvar              temp   1        1        9
blockvar              temp   1        1        8
blockvar              temp   1        1        7
blockvar              temp   1        1        6
blockvar              temp   1        1        5
blockvar              temp   1        1        4
blockvar              temp   1        1        3
blockvar              temp   1        1        2
blockvar              temp   1        1        1

tfront 350  backward
tfront 450  backward
maxvar solconc 'CokeLTO'
maxvar solconc 'CokeITO'
matbal reaction 'WATER'
matbal reaction 'Asphalte'
matbal reaction 'Maltenes'
matbal reaction 'CokeLTO'
matbal reaction 'CokeITO'
matbal reaction 'Gas'
matbal reaction 'O2'
matbal reaction 'N2'
matbal  reaction energy
cchloss
volfrac  'PRODUCER' 'Asphalte'
volfrac  'PRODUCER' 'Maltenes'
volfrac  'PRODUCER' 'Gas'
volfrac  'PRODUCER' 'O2'
volfrac  'PRODUCER' 'N2'
massfrac  'PRODUCER' 'Asphalte'
massfrac  'PRODUCER' 'Maltenes'
massfrac  'PRODUCER' 'Gas'
massfrac  'PRODUCER' 'O2'
massfrac  'PRODUCER' 'N2'
molefrac  'PRODUCER' 'Asphalte'
molefrac  'PRODUCER' 'Maltenes'
```

```
            molefrac  'PRODUCER' 'Gas'
            molefrac  'PRODUCER' 'O2'
            molefrac  'PRODUCER' 'N2'
**============  GRID AND RESERVOIR DEFINITION ================
*grid *cart 1 1 36
**  Tube I.D. = 9.94 cm.  Cross-sectional area is pi*(d/2)**2
**  = 0.0077600166 m2 = L*L.  so equivalent block side is L = 0.088622693 m
**  Total tube length is 1.83 m

*di *con 0.088091
*dj *con 0.088091
*dk *con 0.050833
*por *con 0.400000
*permi *con 12.000000
*permj *equalsi
*permk *equalsi
*end-grid
*rockcp 2.28e6

*thconr 6.048e5
*thconw 5.8147e4
*thcono 1.3392e4
*thcong 4.32e3
*thconmix *simple       ** Simple Volume Weighting (Default Value)
**=============== FLUID DEFINITIONS=======================
**UPDATED TABLE FOR LIGHT OIL from Example sto10.dat converted to SI
*model 8 6 3 1      ** Components are water, Asphalte, Maltenes, N2, Gas, O2, and 2 for
Coke
                ** Standard properties
               ** Gas based on CO/CO2 = 0.168
*compname       'WATER'   'Asphalte'   'Maltenes'    'N2'     'Gas'        'O2'    'CokeLTO'
'CokeITO'
**          ---------------------------------------------------------------------------
*cmm             0.018       1.0928         0.406      0.028     0.0413            0.032
          0.01313    0.01313 ** molecular weight
*pcrit           22107        792           1478       3394      7176       5046                  **
critical pressure
*tcrit           374          904           619        -146.95     22        -119                  ** critical
temp
*molden          0          1059.66          2417.506                                            **
*solid_den  'CokeLTO'     1380.0       0.0       0.0
*solid_den  'CokeITO'     1380.0       0.0       0.0
*cp               0         9.46e-7        9.53e-7
*ct1              0         4.5e-4         5.85e-4
```

```
*kv1            0       0.0         1.140e7                                          **
*kv2            0       0.0          0.0                                  **
*kv3            0       0.0          0.0                                  **
*kv4            0       0.0         -8800                                 **
*kv5            0       0.0         -225                                 **

*cpg1           0       0.0         9.92e2     0      19.8       28.1              **
*cpg2           0       0.0          0.0       0     7.34e-2    -3.68e-6            **
*cpg3           0       0.0          0.0       0     -5.6e-5    1.74e-5             **
*cpg4           0       0.0          0.0       0     1.71e-8    1.065e-9             **
*hvr            0       0           1.03e-4                                  **
*liqphase                                                                  **

**Viscosity from Athabsaca
*avisc          0                   4.89E-25        1.94E-05
*bvisc          0                   33147           5270.4
** Reference and surface conditions
*prsr 100.0
*temr 15.0
*psurf 101.325
*tsurf 15.0

** ---- Chemical Reactions ---- FROM BELGRAVE SPE 20250 && COATS
** All values, Ea FF and Enthalpies reset to those published by Belgrave - DB August
2007

**compname      'WATER'   'Asphaltenes'   'Maltenes'    'N2'     'Gas'      'O2'
'CokeLTO' 'CokeITO'
**          ---------------------------------------------
** 1. Cracking or IT Reactions
** Maltenes --- 0.372 Asphaltenes
*storeac        0          0           1.0         0        0         0         0         0
*stoprod        0        0.372           0         0        0         0         0         0
*freqfac  7.8555e17
*eact     2.347e5
*rorder         0          0           1.0         0        0         0         0         0
** Asphaltenes  --- 83.223 CokeITO, adjusted for Mw of coke
*storeac        0        1.0           0         0        0         0         0         0
*stoprod        0          0           0         0        0         0         0        83.223
*freqfac  3.5113e14
*eact     1.772e5
*rorder         0        1.0           0         0        0         0         0         0
** Asphaltenes  --- 37.683 Gas, adjusted for Mw of gas, based on CO/CO2=0.168
*storeac        0        1.0           0         0        0         0         0         0
*stoprod        0          0           0         0      37.683      0         0         0
```

```
*freqfac  1.1767680e14
*eact     1.763e5
*rorder          0        1.0              0         0        0         0         0          0
** 2. LTO Reactions
** Maltenes + 3.431 O2 = 0.4726 Asphaltenes
*storeac         0          0           1.0         0        0       3.431       0          0
*stoprod         0        0.4726            0         0        0         0         0          0
*freqfac  11.1e9
*eact     86730
*o2pp
*rorder          0          0           1.0         0        0       0.425       0          0
*rxcritcon 'O2' 100.0
*renth 1.295e6
** Asphaltenes + 7.588 O2 =  101.723 CokeLTO
** THE REACTION ORDER IS REPORTED TO BE 4.76
*storeac         0        1.0              0         0        0        7.588       0          0
*stoprod         0          0              0         0        0         0       101.723        0
*freqfac  3.58e9
*eact     1.856e5
*o2pp
*rorder          0        1.0              0         0        0        4.76        0          0
*renth 2.857e6
** 3. HTO Reaction -- 2 identical reactions for CokeLTO and CokeITO
** Stoichiometry from CT#1, x=1.77 and m= 0.168
** 1 Coke + 1.232 O2 = 1 CO2 + 0.565 H2O
** 3.1 For CokeITO                                                    CokeLTO    CokeITO
*storeac         0          0              0         0        0              1.232      0         1.0
*stoprod        0.565       0              0         0       1.0             0          0         0
*freqfac  150.2
*eact     34763  **34763
*o2pp
*rorder          0          0              0         0        0         1.0         0         1.0
*renth 3.5e5
** 3.2 For CokeLTO                                                    CokeLTO    CokeITO
*storeac         0          0              0         0        0              1.232      1.0         0
*stoprod        0.565       0              0         0       1.0             0          0         0
*freqfac  150.2
*eact     34763
*o2pp
*rorder          0          0              0         0        0         1.0         1.0         0
*renth 3.5e5
** ============== ROCK-FLUID PROPERTIES ======================
*rockfluid
*rpt 1 lininterp
** Base Case RP -
```

```
** O-W from Nimr RE reports
** Reasonable Values selected for G-O curves
*swt   **  Water-oil relative permeabilities
**Sw   Krw       Kro   Pcow
0.05 0.00000 1.00000
0.10 0.00039 0.88581
0.25 0.00625 0.58478
0.35 0.01406 0.41869
0.45 0.02500 0.28028
0.65 0.03906 0.08651
0.75 0.05625 0.03114
0.85 0.07656 0.00346
0.95 0.10000 0.00000
1.00 0.12656 0.00000
**Sl=Swc+So
*slt   **  Liquid-gas relative permeabilities
**Sl        Krg       Krog
**----      -------    -------
0.07   0.10000 0.00000
0.16   0.08615 0.00316
0.21   0.06632 0.01262
0.31   0.03711 0.05050
0.41   0.01881 0.11362
0.51   0.00829 0.20199
0.61   0.00296 0.31562
0.71   0.00073 0.45449
0.80   0.00011 0.60106
0.95   0.00000 0.89080
1.00   0.00000 1.00000
SWR 0.07
**  ==============  INITIAL CONDITIONS  ======================
*initial
*pres *con 10300 **KPa
** saturations prior to N2 injection

*sg *con 0.000000
*so *con 0.750000
*sw *con 0.250000

*temp *con 55

*mfrac_oil 'Asphalte' *con 0.084900
*mfrac_oil 'Maltenes' *con 0.915100

**INITIAL GAS COMPOSITION
```

```
** Gas composition
*mfrac_gas 'N2' *con 1.0
** ============== NUMERICAL CONTROL ======================
*numerical
*dtmax 0.005
*newtoncyc 30         ** maximum number of Newtonian cycles
*ncuts 10
*run
** ============== RECURRENT DATA ======================
*time  0   **HEATERS ON
 dtwell .0005
  ** N2 injection and start preheating
WELL 1 'INJECTOR'
         injector mobweight 'INJECTOR'
         incomp gas   0          0          0        1.0       0        0.0
         tinjw 21
         operate stg  1.344000
         PERF  WI  'INJECTOR'   ** i  j  k  wi(gas)
                    1 1 36  1.0
         *heatr *ijk 1 1 34:36  2200000.000000

WELL 2 'PRODUCER'
         producer 'PRODUCER'
         operate bhp 9500.000000
                  ** back pressure is fixed, inlet pressure is variable
         monitor temp 250 stop
         geometry  k  1  1  1  0
         PERF  TUBE-END  'PRODUCER'
            1 1 1  1.0

*time  0.200000
           *heatr con 0      ** Shut off external heaters
         dtwell .0005
         injector mobweight 'INJECTOR'
         incomp gas   0          0          0        0.0522       0        0.9478
         tinjw     21
         operate stg  3.000000
*time  0.500000
         *dtwell .0005
         *injector mobweight 'INJECTOR'
         *incomp water-gas   0.000999          0          0        0.789211       0        0.209790
         *tinjw 50
         *operate stf  1.000000
*time  2.0000000
*stop
```

Appendix B

Sample ANN code

This code is used for wet combustion recovery process

```
clear
clc
format long

load INP4.txt
load OUT4.txt

INP1 = INP4;
OUT1 = OUT4;

P = INP1;
T = OUT1;

%using functional link in the output temperature over distance
P(11,:) = P(1,:)./P(3,:);  %porosity/saturation
P(12,:) = sqrt(P(2,:)./P(1,:));  %permeability/porosity
% check =
P(13,:) = P(4,:).*(P(8,:)-P(7,:));  %air injected
P(14,:) = P(9,:).*P(7,:);       %heat supplied
P(6,:) = P(5,:).*P(10,:);      %amount of water
% P(15,:) = P(6,:)./P(13,:);      %amount of water/air (injection)
P(15,:) = log(P(9,:));
P(16,:) = log((P(10,:)));
P(17,:) = log(P(2,:).*P(1,:));  %permeability/
T(8:11,:) = power((T(8:11,:).*T(4:7,:)),0.5);

%normalising the data
%Pn stands for normalized input and Tn stands for normalized output
[Pn,ps] = mapminmax(P,-1,1);   % gives all values between -1 & 1
[Tn,ts] = mapminmax(T,-1,1);   % gives all values between -1 & 1

[mi,ni] = size(Pn);
[mo,no] = size(Tn);
```

```
%defining some variables required in the network
N_in = mi;   % # of inputs in the network
N_out = mo;  % # of outputs in the network
Tot_in = ni;  %total no. of simulations
N_train = 699;
% N_val = 50;
N_test = 80;

%seperating training, testing & validation data
%when random selection command is available through higher version
%%% dividing random

[Pn_train,Pn_val,Pn_test,trainInd,valInd,testInd] = dividerand(Pn,0.9,0.05,0.05);
[Tn_train,Tn_val,Tn_test] = divideind(Tn,trainInd,valInd,testInd);

val.T = Tn_val;
val.P = Pn_val;
test.T = Tn_test;
test.P = Pn_test;

%Initiating network parameters
%according to the thumb rule total no. neurons should be around 93 in this
%case as Neurons = (total cases(6977))^0.5 + (#inputs(5) + #outputs(14))/2
NNeu1 = 69;
NNeu2 = 62;
NNeu3 = 65;
NNeu4 = 57;  %hidden layer attached to the outermost output layer


% creating the cascade backpropagation network
% load simplefit_dataset
net                                                                    =
newcf(Pn,Tn,[NNeu1,NNeu2,NNeu3,mo],{'logsig','logsig','tansig','purelin'},'trainscg','lea
rngdm','msereg');


%setting training parameters for the network

net.trainParam.goal = 0.0005; %accuracy within this range
net.trainParam.epochs = 12000; % number of iteration sets
net.trainParam.show = 1;
net.trainParam.max_fail = 100000;
net.trainParam.mem_reduc = 60; %to reduce memory requirements
```

```
%starting training the network
[net,tr] = train(net,Pn_train,Tn_train,[],[],test,val);
plotperf(tr)
% pause
%--------------------------------------------------------------------------
%-----------getting data from the trained network ------------------------
%--------------------------------------------------------------------------
Tn_train_ann = sim(net,Pn_train);
Tn_test_ann = sim(net,Pn_test);


%denormalising the data sets obtained
%output reversal
T_train = mapminmax('reverse',Tn_train,ts);
T_test = mapminmax('reverse',Tn_test,ts);
T_train_ann = mapminmax('reverse',Tn_train_ann,ts);
T_test_ann = mapminmax('reverse',Tn_test_ann,ts);

%input reversal
Pn_train = mapminmax('reverse',Pn_train,ps);
Pn_val = mapminmax('reverse',Pn_val,ps);
Pn_test = mapminmax('reverse',Pn_test,ps);

%--------------------------------------------------------------------------

 T_train(8:11,:) = power(T_train(8:11,:),2);
 T_test(8:11,:) = power(T_test(8:11,:),2);
 T_train_ann(8:11,:) = power(T_train_ann(8:11,:),2);
 T_test_ann(8:11,:) = power(T_test_ann(8:11,:),2);

 T_train(8:11,:) = T_train(8:11,:)./T_train(4:7,:);
 T_test(8:11,:) = T_test(8:11,:)./T_test(4:7,:);
 T_train_ann(8:11,:) = T_train_ann(8:11,:)./T_train_ann(4:7,:);
T_test_ann(8:11,:) = T_test_ann(8:11,:)./T_test_ann(4:7,:);
% %--------------------------------------------------------------------------

[m_Te,n_Te] = size(T_test);
NP_test = 1:n_Te;
error_test = ((T_test-T_test_ann)./T_test).*100;


j=0;
for i=1:m_Te
   if i==3 tit = 'error in gas'; xlab = 'case number'; ylab = '% error'; end
   if i==1 tit = 'error in oil'; xlab = 'case number'; ylab = '% error'; end
```

```
        if i==2 tit = 'error in water'; xlab = 'case number'; ylab = '% error'; end
        if i==4 tit = 'error in temp(25%prod.time)'; xlab = 'case number'; ylab = '%
error'; end
        if i==5 tit = 'error in temp(50%prod.time)'; xlab = 'case number'; ylab = '%
error'; end
        if i==6 tit = 'error in temp(75%prod.time)'; xlab = 'case number'; ylab = '%
error'; end
        if i==7 tit = 'error in temp(100%prod.time)'; xlab = 'case number'; ylab = '%
error'; end
        if i==8 tit = 'error in dist.(25%prod.time)'; xlab = 'case number'; ylab = '%
error'; end
        if i==9 tit = 'error in dist.(50%prod.time)'; xlab = 'case number'; ylab = '%
error'; end
        if i==10 tit = 'error in dist.(75%prod.time)'; xlab = 'case number'; ylab = '%
error'; end
        if i==11 tit = 'error in dist.(100%prod.time)'; xlab = 'case number'; ylab = '%
error'; end
        if i==12 tit = 'error in front velocity(25%)'; xlab = 'case number'; ylab =
'%error'; end
        if i==13 tit = 'error in front velocity(50%)'; xlab = 'case number'; ylab =
'%error'; end
        if i==14 tit = 'error in front velocity(75%)'; xlab = 'case number'; ylab =
'%error'; end
        if i==15 tit = 'error in front velocity(100%)'; xlab = 'case number'; ylab =
'%error'; end
        if i==16 tit = 'oil/porosity/sat' ; ylab = '%error'; end

        if rem(i,4)==1
           j=j+1;
           figure(j)

        end
        if rem(i,4)~=0
           subplot(2,2,rem(i,4)): plot([1:n_Te],error_test(i,:));
           axis([1 n_Te -10 10]);
           title([tit]);
           xlabel([xlab]);
           ylabel([ylab]);
           grid on
        else
           subplot(2,2,4): plot([1:n_Te],error_test(i,:));
           axis([1 n_Te -10 10]);
           title([tit]);
           xlabel([xlab]);
           ylabel([ylab]);
```

```
            grid on
        end
    end

    for i=1:m_Te
        if i==3 tit = 'gas actual Vs ANN'; xlab = 'case number'; ylab = 'meter cube'; end
        if i==1 tit = 'oil actual Vs ANN'; xlab = 'case number'; ylab = 'meter cube'; end
        if i==2 tit = 'water actual Vs ANN'; xlab = 'case number'; ylab = 'meter cube';
end
        if i==4 tit = 'temp(25%prod.time) actual Vs ANN'; xlab = 'case number'; ylab =
'degree celcius'; end
        if i==5 tit = 'temp(50%prod.time) actual Vs ANN'; xlab = 'case number'; ylab =
'degree celcius'; end
        if i==6 tit = 'temp(75%prod.time) actual Vs ANN'; xlab = 'case number'; ylab =
'degree celcius'; end
        if i==7 tit = 'temp(100%prod.time) actual Vs ANN'; xlab = 'case number'; ylab
= 'degree celcius'; end
        if i==8 tit = 'dist.(25%prod.time) actual Vs ANN'; xlab = 'case number'; ylab =
'meters'; end
        if i==9 tit = 'dist.(50%prod.time) actual Vs ANN'; xlab = 'case number'; ylab =
'meters'; end
        if i==10 tit = 'dist.(75%prod.time) actual Vs ANN'; xlab = 'case number'; ylab
= 'meters'; end
        if i==11 tit = 'dist.(100%prod.time) actual Vs ANN'; xlab = 'case number'; ylab
= 'meters'; end
        if i==12 tit = 'front velocity(25%)'; xlab = 'case number'; ylab = 'meter/hour';
end
        if i==13 tit = 'front velocity(50%)'; xlab = 'case number'; ylab = 'meter/hour';
end
        if i==14 tit = 'front velocity(75%)'; xlab = 'case number'; ylab = 'meter/hour';
end
        if i==15 tit = 'front velocity(100%)'; xlab = 'case number'; ylab = 'meter/hour';
end
        if i==16 tit = 'oil/porosity/sat' ; ylab = 'CuM/hr.'; end
        if rem(i,4)==1
            j=j+1;
            figure(j)
        end
        if rem(i,4)~=0
            subplot(2,2,rem(i,4)): plot([1:n_Te],T_test(i,:),[1:n_Te],T_test_ann(i,:));
            title([tit]);
            xlabel([xlab]);
            ylabel([ylab]);
            legend('ACTUAL','ANN');
            grid on
```

```
        else
           subplot(2,2,4): plot([1:n_Te],T_test(i,:),[1:n_Te],T_test_ann(i,:));
           title([tit]);
           xlabel([xlab]);
           ylabel([ylab]);
           legend('ACTUAL','ANN');
           grid on
        end


      %    plot([1:n_Te],T_test(i,:),[1:n_Te],T_test_ann(i,:));
      end


      for i=1:m_Te
         if i==3 tit = 'gas actual Vs ANN'; xlab = 'cmeter cube(test)'; ylab = 'meter
cube(ANN)'; end
         if i==1 tit = 'oil actual Vs ANN'; xlab = 'cmeter cube(test)'; ylab = 'meter
cube(ANN)'; end
         if i==2 tit = 'water actual Vs ANN'; xlab = 'cmeter cube(test)'; ylab = 'meter
cube(ANN)'; end
         if i==4 tit = 'temp(25%prod.time) actual Vs ANN'; xlab = 'degree celcius(test)';
ylab = 'degree celcius(ANN)'; end
         if i==5 tit = 'temp(50%prod.time) actual Vs ANN'; xlab = 'degree celcius(test)';
ylab = 'degree celcius(ANN)'; end
         if i==6 tit = 'temp(75%prod.time) actual Vs ANN'; xlab = 'degree celcius(test)';
ylab = 'degree celcius(ANN)'; end
         if i==7 tit = 'temp(100%prod.time) actual Vs ANN'; xlab = 'degree
celcius(test)'; ylab = 'degree celcius(ANN)'; end
         if i==8 tit = 'dist.(25%prod.time) actual Vs ANN'; xlab = 'meters(test)'; ylab =
'meters(ANN)'; end
         if i==9 tit = 'dist.(50%prod.time) actual Vs ANN'; xlab = 'meters(test)'; ylab =
'meters(ANN)'; end
         if i==10 tit = 'dist.(75%prod.time) actual Vs ANN'; xlab = 'meters(test)'; ylab =
'meters(ANN)'; end
         if i==11 tit = 'dist.(100%prod.time) actual Vs ANN'; xlab = 'meters(test)'; ylab
= 'meters(ANN)'; end
         if i==12 tit = 'front velocity actual Vs. ANN(25%)'; xlab = 'meter/hour(test)';
ylab = 'meter/hour(ANN)'; end
         if i==13 tit = 'front velocity actual Vs. ANN(50%)'; xlab = 'meter/hour(test)';
ylab = 'meter/hour(ANN)'; end
         if i==14 tit = 'front velocity actual Vs. ANN(75%)'; xlab = 'meter/hour(test)';
ylab = 'meter/hour(ANN)'; end
         if i==15 tit = 'front velocity actual Vs. ANN(100%)'; xlab = 'meter/hour(test)';
ylab = 'meter/hour(ANN)'; end
```

```
    if i==16 tit = 'oil/porosity/sat' ; xlab = 'CuM/hr.'; ylab = 'CuM/hr.(ANN)'; end


    if rem(i,4)==1
       j=j+1;
       figure(j)
    end
    if rem(i,4)~=0
       subplot(2,2,rem(i,4)): plot(T_test(i,:),T_test_ann(i,:),'*','markersize',3);
       a = min(min(T_test(i,:)),min(T_test_ann(i,:)));
       b = max(max(T_test(i,:)),max(T_test_ann(i,:)));
       xlim([a b]);
       ylim([a b]);
       title([tit]);
       xlabel([xlab]);
       ylabel([ylab]);
       axis equal
       grid on
    else
       subplot(2,2,4): plot(T_test(i,:),T_test_ann(i,:),'*','markersize',3);
       a = min(min(T_test(i,:)),min(T_test_ann(i,:)));
       b = max(max(T_test(i,:)),max(T_test_ann(i,:)));
       xlim([a b]);
       ylim([a b]);
       title([tit]);
       xlabel([xlab]);
       ylabel([ylab]);
       axis equal
       grid on
    end
end
```